AN ABSTRACT OF THE THESIS OF

Daniel M. Wachs for the degree of Masters of Science in Nuclear Engineering and Mechanical Engineering presented on January 6, 1998. Title: A Study of Thermal Stratification in the Cold Legs During the Subcooled Blowdown Phase of a Loss of Coolant Accident (LOCA) in the OSU APEX Thermal Hydraulic Testing Facility.

Redacted for Privacy

Abstract approved: _____

Jose N. Reyes, Jr.

Redacted for Privacy

Abstract approved: _____

Lorin R. Davis

The phenomena of interest in this work is the thermal stratification which occurs during the early stages of a loss of coolant accident (LOCA) in the OSU APEX Thermal Hydraulic Test Facility, which is a scaled model of the Westinghouse AP600 nuclear power plant. Thermal stratification has been linked to the occurrence of pressurized thermal shock (PTS). Analysis of the OSU APEX facility data has allowed the determination of an onset criteria and support for the postulated mechanisms leading to thermal stratification. CFX 4.1, a computational fluid dynamics code, was used to

generate a model of the cold legs and the downcomer and the phenomena occurring within them.

The following are the accomplishments of the work contained within this report;

- Determined the causes of thermal stratification in the cold legs of the Westinghouse Advanced Passive 600 MW (AP600) nuclear power plant.
- Predicted the onset of thermal stratification in the cold legs of the Westinghouse Advanced Passive 600 MW (AP600) nuclear power plant.
- Modeled the phenomena associated with thermal stratification in the cold legs of the Westinghouse Advanced Passive 600 MW (AP600) nuclear power plant.

A Study of Thermal Stratification in the Cold Legs During the Subcooled Blowdown Phase of a Loss of Coolant Accident in the OSU APEX Thermal Hydraulic Test Facility

by

Daniel M. Wachs

A THESIS

submitted to

Oregon State University

in partial fulfillment of
the requirements for the
degree of

Master of Science

Completed January 6, 1998
Commencement June 1998

Master of Science of Daniel M. Wachs presented on January 6, 1998

APPROVED:

Redacted for Privacy

Major Professor, representing Nuclear Engineering

Redacted for Privacy

Major Professor, representing Mechanical Engineering

Redacted for Privacy

Chair of Department, representing Nuclear Engineering

Redacted for Privacy

Chair of Department, representing Mechanical Engineering

Redacted for Privacy

Dean of Graduate School

I understand that my thesis will become part of the permanent collection of Oregon State University libraries. My signature below authorizes release of my thesis to any reader upon request.

Redacted for Privacy

Daniel M. Wachs, Author

Acknowledgment

This work would not have been possible without the tremendous love, patience and support that my wife, Cathy, has given me. She has made countless sacrifices and continues to do so everyday. She and our two children, Alexander and Miranda, are, and always will be, the inspiration that drives me. I would also like to thank my family, Mom, Dad, Brian and Sarah, for their belief in me. I hope that they know that I feel the same belief in them.

I also owe a great deal of thanks to Dr. Jose Reyes Jr., who gave me the opportunity to grow and learn. His genuine decency and dedication are the standard by which I will always measure myself.

TABLE OF CONTENTS

TABLE OF CONTENTS (Continued)

TABLE OF CONTENTS (Continued)

LIST OF FIGURES

LIST OF FIGURES (Continued)

LIST OF FIGURES (Continued)

LIST OF FIGURES (Continued)

A Study of Thermal Stratification in the Cold Legs During the Subcooled Blowdown Phase of a Loss of Coolant Accident in the OSU APEX Thermal Hydraulic Test Facility

1. INTRODUCTION

1.1 DESCRIPTION OF PHENOMENA

A system is described as stabily stratified if the fluid volume within a region can be divided into two distinct regions and the fluid contained within each region is held in that region by some stabilizing force. The stabilizing force can be generated through a variety of physical mechanisms. For example, thermal stratification occurs when the stabilizing force is provided by temperature induced density differences in the fluid. A lake with a thermocline separating the warm surface layer from the cooler bottom layer is an example of a thermally stratified system. Two phase stratification occurs when the stabilizing force is provided by the density difference between a gas and liquid. A nuclear reactor pressurizer is an example of a two phase stratified system. At the pressurizer top there is a large steam bubble while the pressurizer bottom is filled with liquid water. The system would not be fully stratified if boiling were to occur because the liquid region would have steam bubbles mixed in with it. More than one mechanism can contribute to stratification. For instance, a two phase stratified system can also be thermally stratified if the gas is hotter than the liquid.

The phenomena of interest for this research is the stratification that occurs within the cold legs of the OSU APEX test facility (and therefore by scaling

arguments, the Westinghouse AP600) during the early stages of a loss of coolant accident (LOCA). The fluid occupying the cold leg can be resolved into two separate volumes during segments of the LOCA simulations. Reviewing the data collected from thermocouples and level differential pressure (LDP) sensors reveals that both thermal stratification and two phase stratification occurs in most of the simulated LOCAs. In past safety evaluations of nuclear power plants, primary system failure modes due to pressurized thermal shock have been linked to thermal stratification.

1.2 RESEARCH OBJECTIVES

The goal of the research presented here was to develop a model for predicting the onset of thermal stratification that would occur during a LOCA. The model was designed such that it can be scaled up to predict the behavior of the Westinghouse AP600 as well as the OSU APEX facility. It was anticipated that during the development of this model the mechanisms leading up to and causing the stratification to occur would be determined and explained.

1.3 RESEARCH APPROACH

The research was performed by making extensive use of the substantial database generated by the OSU APEX experimental team. This database was used to gain insights into the phenomena leading up to the onset of stratification as well as the stratification itself. Having developed a consistent interpretation of the physical causes for the stratification phenomena, a predictive model was generated using the boundary conditions suggested by the qualitative model. An "off the shelf" computer software package (CFX 4.1) was used to construct the predictive model. Results from

the predictive model were compared to the raw data collected by the OSU APEX facility and ROSA facility.

2. REVIEW OF LITERATURE

Pressurized Thermal Shock (PTS) is a commonly postulated accident sequence that was first recognized in the early 1980s. Since that time it has received a great deal of attention in the literature as appropriate models and analytical tools were developed to determine the actual safety risk that PTS presented. Definitive studies were performed on each of the common commercial power reactor types that were operating in the U.S. at the time, including reactors manufactured by Westinghouse, Babcock and Wilcox, and Combustion Engineering. Only a few reactors were recognized to be at risk and steps were taken to reduce the chance of PTS in each.

A resurgence of interest in the nuclear power industry has lead to the development of several new reactor designs. Each of these designs must be certified by the U.S. Nuclear Regulatory Commission (NRC) before they can be built and operated. A major part of this certification process is the characterization of the reactor safety systems. The NRC evaluates these systems by presenting the plant with a series of postulated accidents that could expose failure modes of the reactor. They then analyze the plant and determine how the plant will perform. One of these potential failure modes is PTS. A PTS event can only occur if all of the following conditions exist simultaneously;

- The reactor pressure vessel has incurred radiation embrittlement,
- A flaw exists in the vessel material and is large enough to propagate,
- The reactor coolant near the pressure vessel flaw cools rapidly,
- Heat is transferred quickly from the vessel wall to the fluid,

- The primary system is at high pressure.

Many of the tools necessary to analyze the risk of PTS, including vessel embrittlement and non-destructive testing for material flaws, have been developed and are directly applicable to the Westinghouse AP600. New thermal hydraulic analysis must be done though, because it is very dependent upon the system of interest. The safety injection for most of the plants previously analyzed occurred within the cold legs. In the APEX facility it occurs within the steam generator lower plenum (PRHR injection) and the reactor pressure vessel. Direct vessel injection (DVI) has already been examined for the Westinghouse two-loop plants and the downcomer behaves very similarly to those previously modeled (2). This leaves the mixing behavior within the cold leg as the only unsettled PTS issue.

2.1 Onset Criteria

It has been repeatedly recognized that a well-mixed cold leg (i.e. non-stratified) is unlikely to lead to a PTS event (3,6,8,12-14,20-23). Theofanous, therefore, generated an onset criteria to quickly determine if a particular combination of loop flow (be it forced or natural circulation) and safety injection flow could potentially be stratified at the cold leg exit. Theofanous pointed out that for the cold leg flow to be well-mixed there must be sufficient loop flow to break up the high pressure safety injection (HPI) plume (or PRHR injection plume in this case) and to produce a stable exit of flow into the downcomer. The boundary of stability is expressed in terms of the local Froude number by:

$$Fr_{CL} = 1 \tag{2.1}$$

which is the degenerate case of the more general condition

$$Fr_1^2 + Fr_2^2 = 1 \tag{2.2}$$

expressing the stationarity of long waves at the interface of two parallel flowing liquid layers of different density (26). These conditions are analogous to flow choking (or flooding) in the sense that the two-layer flow cannot be changed gradually through a state where equation 2.2 applies without leading to a violent disruption of the flow by internal discontinuities (i.e. hydraulic jump).

The condition expressed by equation 2.1 is applied with the total loop flow Q_T defined as:

$$Q_T = Q_{loop} + Q_{HPI} \tag{2.3}$$

at the mixed mean temperature defined by the following equation;

$$T_m = \frac{Q_{loop}}{Q_{loop} + Q_{HPI}} T_{loop} + \frac{Q_{HPI}}{Q_{loop} + Q_{HPI}} T_{HPI} \tag{2.4}$$

equation 2.2 can then be expressed as;

$$\frac{Q_T}{A_{CL}} = \left\{ g D_{CL} \frac{\rho_M - \rho_{loop}}{\rho_M} \right\}^{1/2} \tag{2.5}$$

The density ratio may be approximated by expressing it in terms of the component flows and densities by employing a "average" expansion coefficient;

$$\frac{\rho_M - \rho_{loop}}{\rho_M} \cong \beta_M \left(T_{loop} - T_M \right) \tag{2.6}$$

$$\frac{\rho_{HPI} - \rho_{loop}}{\rho_{HPI}} \cong \bar{\beta}_{HPI}\left(T_{loop} - T_{HPI}\right) \tag{2.7}$$

Combining these approximations with equation 2.4 allows the Froude number condition to be written as;

$$Fr_{HPI,CL} \cong \left\{1 + \frac{Q_{loop}}{Q_{HPI}}\right\}^{-3/2} \left(\frac{\dot{\beta}_M}{\dot{\beta}_{HPI}}\right)^{1/2} \tag{2.8}$$

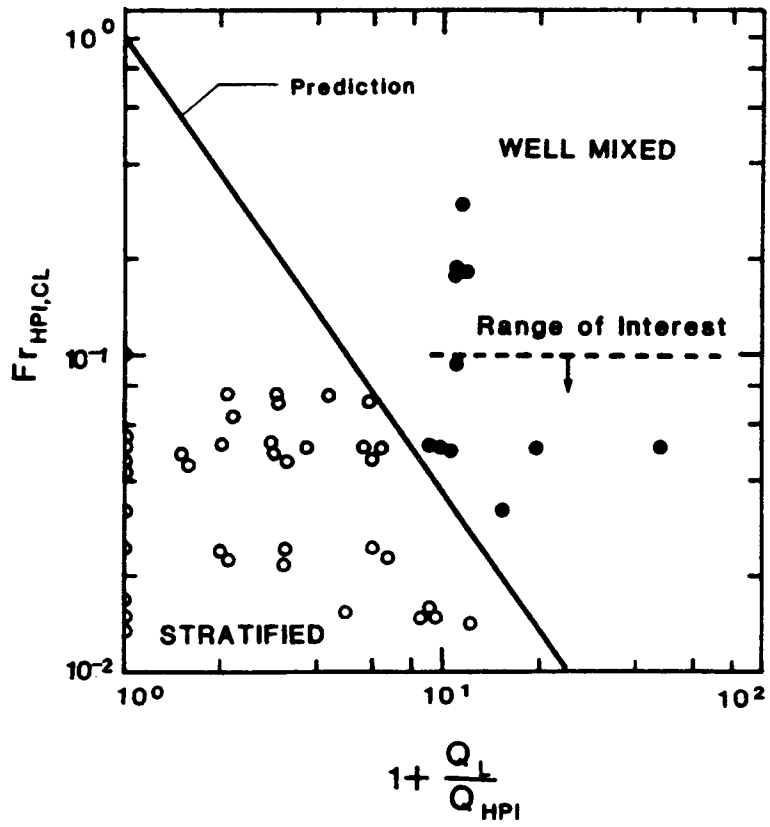

Figure 2-1 - Comparison of theoretical stratification criteria with the CREARE 1/5 scale test results

The effect of β-T non-linearity, as deduced by exact calculations, is to slightly change the flow ratio exponent in the previous equation such that it takes the following form;

$$Fr_{HPI,CL} \cong \left\{1+\frac{Q_{loop}}{Q_{HPI}}\right\}^{-7/5} \tag{2.9}$$

Theofanous compares the stratification/mixing boundaries expressed by these equations to the experimental data collected from the CREARE 1/5 scale mixing facility in Figure 2-1. Excellent agreement is noted. The equations do not predict the degree of stratification. They simply provide a uncomplicated tool for establishing an estimate of loop flow for which stratification can be ignored and a well-mixed condition can be assumed to exist.

2.2 Cold Leg Mixing Models

2.2.1 Well-Mixed Model

The well-mixed model assumes complete mixing between the two streams, loop and HPI. The temperature of this stream can be calculated using equation 2.4. This method is not applicable to a stagnant loop condition (i.e. no loop flow) because the well-mixed assumption ignores the transient cooldown behavior and would predict a cold leg filled entirely with water at the HPI inlet temperature. This condition is far too conservative for accurate, realistic analysis. While at the opposite extreme, a well-mixed cold leg with moderate loop flows may not be conservative enough. It has been observed that small loop flows may not be sufficient to generate complete mixing and stratification may occur. For the stratified case, a cold stream that may be significantly colder than the well-mixed model predicted could fall into the downcomer. This would subject the vessel wall to a cooldown transient much more

severe than anticipated. The well-mixed model is still useful when the onset criteria predicts that the cold leg is well-mixed.

2.2.2 Regional Mixing Model

Theofanous (20-23) recognized that very small loop flows were sufficient to break up any injection plume that might exist therefore generating a well-mixed condition in the cold leg. This led him to create the Regional Mixing Model (RMM) which allowed the quantitative description of thermal stratification in a stagnant loop. Theofanous stated that a counter-current flow condition would form due to incomplete mixing of the HPI plume. The cold HPI plume would entrain some of the hot ambient fluid near the injection point and would therefore take that fluid with it as the stream moved down the cold leg and into the downcomer. To satisfy continuity the hot entrained fluid must be replaced and a counter-current stream of hot fluid from the downcomer forms in the upper cold leg.

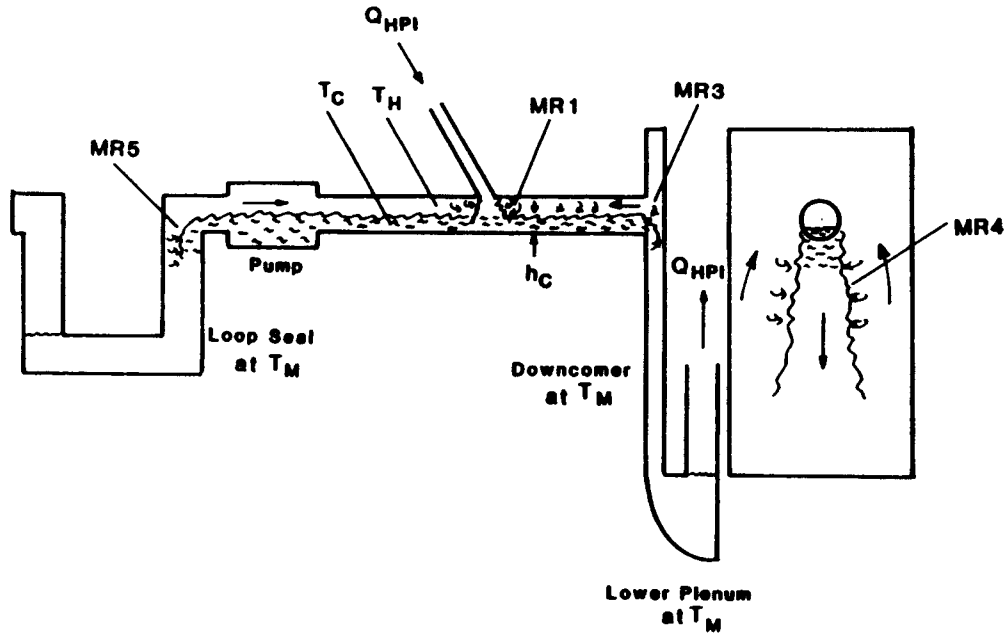

Figure 2-2 - Conceptual definition of the Regional Mixing Model.

To model this behavior Theofanous starts by identifying four mixing regions within the cold leg and downcomer. Figure 2-2 shows a diagram of the cold leg and clarifies the location of these regions. The first mixing region is the injection point of the HPI (MR 1). This is the most significant region for the description of thermal stratification. The second mixing region (which is not noted on the diagram) is the interface between the hot and cold stream. These streams are assumed stable and mixing at this interface is assumed negligible. Mixing regions three (MR 3) and five (MR 5) occur where the cold leg stream transitions from a horizontal flow condition to a falling plume. These conditions occur at the downcomer and loop seal entrances. The fourth mixing region is the planar plume which develops in the downcomer (MR 4).

Due to the large volume of the whole system relative to the HPI flow rate, and except for a short-duration initial transient associated with the establishment of the overall circulation pattern, the temperatures decay slowly compared to the residence time in the cold stream portion of the circuit. The whole process can be viewed as a decay (by mixing-entrainment) of highly buoyant jets and plumes in a slowly varying ambient. That is, the cold layer temperatures are estimated quasi-statically on the basis of the instantaneous "ambient" temperature, which is found as a continuous function of time for the duration of the transient.

This procedure is based on the observation that significant decay of the HPI plume occured right at the point of injection. This yields a relatively small degree of stratification in the horizontal portion of the cold leg. The temperature difference between hot and cold streams is further reduced by mixing in the regions near the entrance to the loop seal and downcomer volumes. Thus, from an overall energy balance point of view these volumes as well as that of the lower plenum are taken as well mixed, at T_M. Taking into account the heat conducted from the metal walls, Q_W, the T_M transient may be found from:

$$\rho V_T C_P \frac{dT_M}{dt} = \dot{Q}_W - Q_{HPI}\rho C_P\left(T_M - T_{HPI}\right) \tag{2.10}$$

$$\dot{Q}_W = \sum_i h_i S_i\left(T_{WS_i} - T_M\right) \tag{2.11}$$

The wall surface temperature, T_{WS}, is found numerically by solving the conduction equation in an appropriate number of metal slabs (corresponding to the vessel and pipe walls and the thermal shield). The local heat transfer coefficient, h_i, is obtained

from an approximate mixed convection correlation or, a rough, constant, and uniform value may be utilized. The stainless steel vessel wall cladding is also taken into account.

The temperature T_M physically exists in the major portions of the loop seal, downcomer, and lower plenum. In the cold leg and pump and in the upper part of the downcomer, however, T_M represents an "average" of the hot and cold stream temperatures, and it can be partitioned by:

$$V^* T_M = V_H T_H + V_C T_C \tag{2.12}$$

$$V^* = V_H + V_C \tag{2.13}$$

V_H includes the volume of the top layer of the cold leg and pump, as well as an upper section of the downcomer, extending two cold leg diameters below the cold leg centerline, which is essentially at the hot stream temperature. As neither the volumes, nor the temperatures of the two streams in the cold leg are known, additional constraints are required to complete the partition.

At the point of injection (MR 1) the cold plume decay depends upon the injection Froude number (Fr_{HPI}) and the length, h_H, of the plume exposed in the hot stratum. A κ-ε-θ' turbulence model was utilized to compute this decay. The results for total plume flow (Q_{HPI} plus entrainment) and mixed mean plume temperature are given in Figure 2-3 and Figure 2-4.

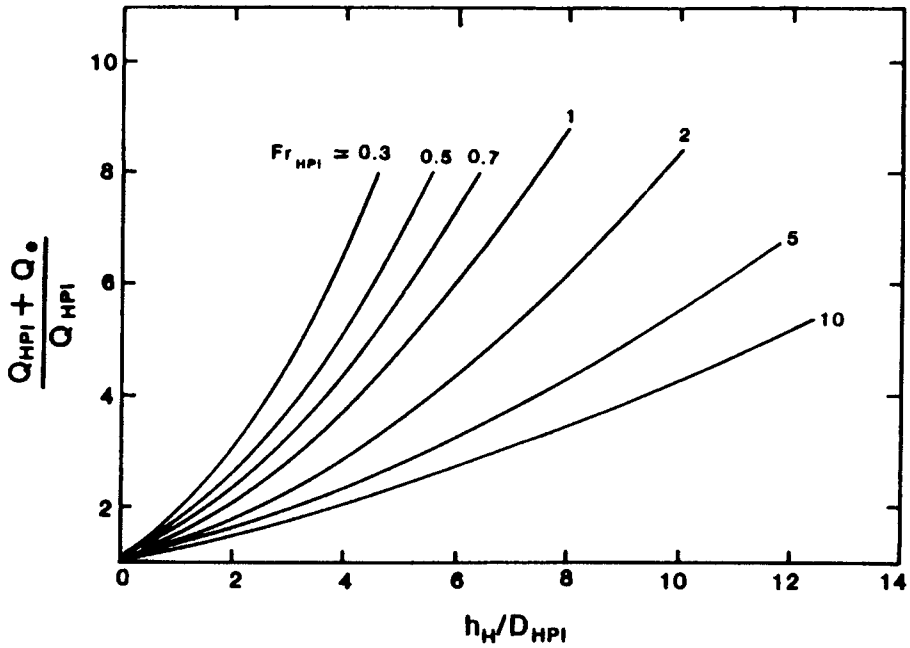

Figure 2-3 - Prediction of total flow in axisymmetric plumes (jets).

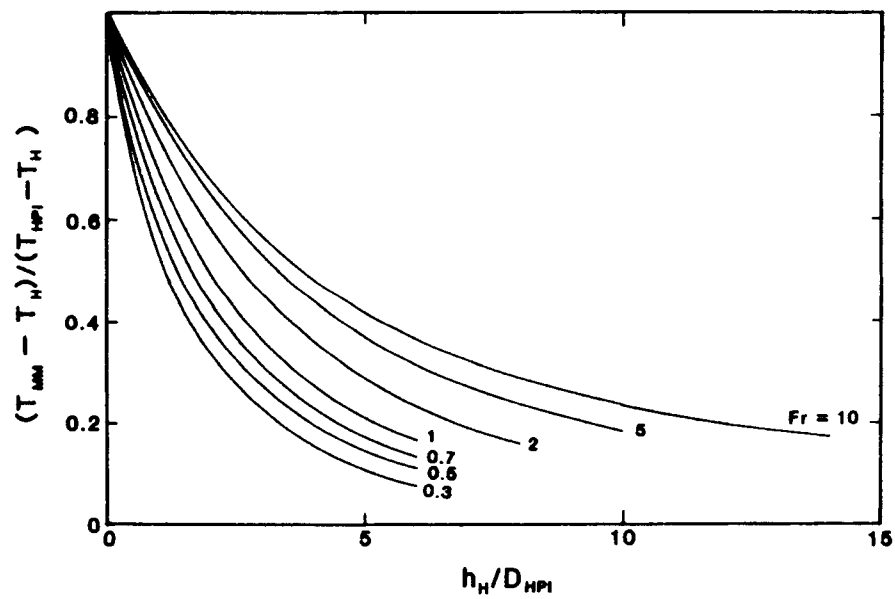

Figure 2-4 - Prediction of mixed mean (radially averaged) temperature for axisymmetric jets (plumes).

In the area of interest these results may be represented by:

$$\frac{Q_e}{Q_{HPI}} = 0.5176\left(\frac{h_H}{D_{HPI}}\right)^{1.236} Fr_{HPI}^{-0.414} \tag{2.14}$$

for: $0.2 < Fr_{HPI} < 1.0$ and $0.5 < h_H/D_{HPI} < 4$

$$\frac{T_{MM} - T_H}{T_{HPI} - T_H} = \left(1 + \frac{Q_e}{Q_{HPI}}\right)^{-1} \tag{2.15}$$

which were utilized, for convenience, in the computations. The stratification in the horizontal travel (MR 2) is stable and any additional mixing is neglected, that is,

$$T_C = T_{MM} \tag{2.16}$$

The essential control of the overall process, that is problem closure, is provided by the counter-current flow condition at the two ends of the cold leg, i.e. the cold stream will accelerate until it reaches a value consistent with plume decay and hot stream entrainment requirements as expressed by the condition of stationarity of long waves (equation 2.2). The algebra for circular cross sections was carried out by Gardener (9) in connection with a different application, and the result indicates a Froude number definition with a length scale expressed as the ratio of the stream cross sectional area and the width, W, of contact between the two streams, i.e.,

$$\frac{\left(Q_C/A_C\right)^2}{g\frac{A_C}{W}\frac{\rho_C - \rho_H}{\rho_C}} + \frac{\left(Q_H/A_H\right)^2}{g\frac{A_H}{W}\frac{\rho_C - \rho_H}{\rho_H}} = 1 \tag{2.17}$$

The flow areas may be expressed in terms of the stream height, h_C, h_H, by:

$$A_C = (\pi - \alpha)\frac{D_{CL}^{\,2}}{4} + (0.5 \cdot D_{CL} - h_H)h_H^{1/2}(D_{CL} - h_H)^{1/2} \quad \text{for } h_C > \frac{D_{CL}}{2} \qquad (2.18)$$

where,

$$\alpha = \arctan\left\{h_H^{1/2}(D_{CL} - h_H)^{1/2} \Big/ (0.5 \cdot D_{CL} - h_H)\right\}$$

and:

$$A_C = \alpha\frac{D_{CL}^{\,2}}{4} - (0.5 \cdot D_{CL} - h_C)h_C^{1/2}(D_{CL} - h_C)^{1/2} \quad \text{for } h_C < \frac{D_{CL}}{2} \qquad (2.19)$$

where,

$$\alpha = \arctan\left\{h_C^{1/2}(D_{CL} - h_C)^{1/2} \Big/ (0.5 \cdot D_{CL} - h_C)\right\}$$

while,

$$A_{CL} = A_C + A_H \text{ and } D_{CL} = h_H + h_C \qquad (2.20)$$

In the calculations presented here we apply equation 2.17 at the vessel junction of the cold leg. To make up for this simplification we assume symmetry, i.e. equal amounts of HPI plume entrainment, Q_e obtained from each side of the cold leg. Thus for the left-hand portion of the cold leg the hot streams will each move at a rate of ½ Q_e while mass conservation on the right-hand portion requires that:

$$Q_H = \frac{1}{2}Q_e \qquad (2.21)$$

$$Q_C = Q_{HPI} + \frac{1}{2}Q_e \qquad (2.22)$$

Equations 2.12 to 2.22 are solved by iteration with the help of the equation of state, $\rho=\rho(T)$. For each time of interest, T_M is obtained from equations 2.10 and 2.11, values of T_H and h_H are guessed and updated until all the equations, in particular the conditions expressed by equations 2.12 and 2.17, are satisfied. The temperatures in the downcomer may be estimated on the basis of the temperature transient of the cold stream spilling over the cold leg. Visualization experiments indicate that within ~ 1 cold leg diameter the flow is highly three dimensional with a tendency of the plume to descend closer to the core-side of the downcomer width. From the point of view of fluid temperature in the vicinity of the vessel wall this behavior may be closely bounded by considering two extreme cases: (a) the plume is totally contained between the core barrel and thermal shield (if present), and the temperature along the vessel wall is nearly uniform and given by T_M, (that is, it descends as a planar plume, with an initial width obtained, by continuity, from the flow in the cold stream) and decays by entrainment from its sides. The centerline (minimum) temperature of such a plume is estimated from the results of the turbulence mixing model shown in Figure 2-5.

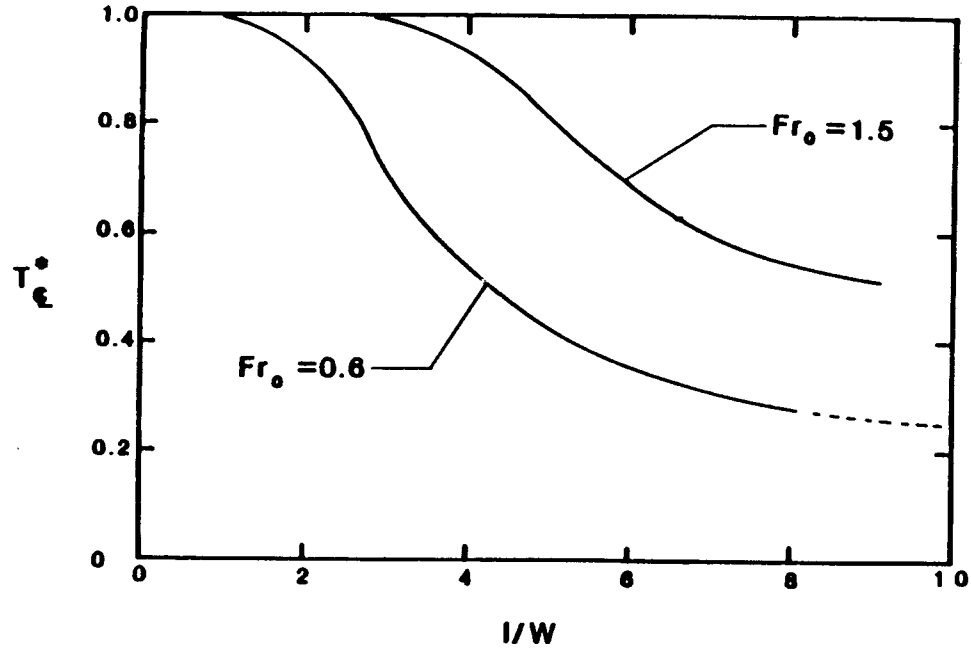

Figure 2-5 - Prediction of centerline temperature in planar plumes, as function of axial position. Fr_0 is based on the plume width and velocity at the entrance to the downcomer

The whole computation has been automated in a user-convenient form in the code REMIX (for REgional MIXing model). The code was then applied to several experimental facilities and excellent agreement was obtained.

2.3 Three-Dimensional Computer Codes

The mixing behavior of the cold legs were also modeled using a computer program called COMMIX (3,4,7,8). COMMIX is a general purpose, three-dimensional single-phase steady-state/transient computer program for thermal hydraulic analysis of single and multi-component systems which uses the new porous media formulation. The program was originally developed by Argonne National

Laboratory for analyzing liquid metal fast breeder reactors (LMFBR), but was easily adapted to PWR analysis. The program solves the conservation of mass, momentum and energy equations as boundary value problems and as initial-value problems in time. Early versions of the code however did not include a true turbulence model. Turbulence was simulated using a global constant input value for the effective turbulent viscosity and thermal conductivity.

The code was applied to the mixing problem within the cold leg and was checked against data from experimental facilities. Even though the results appeared to coincide with the experimental data, the lack of a turbulence model became an issue. Any mixing behavior that the program predicted was attributed to numerical diffusion. At this point the authors responded by adding several turbulence models to the program, the highest order of which was the κ-ε turbulence model. The authors then once again compared the code results to data from the experimental facilities and found good agreement.

The objective of this work was to analyze the thermal hydraulic behavior of the OSU APEX facility cold legs during the high pressure stages of a LOCA. Several approaches have been documented for currently operating reactor designs. The well-mixed model is simply not conservative enough and is therefore not considered. The RMM could potentially be adapted to describe the OSU APEX system, but calculation of Q_e would require the generation of entrainment functions that would describe mixing at several locations, including the mixing occurring at the PRHR injection point, the mixing that occurs as the cold stream falls into the reactor coolant pump chamber and the mixing that occurs as the flow goes from a falling condition

back to horizontal. Modeling of this mixing becomes very difficult and may not be possible without the generation of empirical data gathered from geometry specific tests. The application of three-dimensional computer codes therefore appears necessary. Many computational fluid dynamics (CFD) codes are available "off-the-shelf". The function of all of these programs is fundamentally the same. Each program is equipped with subtle differences in the correlations they employ and the interface that the user encounters. For the purposes of this work CFX4.1 by AEA Technologies has been selected.

3. DESCRIPTION OF FACILITIES

3.1 GENERAL DESCRIPTION

The OSU APEX Test Facility (1) is a one-fourth height, one-half time scale, reduced pressure integral systems test facility. It accurately models the details of the AP600 geometry including the primary system, the passive safety systems, and parts of the non-safety grade chemical and volume control systems (CVCS) and residual natural circulation system (RNCS). The interconnecting pipe routings are also duplicated in the model.

All of the primary system components are fabricated of stainless steel and are capable of prolonged operation at 400 psia and saturation conditions.

3.1.1 Primary System

The APEX primary system includes the following components:

- A *Reactor Pressure Vessel (RPV)* that models the upper and lower reactor internals, the core barrel, the downcomer, and the core. Connections for the hot and cold legs and DVI lines are provided. The RPV houses 48 electric heater rods each having a 1 inch (2.54 cm) diameter and a heated length of 36 inches (91.44 cm). The maximum core power is 600 kW.
- *Reactor coolant loop piping* that models two primary loops, each consisting of one hot leg and two cold legs. Break spool pieces have been installed on the hot and cold legs, the Direct Vessel Injection (DVI) line, and the Core Makeup Tank Pressure Balance Line (CMT-PBL) to simulate

pipe breaks. The discharge from these valves vent to the Break and Automatic Depressurization System (ADS) Measurement System (BAMS) to separate and measure break flow rates.

- Two Steam Generators (*SGs*), one on each loop, each having tube and shell dimensions scaled to simulate a Westinghouse Delta-75 SG.
- Four Reactor Coolant Pumps (*RCPs*), two attached to the lower channel head of each SG.
- A *Pressurizer* with internal heaters capable of controlling pressure and minimizing pressure spikes in the Reactor Coolant System (RCS).

3.1.2 Passive Safety System

The APEX facility includes the following passive safety systems:

- Two Core Makeup Tanks (*CMTs*) each having a pressure balance line that connects the CMT head to the cold leg. Each CMT also has an injection line that permits draining of the CMT into one of two DVI lines connected to the reactor downcomer. Check valves and isolation valves have been included.
- An *ADS* that includes three valves off the top of the pressurizer. The flow from ADS 1-3 is directed to a sparger that vents directly into the In-Containment Water Storage Tank (IRWST). The ADS 1-3 flow nozzles are sized to represent two-trains of ADS 1-3 in the AP600. Fourth stage ADS is modeled by a single valve located off the top of each hot leg. The ADS 4 flow nozzles are sized to model two trains of ADS 4 on each hot leg in

the AP600. Failure of the ADS 1-4 valves can be simulated by installing different flow nozzles.

- Two *Accumulators* pressurized with nitrogen to provide safety injection during depressurization events. Each accumulator has an injection line that connects to one of two DVI lines. Check valves and isolation valves have been included.
- An *IRWST* having two injection lines that connect to each DVI line. The IRWST is capable of being pressurized to 80 psia (0.55 MPa) to simulate containment backpressure. Return lines to the DVI lines are provided to represent containment sump recirculation lines.
- A Passive Residual Heat Removal *(PRHR)* heat exchanger located inside the IRWST. The PRHR is driven by natural circulation. It draws liquid from one hot leg, rejects heat to the IRWST liquid, and returns cooled liquid into the lower channel head of one SG.

Figure 3-1 and Figure 3-2 present schematics of the APEX Test Facility.

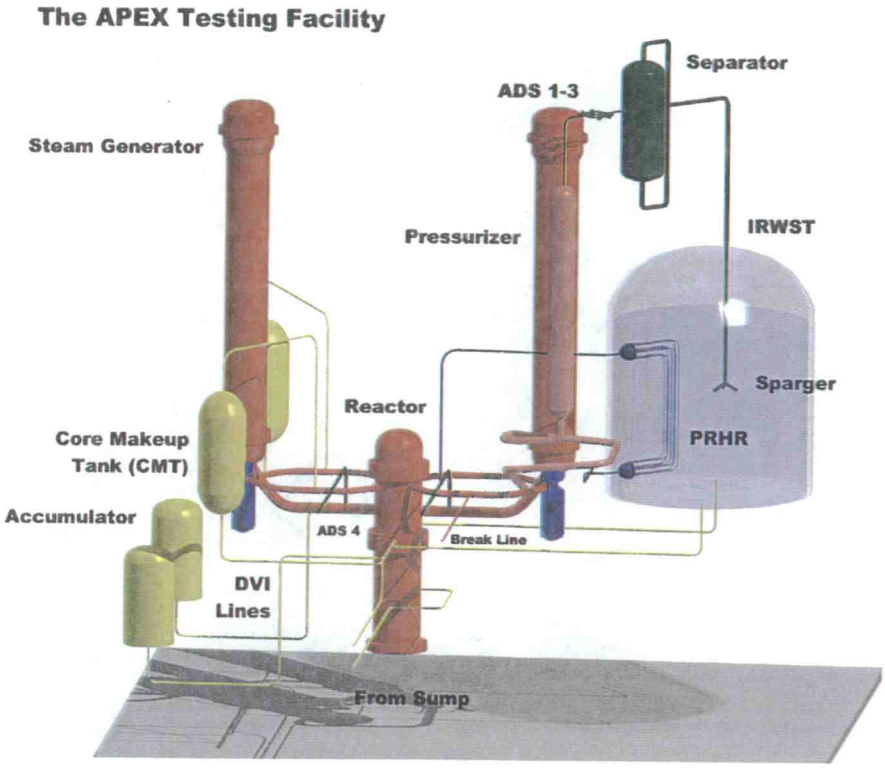

Figure 3-1 - Layout of the OSU APEX facility

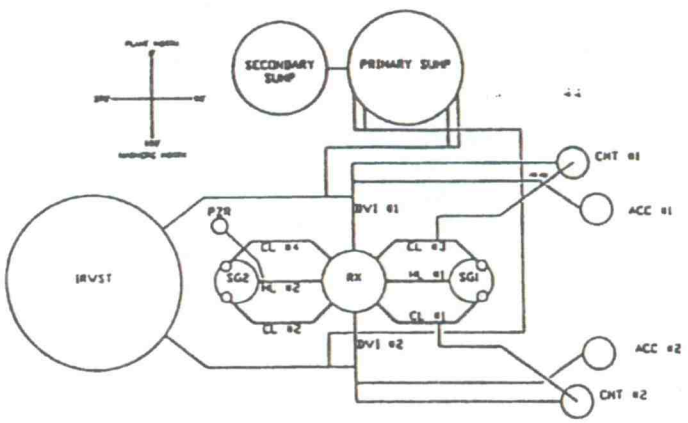

Figure 3-2 - Line diagram of OSU APEX facility

3.1.3 Break and ADS Measurement System

The BAMS is used to measure two-phase flows from breaks and the ADS measurement system. The two-phase flow is directed to a separator where the flow is separated into liquid and vapor. The liquid flow is measured and directed to the appropriate tank (IRWST or Primary Sump). The vapor flow is measured and vented from the test facility. Vapor flow from ADS 1-3 is directed into the IRWST. Electrical strip heaters are used to maintain boundary conditions at approximately 200 F (93.3 C). The system is capable of being pressurized to 80 psia (0.55 MPA) to simulate containment backpressure.

The BAMS contains the following components:

- The *Primary and Secondary Sumps* - Simulate the containment compartment volumes below the normal floodup elevation. The Primary and Secondary Sumps are connected with a line at a level simulating the curb overflow level in the AP600. The liquid overflow from the IRWST is also collected in the Secondary Sump. Both tanks are capable of being pressurized to 80 psia (0.55 MPA) to simulate containment backpressure. Return lines to the DVI are connected to the Primary Sump to represent the containment sump recirculation lines.
- *Four Moisture Separators* - Three ADS separators and one break separator sized based on maximum expected flowrates. Separation is primarily accomplished by the use of gravity and a swirl vane moisture separator element. Each separator is provided with a loop seal line on the liquid discharge to ensure vapor flow does not bypass the separator.

- *Containment Sump Return System* - Heated water from a hold-up tank is pumped into the Primary Sump and the IRWST at a mass flow rate equivalent to the mass flow rate of the vented steam. This heated liquid simulates the flow of condensate from the steam vented into the containment building. This steam would be condensed and would drain into the IRWST or the containment (primary) sump.

3.1.4 Instrumentation

APEX includes the following types of instruments:

- *Thermocouples (TF/TFM/TH/TW)* are used to measure fluid temperatures. They are also used to measure the temperature distribution in the CMT walls and core heater rods. Premium grade thermocouples have been used and connected to the DAS through controlled purity thermocouple wire.
- *Magnetic Flowmeters (FMM)* are used to measure all single-phase liquid flow rates.
- *Pressure Transducers (PT)* are used to measure the static pressures within the various tanks and piping.
- *Differential Pressure (DP)* transducers are used to measure liquid levels in various tanks and piping. They are also used to determine pressure drops.
- *Vortex Flowmeters (FVM)* are used to measure all steam flow rates.
- *Heat Flux Meters (HFM)* are used to measure heat loss from individual tanks and components.
- *Heated Phase Switches (HPS)* are used to determine the fluid phase at various points inside system piping. Each HPS measures: 1) fluid

temperature, 2) temperature difference between the fluid and the heater, and 3) a relative heat transfer coefficient.

- *Load Cells (LC)* are used to measure the weight of liquid inside the IRWST, the Primary Sump, and the Secondary Sump.

Ambient air temperature and barometric pressure are also recorded. All of the instruments are monitored and recorded by the DAS. Additionally, a sequence-of-events program is used to monitor various pumps and valves in the test facility.

3.2 DETAILED DESCRIPTION OF CRITICAL COMPONENTS

3.2.1 Critical Components

A small group of reactor components have a particularly strong influence on the behavior and condition of fluid within the cold leg. These components include the cold legs, downcomer, the core make-up tank pressure balance lines (CMT-PBLs), the PRHR system and the steam generators. A brief description of these components, their interaction and their function follows.

The purpose of the cold legs during normal operation is to return cooled water from the steam generator to the reactor. There are four cold legs in the reactor. Two cold legs serve each of the steam generators. The cold legs are horizontal and attach to the reactor coolant pumps directly below the steam generators. Unlike previous Westinghouse designed reactors, the cold legs do not have a loop seal. For safety

system purposes the plant can be divided into two distinct halves; the CMT side and the PRHR side. The CMT side of the facility consists of steam generator #1 and cold legs #1 and #3. The CMT-PBLs are attached to cold legs #1 and #3. The PRHR side of the facility consists of steam generator #2 and cold legs #2 and #4. The cold PRHR flow is injected into the lower plenum of steam generator #2 from which it can propagate into the downcomer.

The purpose of the CMT-PBL is to provide a balancing force and a refill route so that the CMTs can drain into the reactor due to buoyancy forces. Initially the CMT is filled with water at the ambient containment temperature and is isolated from the reactor primary system. When a LOCA occurs, the safety systems are actuated and this isolation is broken. The high density cold water falls into the reactor. As the CMT injection begins, the cold injected fluid is replaced by hot fluid rising up from the cold leg through the CMT-PBL. The replacement fluid is much warmer than the initial CMT fluid so the recirculation slows substantially as the LOCA progresses. Eventually the recirculatory flow stops altogether when a vapor bubble forms at the top of the CMT-PBL and a flow path between the cold leg and CMT no longer exists. At this time the CMT begins to empty rapidly.

The PRHR system is designed to remove the decay heat generated by the reactor fuel rods. The PRHR takes water from the hot leg and injects it into the base of steam generator #2. Prior to being injected, the water is cooled by passing it through a heat exchanger within the IRWST. The PRHR injection stream is injected vertically upward into the lower plenum of the steam generator and forms a mixing plume. The PRHR flow and the fluid it entrains during mixing has a higher density

than both the ambient downcomer and cold leg fluid density. The lower plenum therefore drains into the downcomer through the cold leg. As the steam generator liquid volume decreases, the bulk fluid temperature in the lower plenum becomes more affected by the PRHR injection stream and the cold leg temperature decreases. Once this stream reaches the downcomer a falling plume forms and the PRHR flow is once more diluted as it mixes with the ambient downcomer fluid.

3.2.2 Critical Instruments

Some key instruments have been identified and are described in greater detail here. These instruments include level differential pressure (LDP) transducers and thermocouples on components closely related to the cold leg and its behavior. The DAS collects measurements from the instruments at approximately every 8 seconds at the normal scanning rate and every 1 sec in burst mode

Two rakes of thermocouples provide the instrumentation necessary to evaluate the occurrence of thermal stratification. Each rake consists of six thermocouples located at the elevations shown in Figure 3-3. Rake 1 is located in cold leg #3 on the CMT side of the facility and rake 2 is located in cold leg #4 on the PRHR side of the facility.

There are thermocouples dispersed throughout the downcomer at varying elevations and radial positions. These thermocouples provide an estimation of the vertical temperature profile in the reactor downcomer, steam generators, PRHR and CMTs. Figure 3-4 is a diagram describing the relative locations of the thermocouples

in the downcomer and cold legs. The thermocouple radial position in the downcomer is also listed.

Level differential pressure sensors are also installed in the downcomer, steam generators, CMTs, CMT-PBLs and cold legs. A diagram of the pressure taps into the downcomer is given in Figure 3-5.

Additional diagrams showing the locations of both thermocouples and LDPs in the CMTs (Figure 3-7 and Figure 3-8) and steam generators (Figure 3-6) are also provided.

The volumetric flow rate of the PRHR liquid into the SG is also measured.

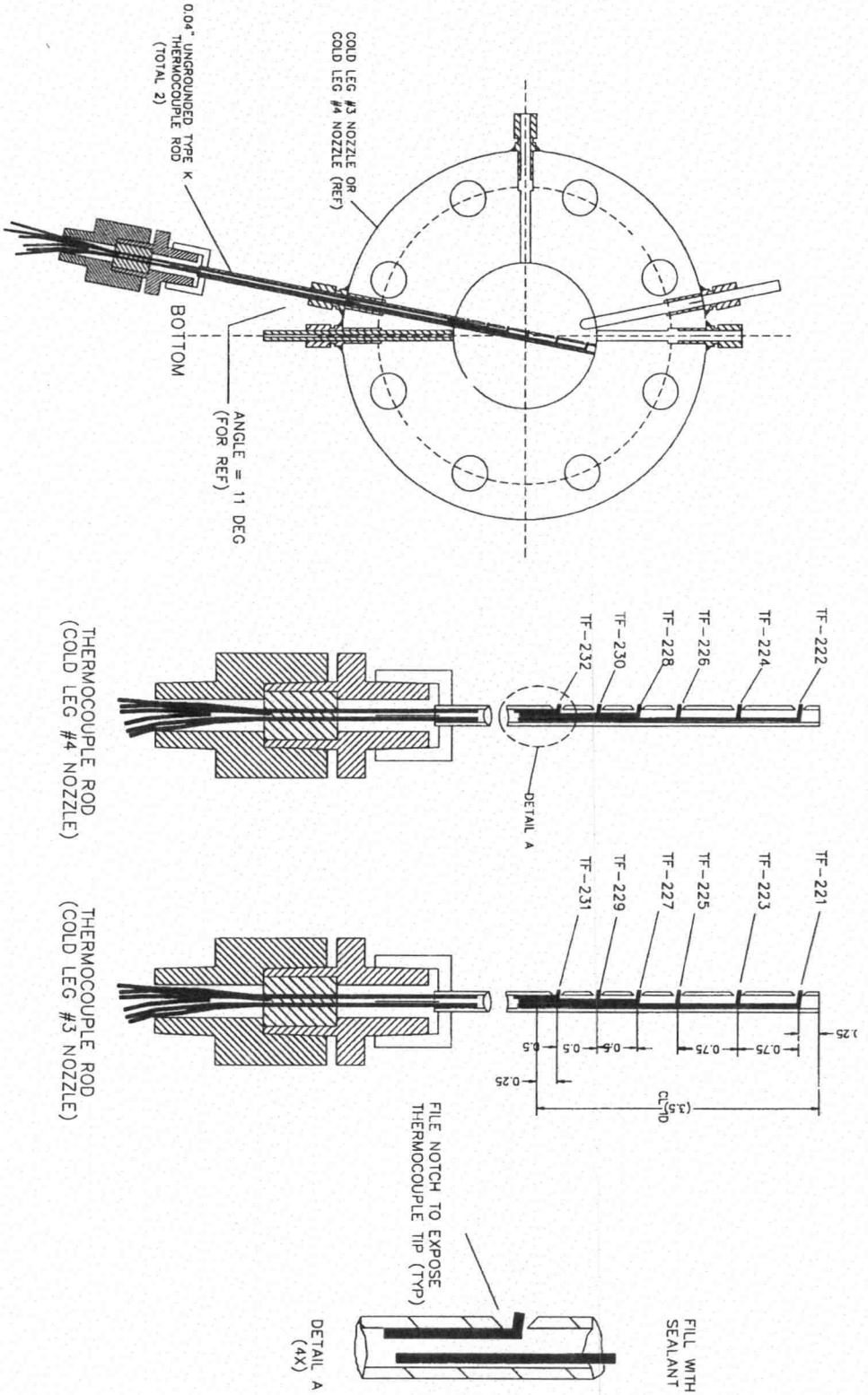

Figure 3-3 - Cold leg thermocouple rake description.

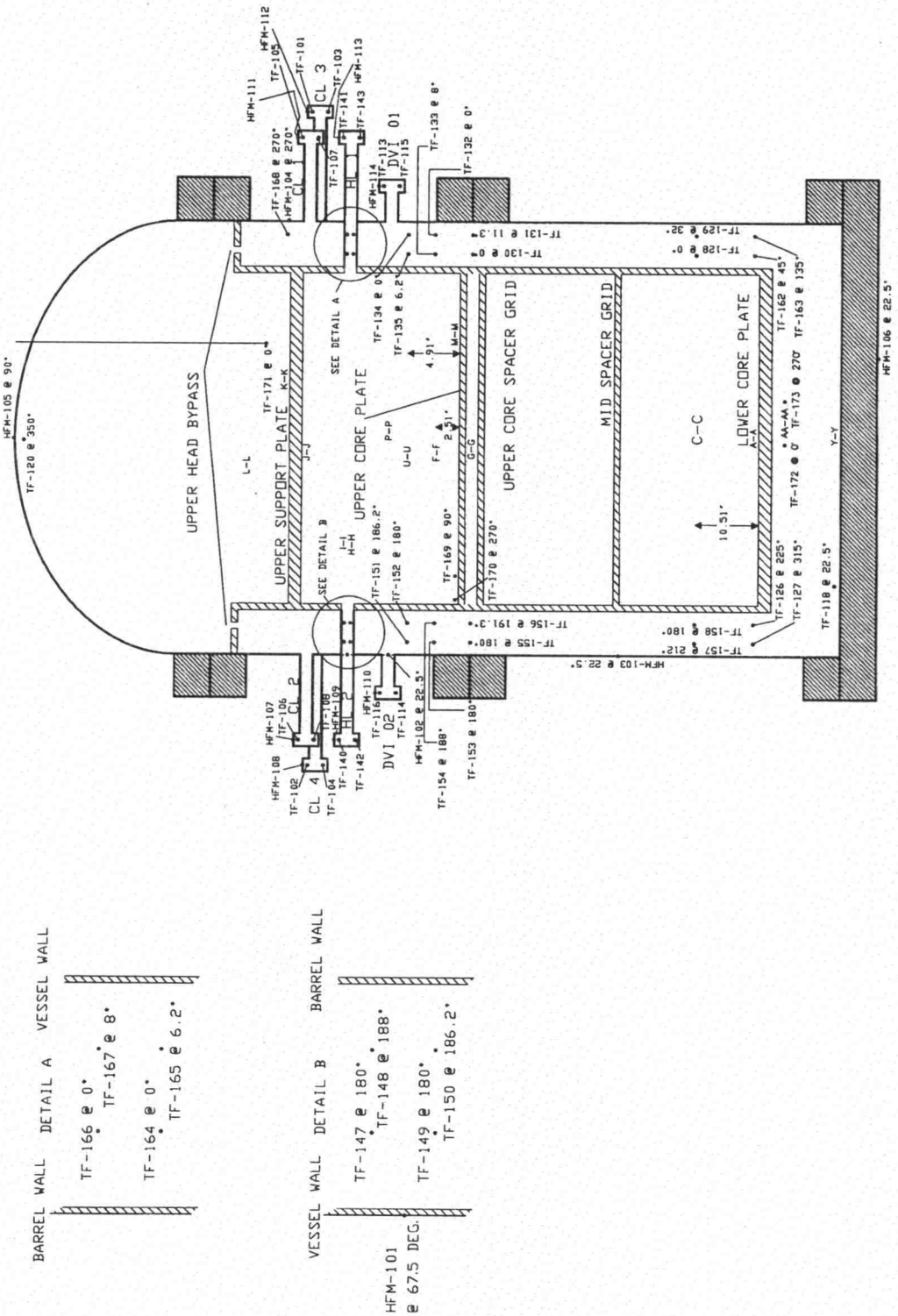

Figure 3-4 - Thermocouple instrumentation diagram for the reactor pressure vessel.

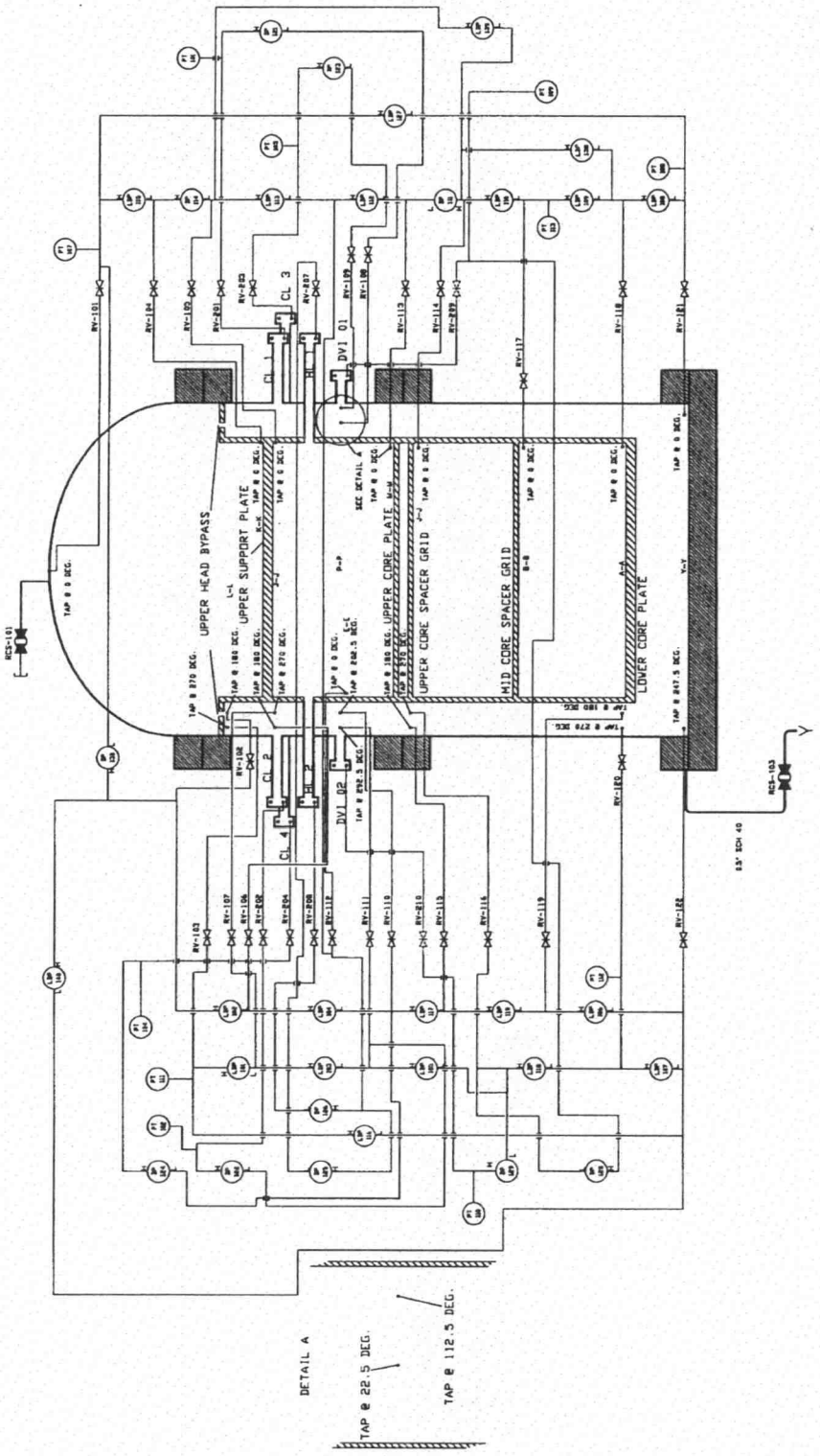

Figure 3-5 - Level differential pressure transducer location diagram for the reactor pressure vessel.

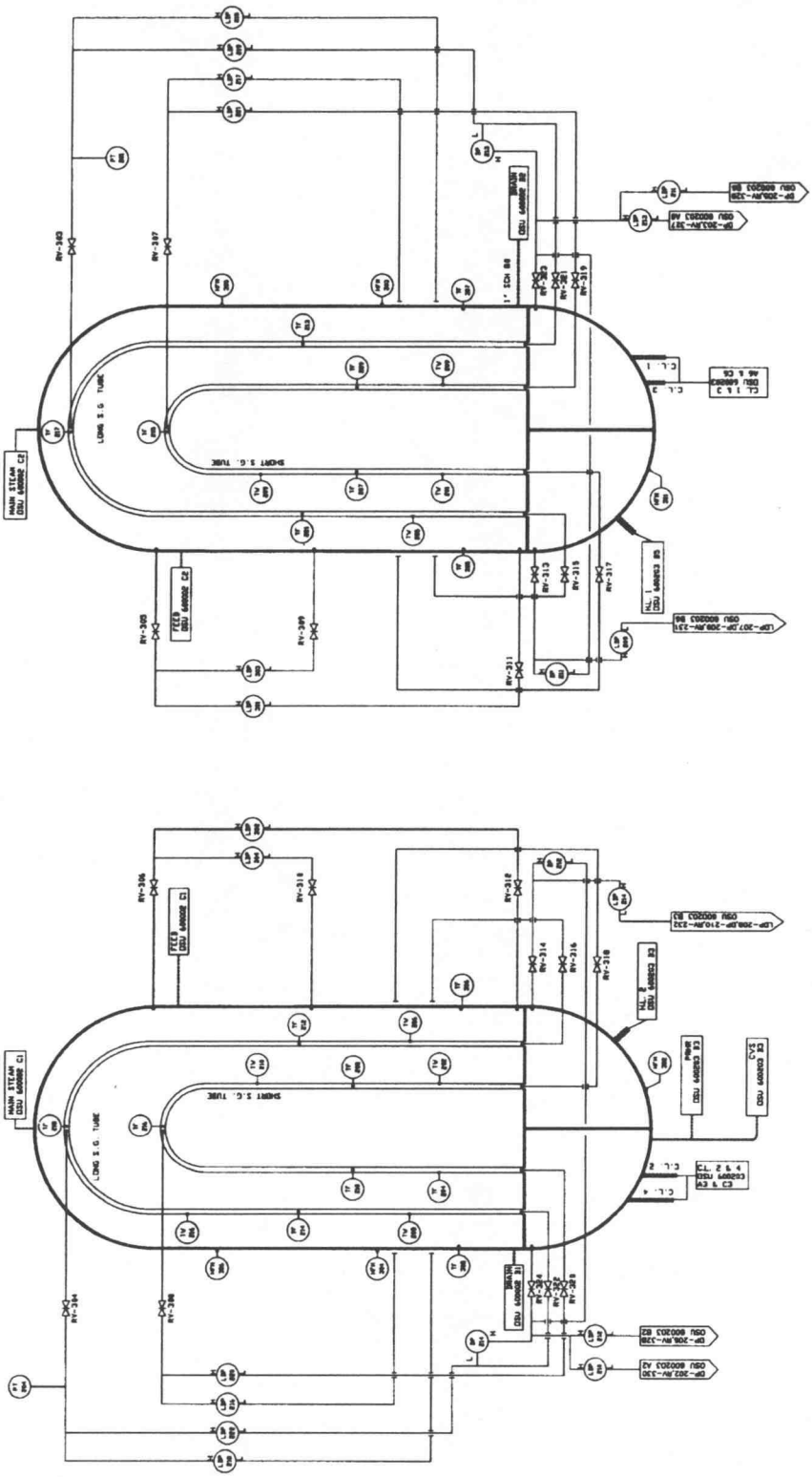

Figure 3-6 - Steam generator instrumentation diagram.

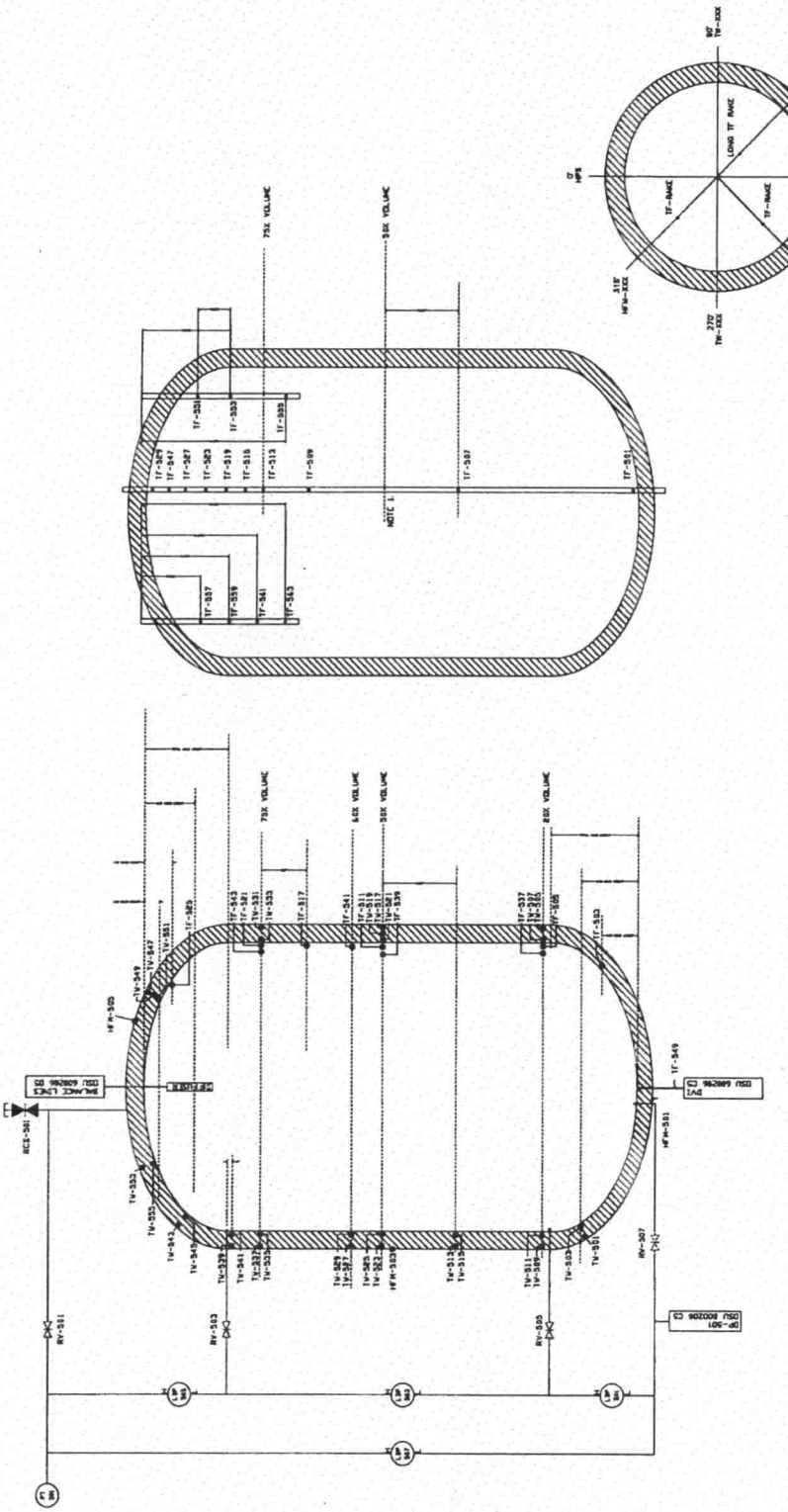

Figure 3-7 - Instrumentation diagram for core make-up tank #1 (CMT #1).

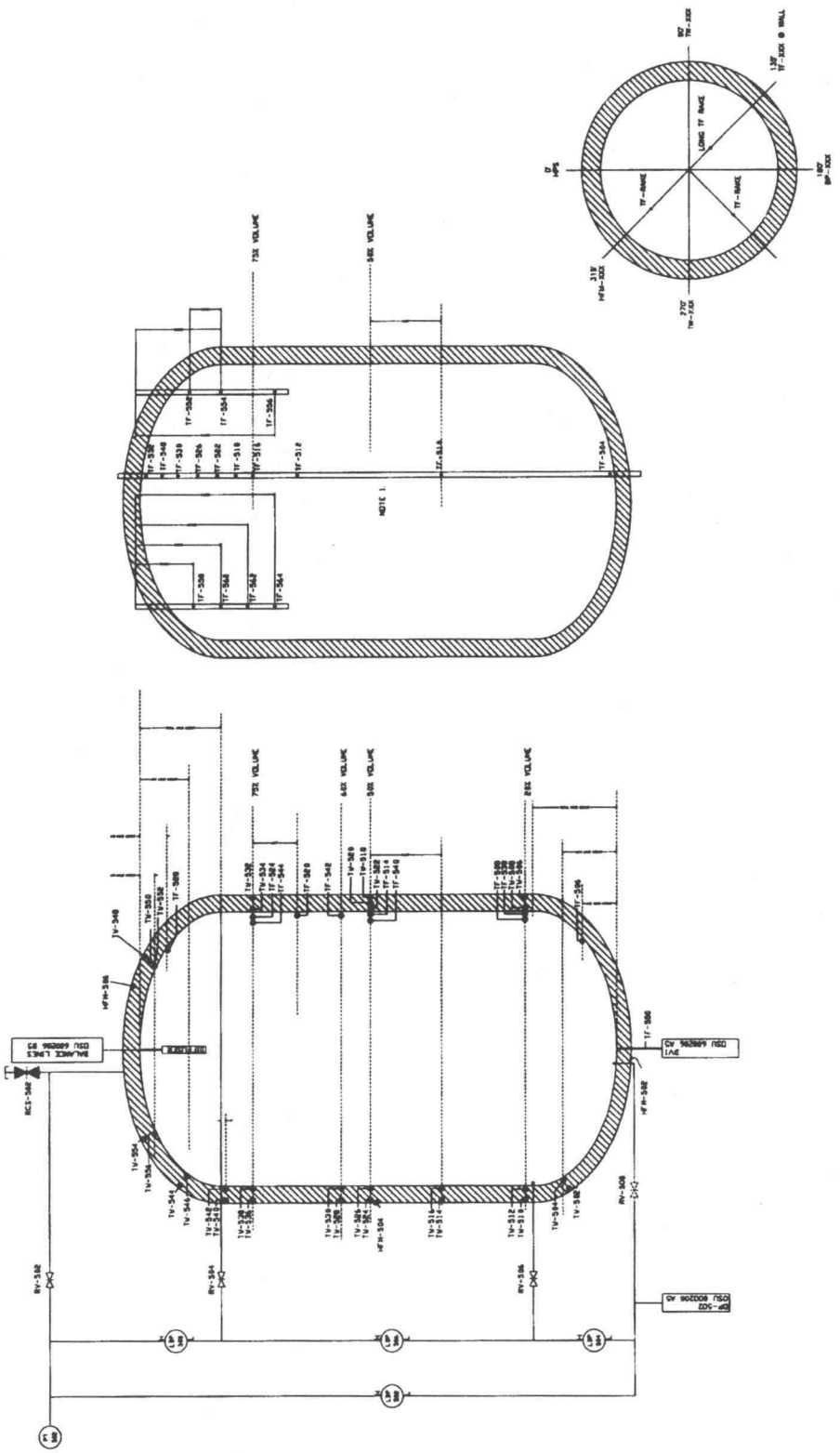

Figure 3-8 - Instrumentation diagram for core make-up tank #2 (CMT-2)

4. DESCRIPTION OF PHENOMENA

The essential difference between the AP600 (and therefore the APEX facility) and other common reactors currently available lies in the safety systems that have been employed to mitigate loss of coolant accidents (LOCAs). The OSU APEX facility has been constructed to perform tests on the AP600 system's LOCA response. This plant is designed to initiate a regular, repeatable safety sequence in response to a LOCA. The objective of this sequence is to depressurize the reactor primary system and to bring the system into a state of natural circulation that provides enough cooling to dissipate the decay heat of the core without resulting in a breach of containment.

4.1 Test Evolution

Prior to the start of a test, the OSU APEX facility was run at a steady state condition representative of normal operation. To initiate the test, the break valve at the cold leg (normally at the bottom of cold leg #3) is opened and an "S" signal is generated which trips the reactor coolant pump (RCPs) and opens the CMT-PBL, CMT injection, and the PRHR heat exchanger isolation valves. Figure 4-1 shows the pressure history of the pressurizer. The standard sequence-of-events for a LOCA test in the APEX facility can be categorized into a subcooled blowdown phase, natural circulation phase, ADS operation, IRWST injection phase and sump recirculation phase. A thorough description of each phase follows.

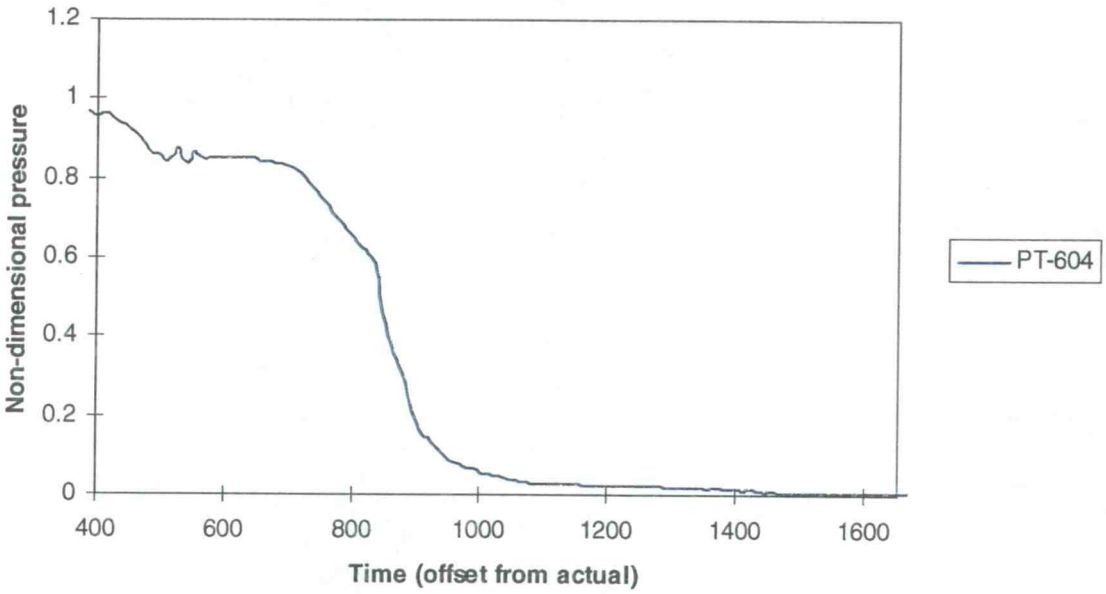

Figure 4-1 - Pressurizer pressure.

4.1.1 Subcooled Blowdown Phase

This phase is distinguished by a rapid depressurization of the primary system due to the flow of subcooled liquid out of the break. The subcooled blowdown phase begins immediately upon opening the break and ends when the break reaches saturation conditions which corresponds to the secondary side pressure. The duration of this phase for the two-inch break case is relatively short. During this phase, subcooled, buoyancy driven circulation is established in the CMT-PBLs and PRHR loops immediately after opening their respective isolation valves. This is illustrated in Figure 4-2 and Figure 4-3.

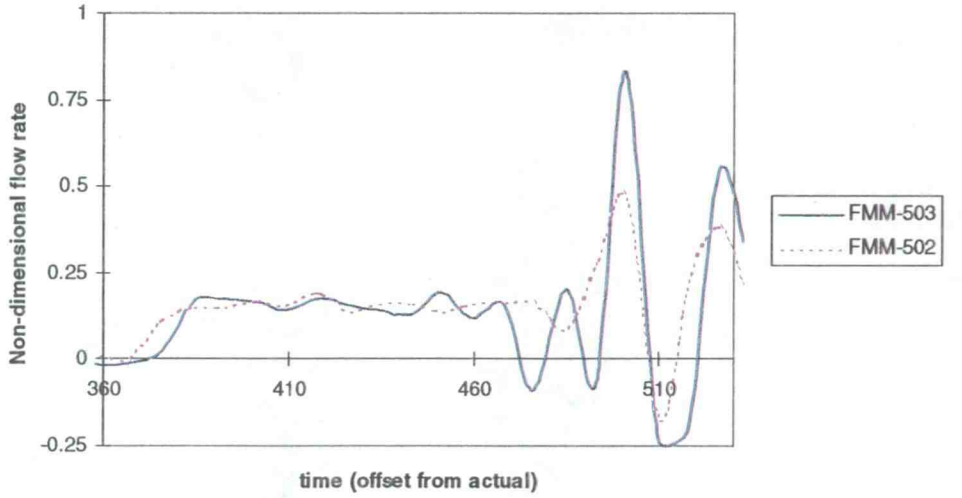

Figure 4-2 - CMT-PBL recirculation flow. FMM-503 is attached to the cold leg containing the break.

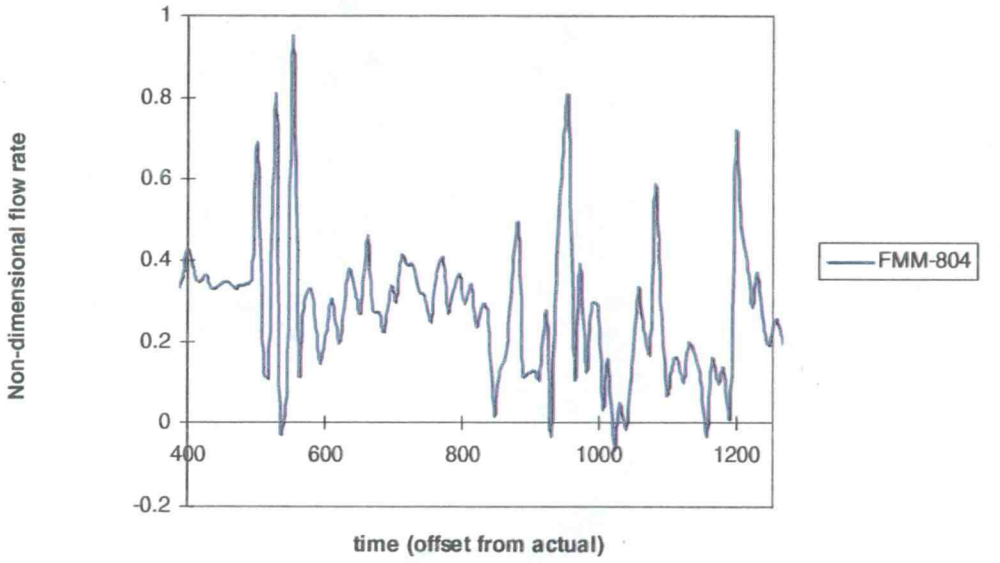

Figure 4-3 - PRHR recirculation flow.

4.1.2 Natural Circulation Phase

Upon reaching saturation conditions at the break, the primary system pressure remained relatively constant and saturated natural circulation was established in the primary, the CMT-PBLs and the PRHR loops. Cold liquid from each CMT was gradually replaced by hot liquid entering the CMT through the CMT-PBLs. The cold liquid leaving the CMTs passes through the CMT injection lines, the DVI line, and into the reactor pressure vessel (RPV) downcomer. For the CMT1-PBL the duration of the recirculation mode was 120 seconds while for CMT2-PBL, it was 160 seconds. During this phase, the CMTs were full of liquid. The water in the CMTs gradually warmed as it was replaced by the circulating hot water from the CMT-PBLs. This resulted in a gradual decrease in the buoyant head (i.e., decrease in recirculation flow rate) and the development of a thermal layer at the upper portion of the CMTs. With continuous depressurization, the hot water in the thermal layer flashed into steam after reaching the saturation temperature as shown in Figure 7. This interrupted the flow through the CMT-PBLs. Upon interruption of the liquid natural circulation path, CMT 1 started to drain, followed shortly by CMT 2.

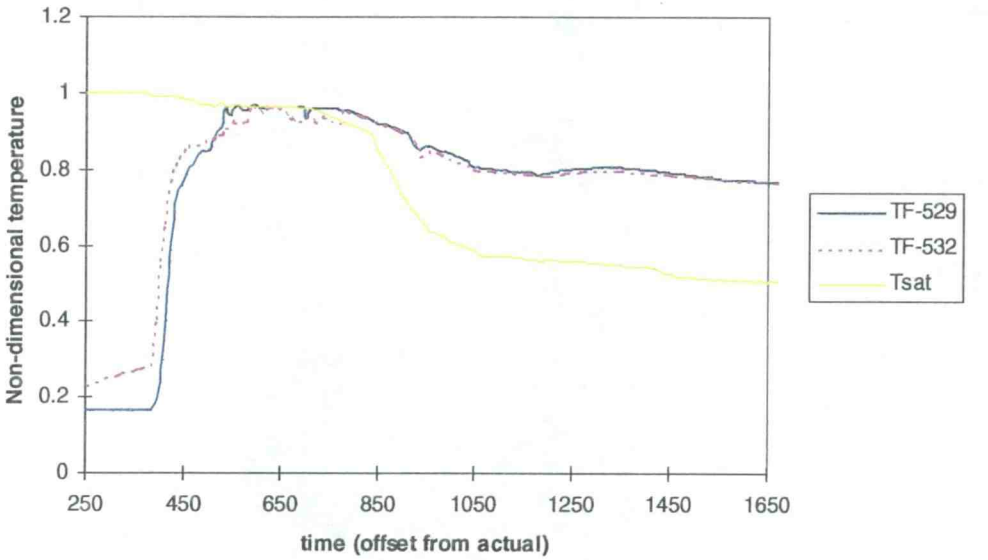

Figure 4-4 - Fluid temperature in the CMT heads.

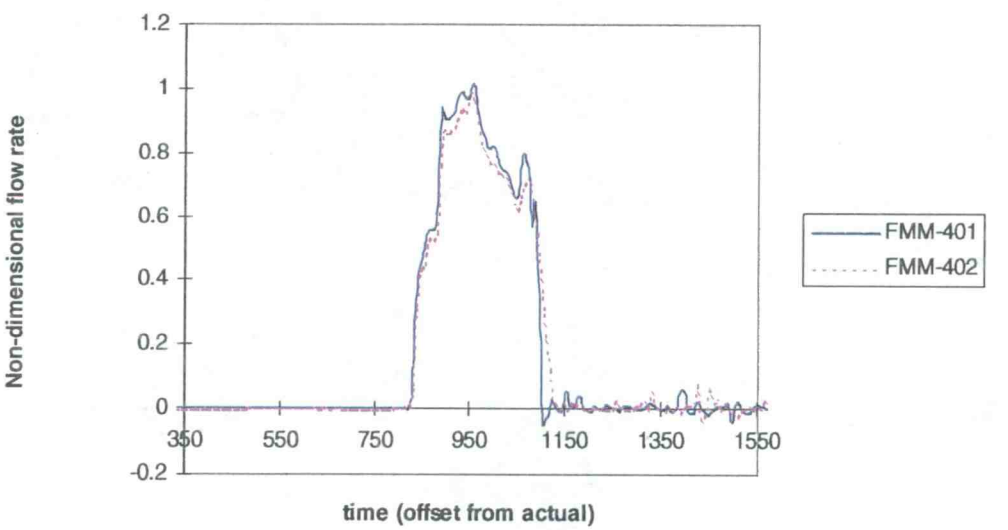

Figure 4-5 - Accumulator 1 and 2 injection flow rates.

4.1.3 ADS Operation Phase

This phase started when the liquid level in CMT 1 dropped to 60% of full at time equal to 820 seconds and ended when the system pressure reached the IRWST injection pressure at time equal to 1625 seconds. Upon opening ADS 1, at time equal to 840 seconds, the primary system pressure dropped below 65% of the initial pressure, leading to accumulator injection. Accumulator injection essentially halted CMT draining. The ADS 2 valve was opened at approximately 890 seconds (i.e., one minute after the actuation of the ADS actuation signal). The ADS 3 valve, (with flow area rescaled for property similitude) was opened at approximately 950 seconds causing further depressurization and leading to the emptying of the ACCs at approximately 1100 seconds. This is shown in Figure 4-5. After emptying the ACCs, the injection from the CMTs was resumed.

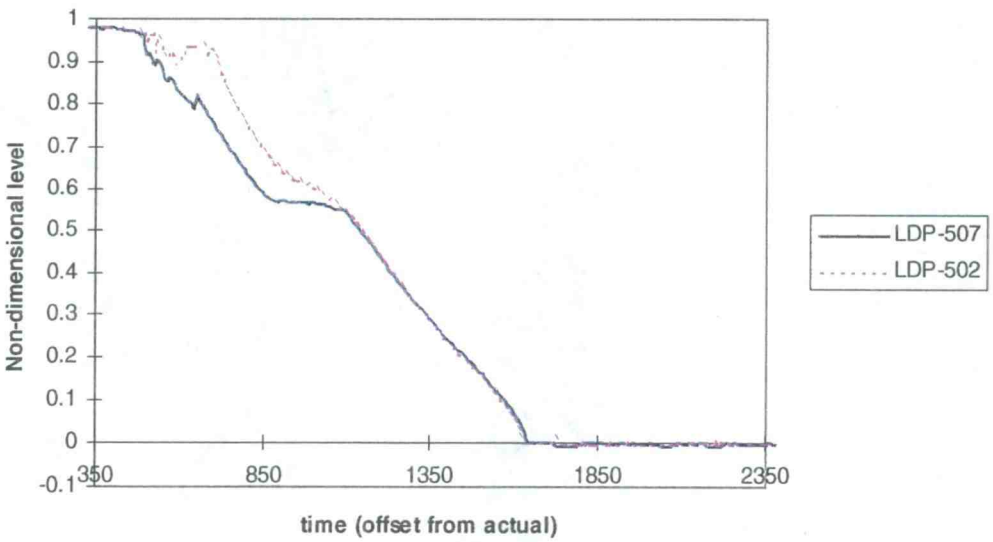

Figure 4-6 - Liquid level histories for the CMTs.

The resumption of CMT draining was due to the drop in Cold Leg #3 liquid level that occurred following the conclusion of accumulator injection. This drop in level allowed steam from the cold legs to flow through the PBLs into the CMTs. Permitting the CMTs to drain. The ADS 4 valves opened at time equal to 1400 seconds leading to further depressurization and thus emptying CMT 2 at time equal to 1620 seconds while CMT 1 emptied 9 seconds after the start of the IRWST injection. After emptying the CMTs, they were isolated to prevent any further refilling. Figure 4-6 presents the liquid level histories for the CMTs.

4.1.4 IRWST Injection Phase

This phase began at time equal to 1657 seconds when the primary pressure was low enough to allow for gravity driven injection from the IRWST and ended at time equal to 15,800 seconds when the flow was established from the containment sump to the RPV. This occurred when the IRWST liquid level reached approximately 18% of the initial liquid level. Figure 4-7 presents the liquid level history for the IRWST during the injection phase.

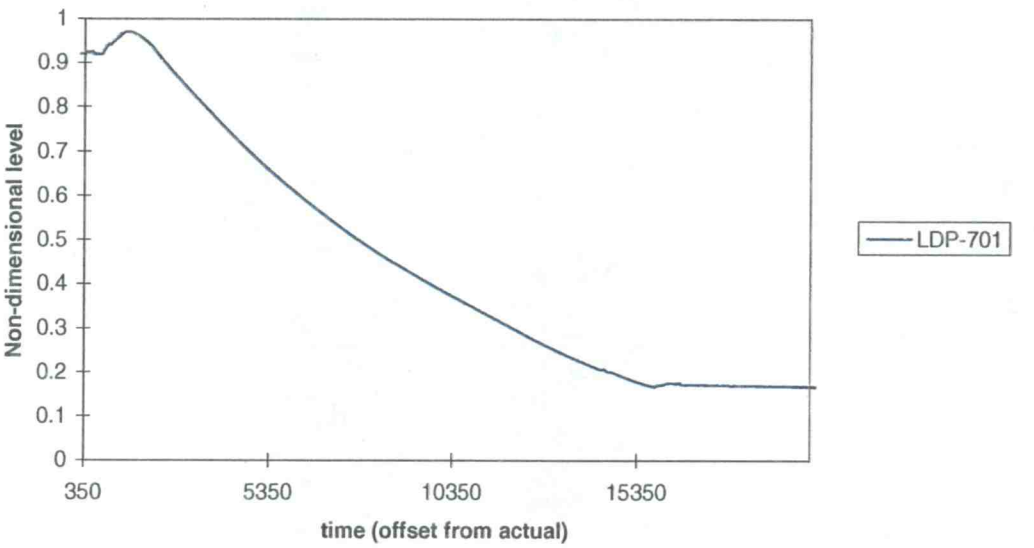

Figure 4-7 - IRWST liquid level during IRWST injection phase.

When the core reached saturation conditions at time equal to 7,970 seconds a set of flow, level and pressure oscillations were observed. These oscillations affected the entire system as shown in Figure 4-8 through Figure 4-11.

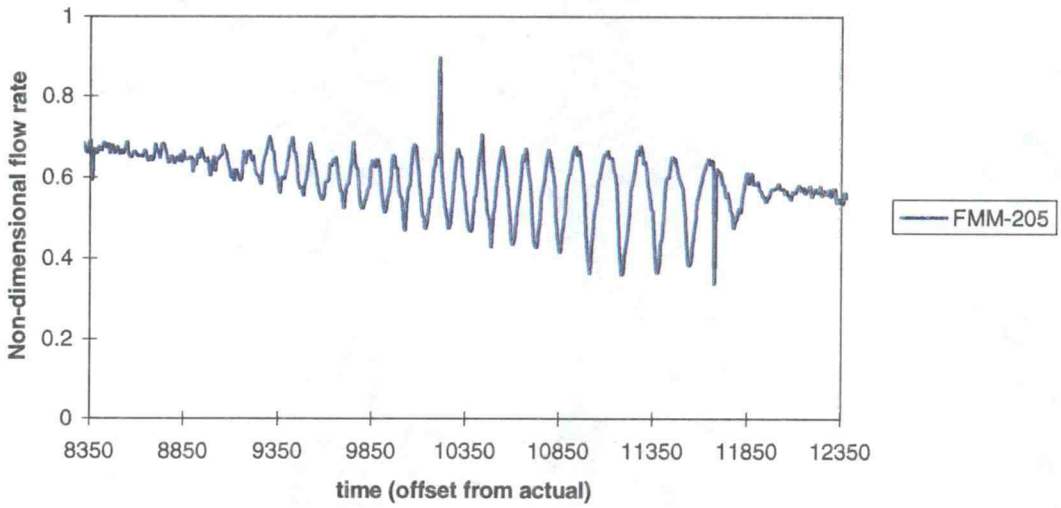

Figure 4-8 - DVI-1 liquid flow oscillations during IRWST injection.

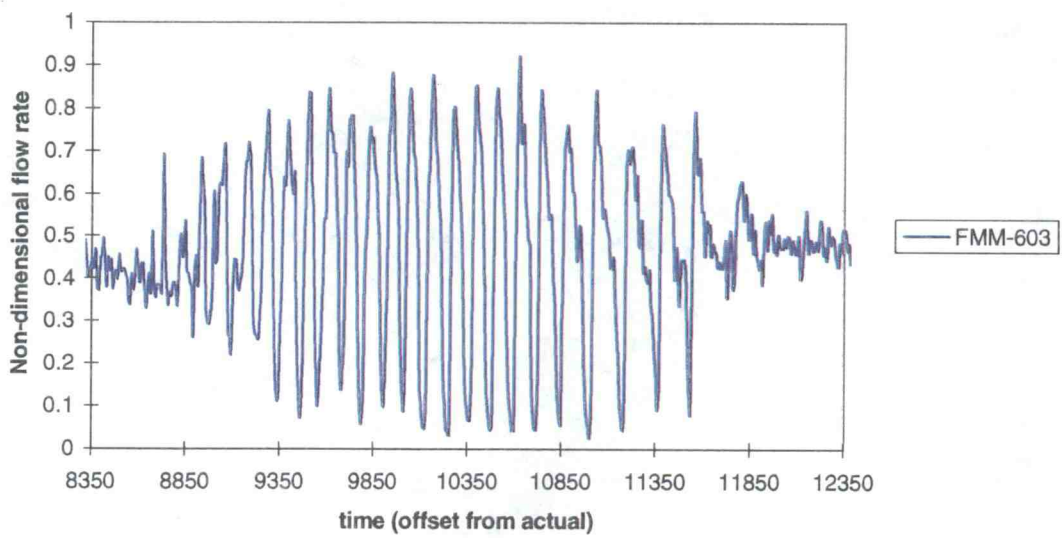

Figure 4-9 - ADS 4 liquid level oscillations during IRWST injection.

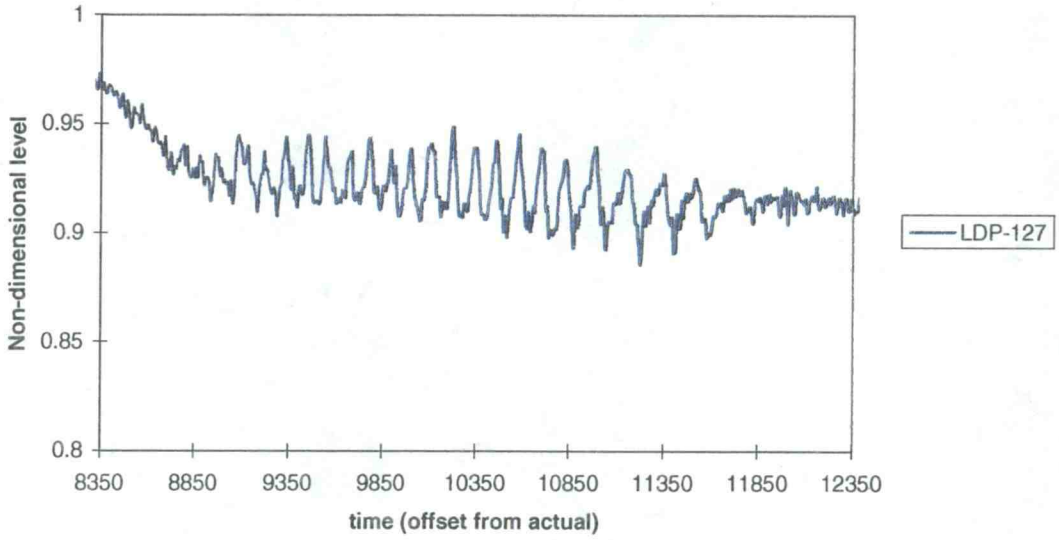

Figure 4-10 - Core liquid level oscillations during IRWST injection.

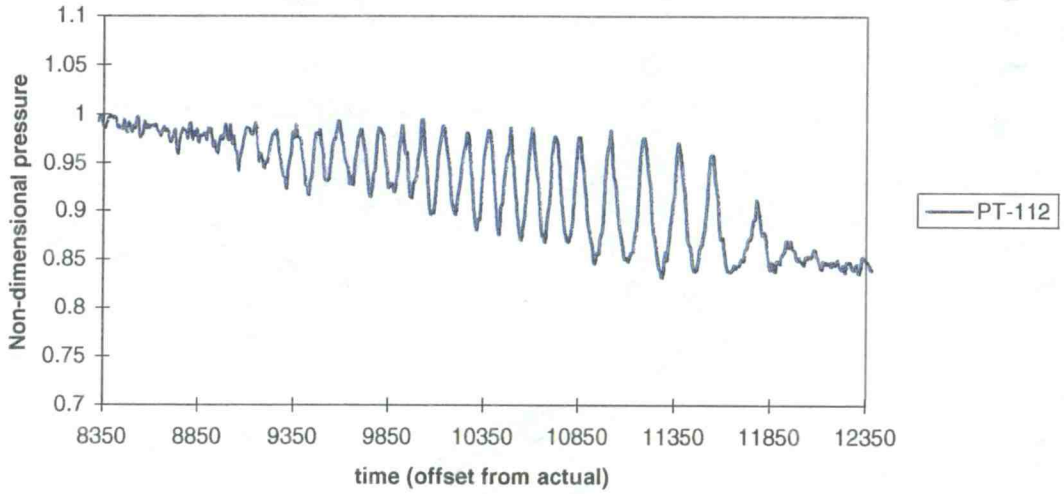

Figure 4-11 - Core Pressure Oscillations during IRWST injection.

The oscillations continued until just before to the start of sump recirculation.

4.1.5 Long Term Cooling System Recirculation Phase

This phase began at approximately 15,800 seconds when valves were opened to equalize liquid level in the IRWST and the primary sump. The primary sump liquid level had reached the overflow line as shown in Figure 4-12. After the levels equalized, a constant flow condition was established between the primary sump and the RPV. As steam and liquid were vented through ADS 4, the liquid leaving the system was directed to the sump. As shown in Figure 16, the liquid in the sump gradually began to increase in temperature as it was recirculated from the sump through the core and back to the sump. The test was terminated at 23,000 seconds, approximately two hours from the start of the LCS recirculation phase.

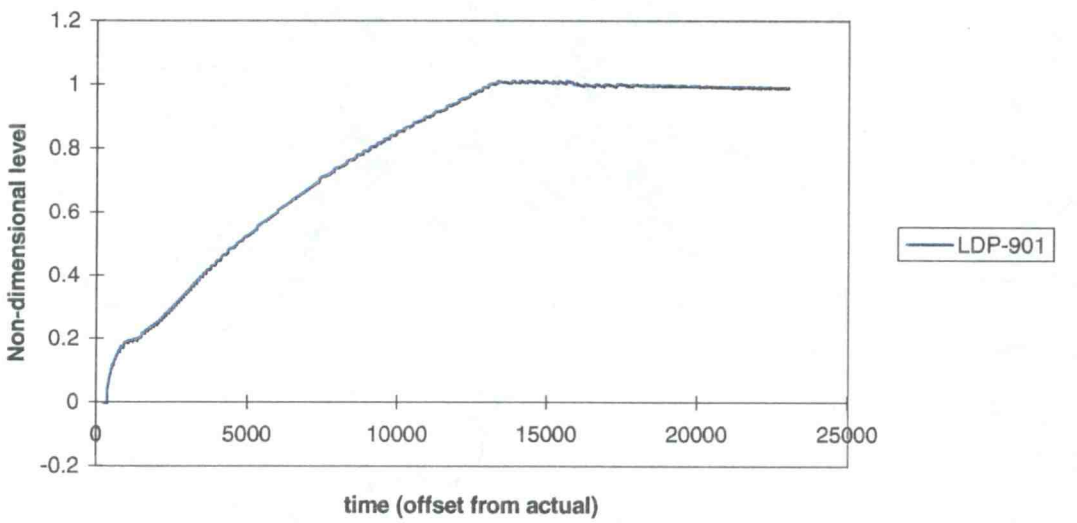

Figure 4-12 - Primary sump liquid level.

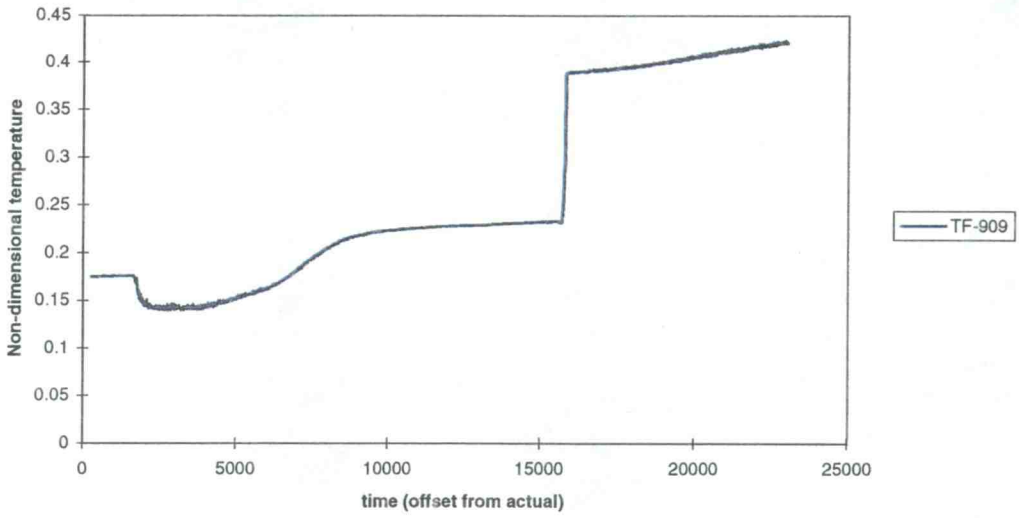

Figure 4-13 - Fluid temperature in the sump/DVI-1 line.

The purpose of this report is to examine the cold leg flow conditions so that the probability of pressurized thermal shock (PTS) can be evaluated. For PTS to occur the reactor pressure must be high. All but the first two stages, subcooled blowdown and natural circulation, can therefore be ignored.

Of primary interest during this early part of the transient is the temperature profile in the cold legs. As described in the literature review section, a stratified cold leg was recognized to pose a greater risk of PTS than a well mixed one. Stratification is regularly encountered in all normal small break LOCA tests performed at the APEX facility. An explanation of this phenomena is therefore necessary.

4.2 Description of Thermal Stratification

To reasonably predict thermal stratification and to reduce the amount of modeling necessary the problem must be simplified. To do this a qualitative analysis was performed initially to establish which components were significant to the study of thermal stratification as it affected PTS. Data from the OSU APEX facility was used to generate and support assumptions regarding the conditions within the cold leg, downcomer, core makeup tanks (CMTs) and steam generators and to explain the interactions between them. The OSU APEX tests predominately included simulations of 1 and 2 inch cold leg breaks. Data from a sample test is included in the descriptions to illustrate the event and timing of critical phenomena. The chosen sample test is NRC 5111, a 2 inch break in the bottom of cold leg #3. The reactor is symmetric and may therefore be broken into two distinct halves, the CMT-side of the facility which is affected by the presence of the CMT-PBLs and the PRHR-side of the facility which contains the PRHR injection line at the base of the steam generator. A rough schematic of the reactor primary system is shown in Figure 4-14.

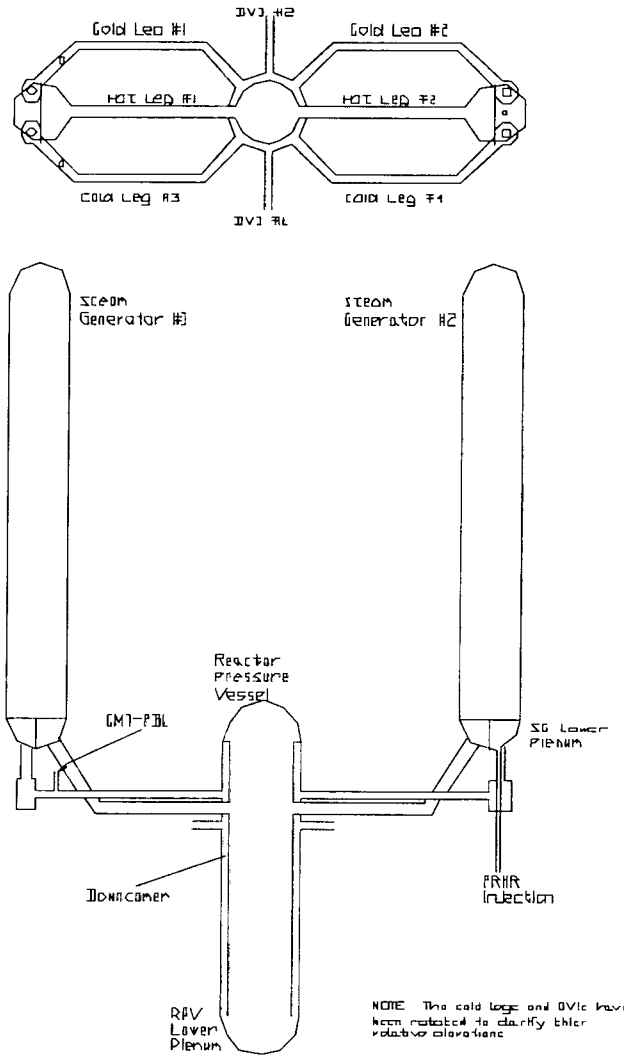

Figure 4-14 - Schematic of APEX primary system.

4.2.1 Thermal Stratification on the CMT-Side

During the early stages of the LOCA the fluid in the CMT-side cold legs transitions between four conditions. A plot of the vertical temperature profile in cold leg #3, the CMT-side cold leg containing the break, as measured by the thermocouple rake described in the critical instruments chapter, is shown in Figure 4-15.

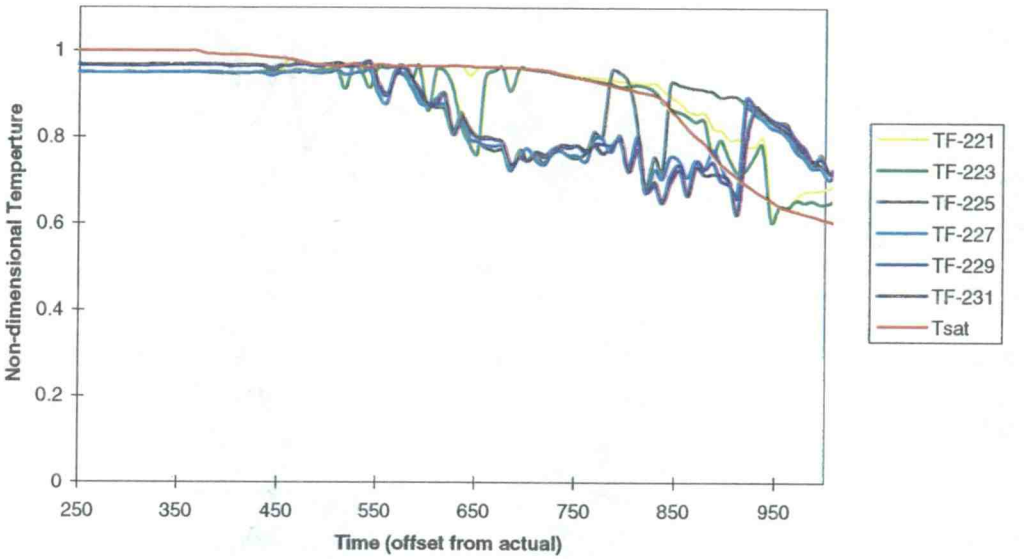

Figure 4-15 - Cold leg temperature profile as measured by the thermocouple rake in cold leg #3.

Most OSU APEX tests simulate the LOCA with a break in the cold leg. When the simulated break occurs mass flows out of the primary system piping and the LOCA transient begins. Thermal stratification is observed to be a part of this transient. The events leading to thermal stratification in cold legs #1 and #3 and subsequent CMT draining can be broken down into the following four stages;

1. natural circulation,
2. cold leg stagnation,
3. two phase stratification in the cold legs and
4. vapor filled (empty) cold legs.

The beginning of the third stage (two-phase stratification) was chosen as the time of onset for thermal stratification. A thorough description of the events leading up to the onset of thermal stratification in the CMT-side cold legs follows.

Prior to the beginning of the LOCA, the reactor is operating under normal conditions. High pressure, subcooled water is flowing up through the reactor core and out of the vessel through the hot legs. From the hot legs the water moves into the steam generators where it cools and is pumped back into the reactor vessel through the cold legs. Once in the vessel, the water is again heated by the reactor core and the circulation continues. A schematic of normal operation is shown in Figure 4-16.

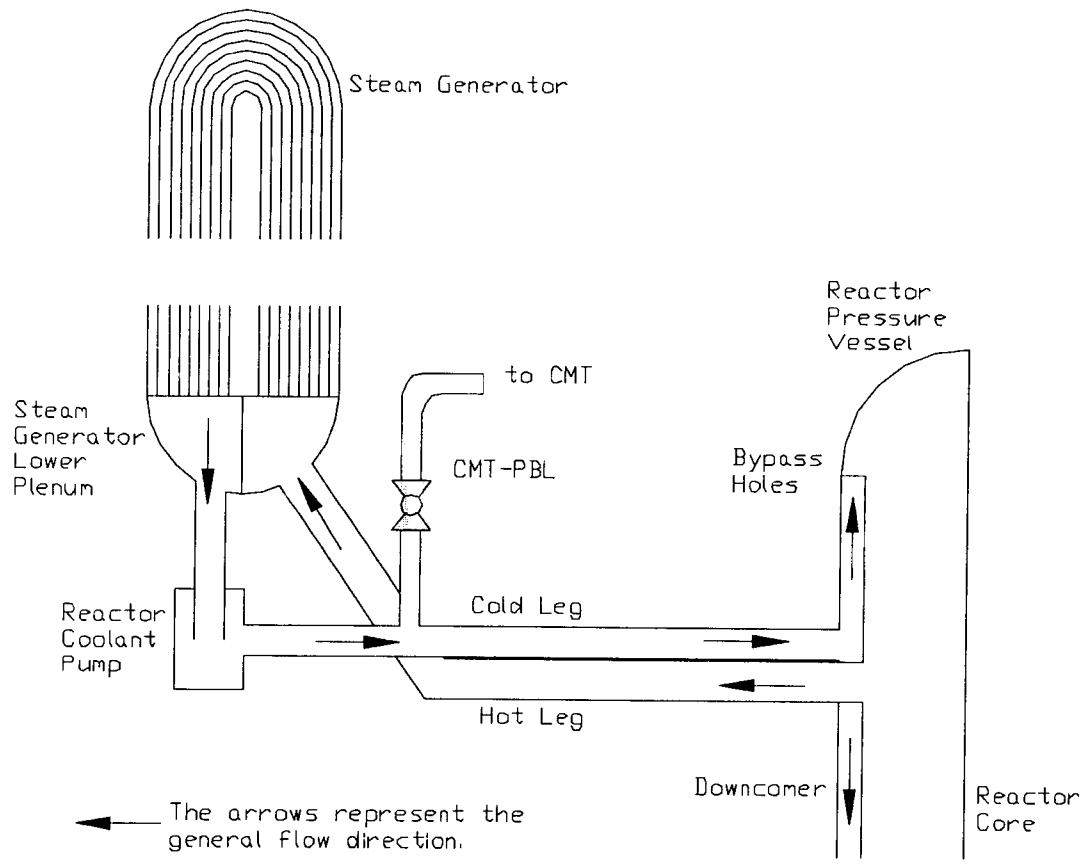

Figure 4-16 - Schematic of normal operation.

4.2.1.1 Stage 1 - Natural Circulation

When the simulated break occurs, the safety systems are actuated and the reactor trips (i.e. the coolant pumps stop and the reactor heater rods go into decay heat mode). Even though the pumps have tripped, the primary coolant loop continues to circulate due to natural convection. The flow patterns are similar to normal operation, but with significantly lower flow rates. On the CMT-side of the facility, cold water is not injected into the cold legs at any point during the transient. During this stage there is no mixing occurring and the cold leg temperature is therefore the same as the steam generator temperature, resulting in a uniform temperature profile. Throughout this stage the reactor pressure remains high and the liquid in the cold leg stays subcooled as is the liquid in the core makeup tanks (CMTs) and their pressure balance lines (CMT-PBL). A plot of the fluid temperature near the top of the CMT is shown in Figure 4-17. This figure shows that the fluid near these thermocouples stays subcooled for a long period of time (until approximately 500 seconds).

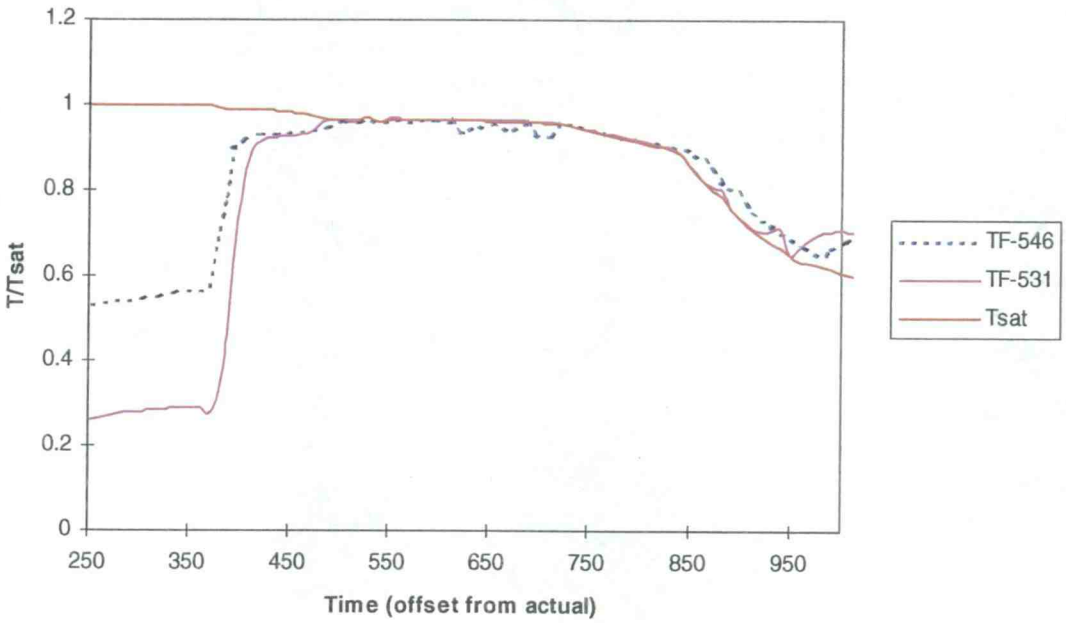

Figure 4-17 - Non-dimensional temperature at the top of CMT-1 (TF-531) and CMT-2 (TF-546).

As mass is vented from the primary system through the break the reactor pressure drops and steam bubbles begin to form as hot regions in the core reach saturation conditions and flash to steam. The bubbles rise to the top of the reactor and collect within the vessel head, pressurizer and steam generator U-tubes. The CMTs are another high point in the reactor but they do not gather a vapor bubble. This occurs because early in the transient the fluid in the CMT is very subcooled and the CMT vessel walls are cold. This allows the CMTs to condense any vapor which may reach them for a long period of time. Eventually, the bubbles in the steam generators grow large enough that they interrupt natural circulation through the reactor. The

growth of the steam bubble can be seen in Figure 4-18 as the collapsed liquid level drops. The bend in the U-tubes becomes uncovered at approximately 80% of full.

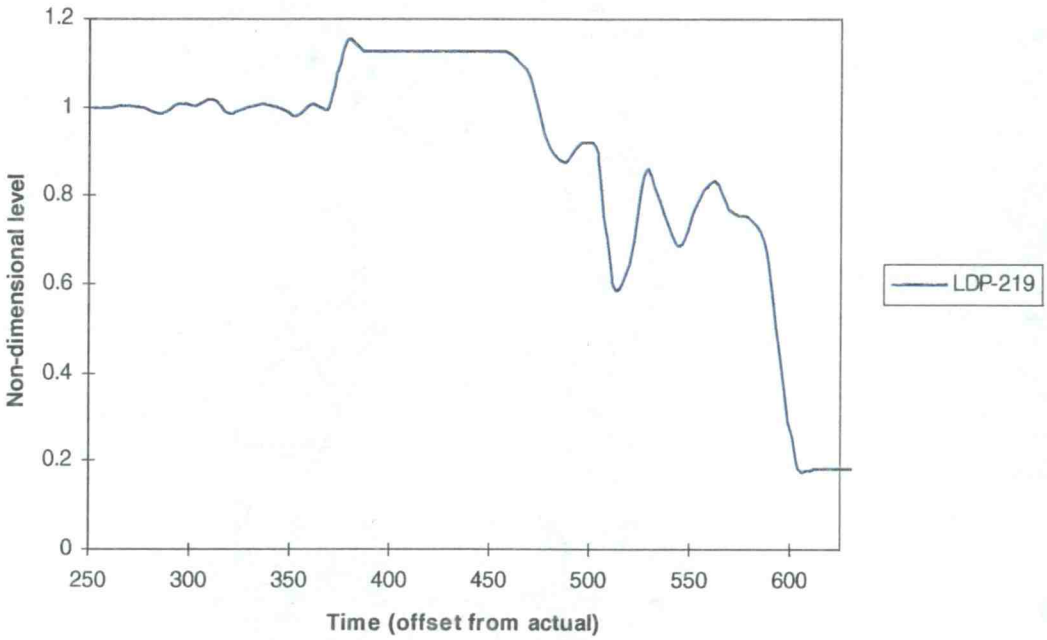

Figure 4-18 - Steam generator #1 collapsed liquid level.

When the steam bubble becomes large enough to fill the U-tube bends, natural circulation through the steam generator stops and the cold legs are considered "stagnant." The loop stagnation condition does not necessarily mean that there is not any movement within the cold legs, because this is certainly not the case. It only means that flow through the steam generator is essentially stopped with the end of natural circulation. The break, though, still draws fluid into the cold leg. The CMT is

still in a natural circulation mode and is also drawing fluid into the cold leg. This flow must come from the downcomer, which is the beginning of stage 2.

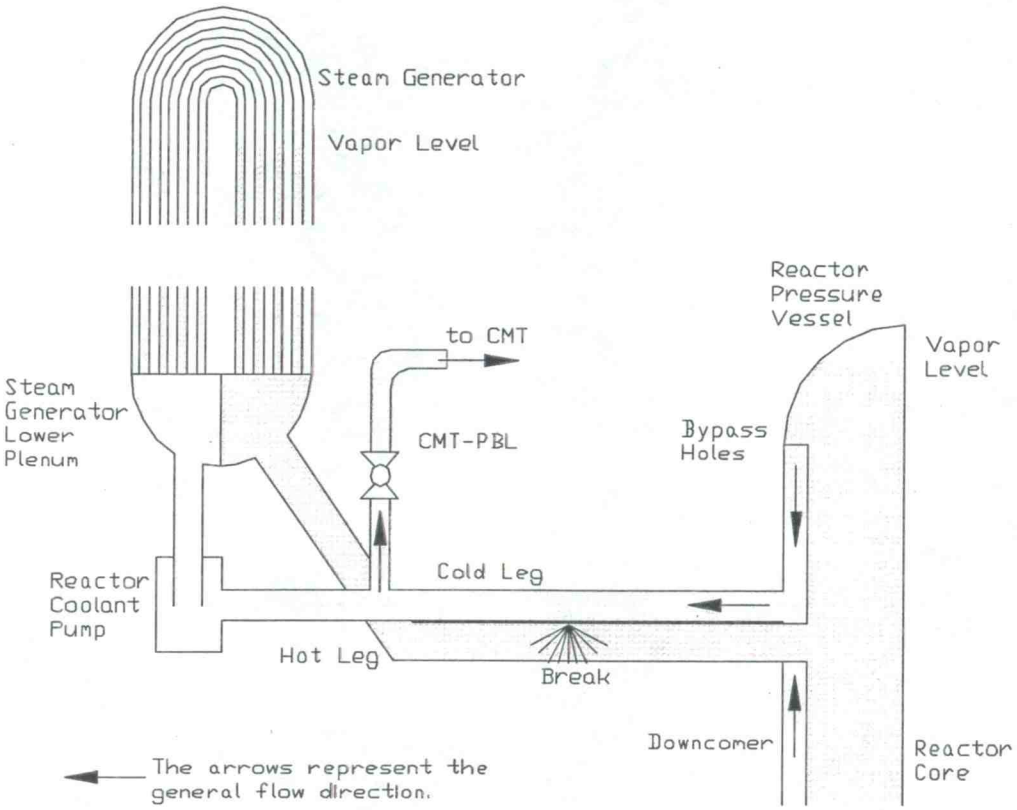

Figure 4-19 - Schematic of loop stagnation.

4.2.1.2 Stage 2 - Loop Stagnation

A schematic of loop stagnation is shown in Figure 4-19. Because natural circulation through the steam generators has stopped, the primary loop is considered "stagnant" and break and CMT recirculation flow is supplied by the downcomer. The lower downcomer temperature steadily drops throughout the transient while the upper downcomer temperature quickly becomes saturated. This is apparent in Figure 4-20, which shows several downcomer temperature readings from the thermocouples

located at varying heights between cold legs #1 and #3 and just above and below the hot leg and DVI.

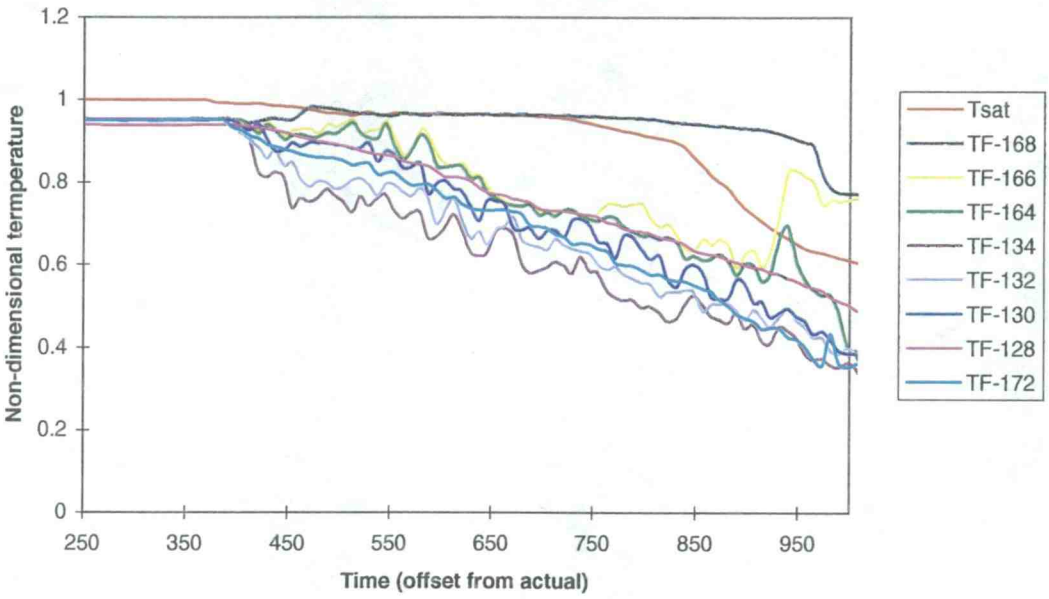

Figure 4-20 - Non-dimensional downcomer temperature profile. All the thermocouples are located on a vertical axis with the DVI, directly between the CMT-side cold legs.

The low temperature of the lower downcomer is attributed to the entrance of cold water into the downcomer through the DVI and PRHR (after mixing in the steam generator lower plenum and cold leg) at or below the cold leg level. In fact the DVI plume and its decay are clearly evident in the figure by examining TF-134 , TF-132 and TF-130.

The high temperature of the upper downcomer is caused by the flow of steam (or initially hot water) through the downcomer bypass holes in the top of the

downcomer. Eventually the upper downcomer is filled with saturated steam which begins to be drawn into the cold leg. This marks the onset of thermal stratification in the cold legs and the beginning of stage 3.

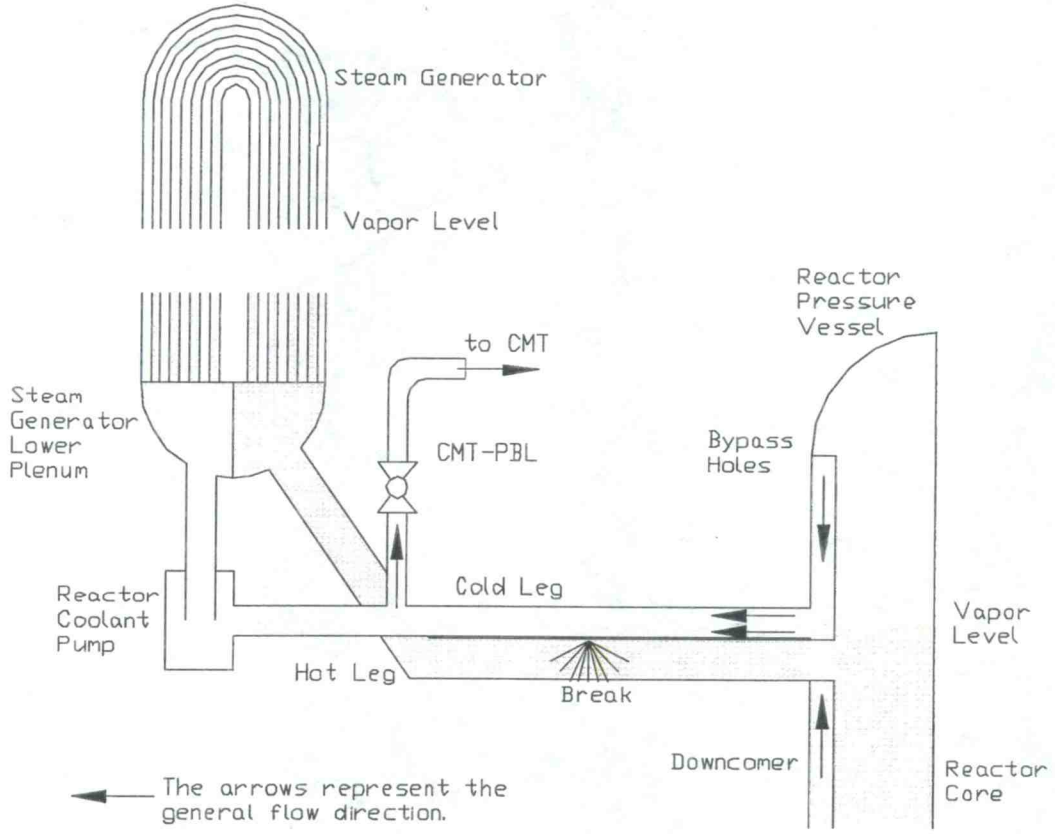

Figure 4-21 - Schematic of two-phase stratification.

4.2.1.3 Phase 3 - Two Phase Stratification in the Cold Legs

A schematic of two-phase stratified conditions is shown in Figure 4-21. The two phase stratification stage begins when the vapor bubble in the reactor vessel grows large enough to drop the liquid level below the reactor bypass holes. This allows vapor to flow into the upper downcomer and form an annular region of steam.

The level in the reactor vessel and the upper downcomer drops until it approaches the top of the cold leg. Figure 4-22 shows the collapsed liquid level in cold leg #3 with the cold leg temperature profile. The plot shows that the cold leg does not stratify before the steam enters the cold leg. (The large drop in the cold leg level at approximately 350 seconds is due to the shutoff of the reactor coolant pumps.) As further support, Figure 4-23 shows that as the upper downcomer drains, it goes through a rapid temperature change from subcooled to saturated. This means that if there is a layer of saturated liquid in the upper downcomer it is very thin and any single phase stratification that may occur is short lived.

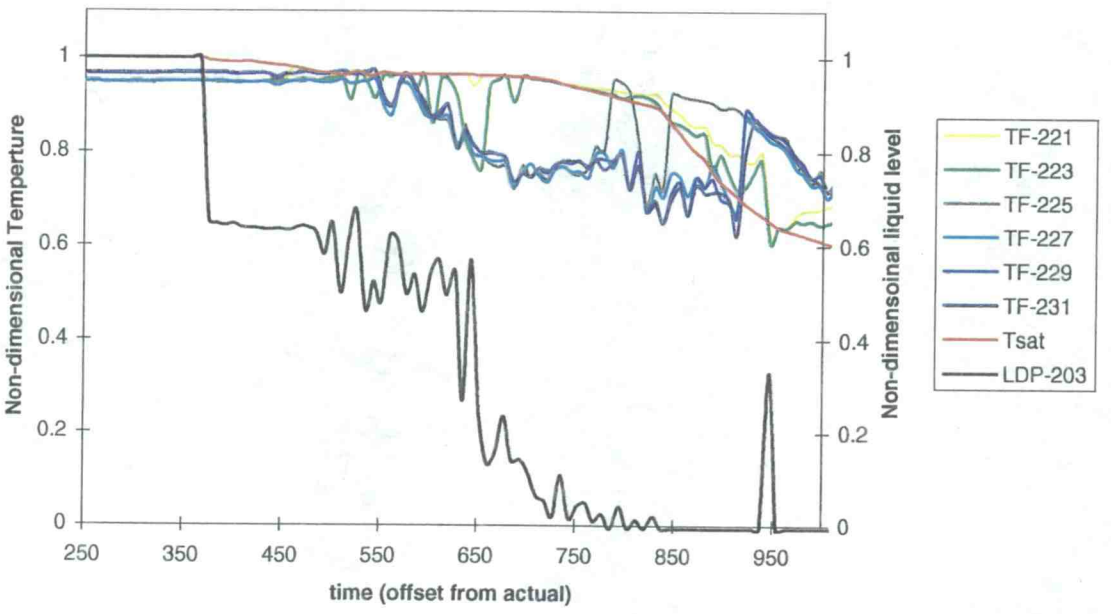

Figure 4-22 - Cold leg #3 temperature profile and the cold leg collapsed liquid level.

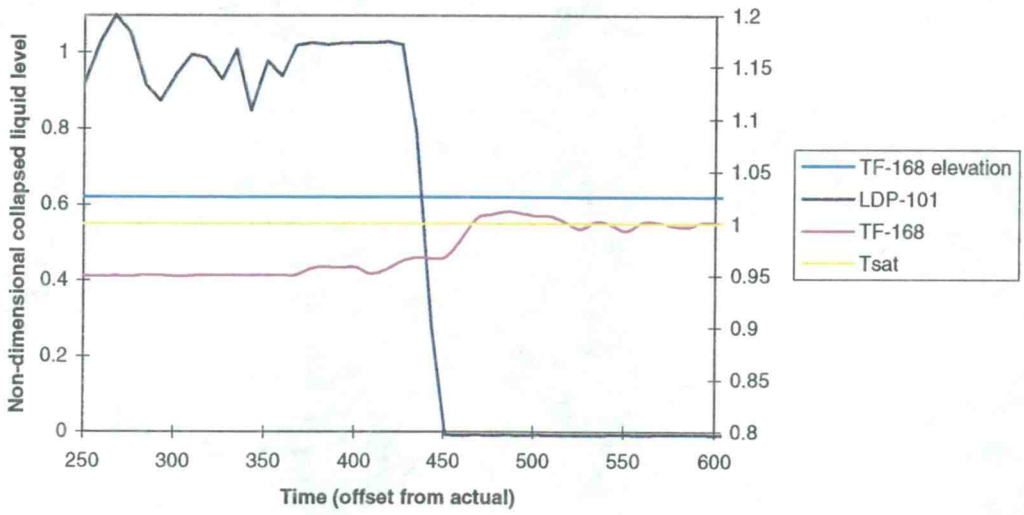

Figure 4-23 - Upper downcomer collapsed liquid level and temperature.

The cold leg containing the break will be the first to draw in steam. This occurs because the break creates an added driving force that will depress the liquid level in the downcomer near the cold leg inlet thereby allowing the early entrance of steam. Steam which has been drawn into the cold leg flows along the top of the cold leg and into the CMT-PBL where it is either condensed or coalesces to form a vapor bubble allowing the CMT to begin draining. The plot of the CMT-PBL collapsed liquid level in Figure 4-24 and Figure 4-25 shows large fluctuations. This implies that there is a great deal of vapor moving through it in large slugs. It should also be noted that CMT #2 begins draining before CMT #1 due to early stratification in cold leg #3.

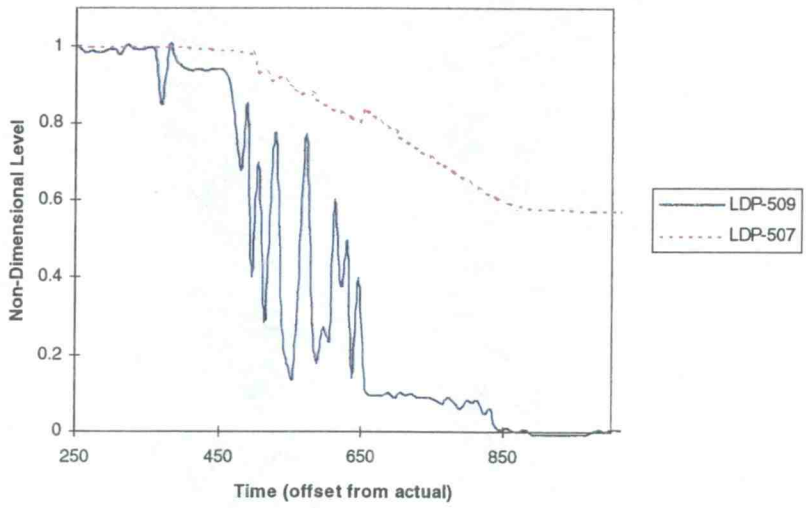

Figure 4-24 - Non-dimensional CMT #2 (LDP-507) and CMT-PBL #2 (LDP-509) collapsed liquid levels. CMT #2 is attached to cold leg #3.

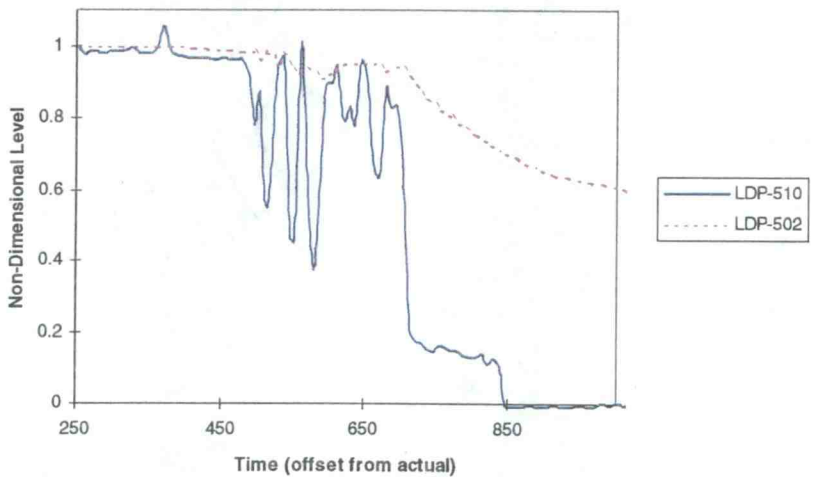

Figure 4-25 - Non-dimensional CMT #1 (LDP-502) and CMT-PBL #1 (LDP-510) collapsed liquid levels. CMT #1 is attached to cold leg #1.

The second stream in the cold leg comes from the downcomer. It is subcooled and runs along the bottom of the cold leg. The temperature of this stream matches that of the downcomer which is affected by the DVI and PRHR flow (after mixing in the steam generator lower plenum and PRHR-side cold legs) coming into the downcomer. The top stream will always be at the system saturation temperature and the bottom stream will control the degree of stratification.

The upper downcomer level continues to drop as the reactor vessel bubble grows. Eventually it drops below the top of both cold legs #1 and #3 and steam is drawn into the cold legs without the additional driving force of the break flow. The vapor then flows steadily up into CMT #1 which, like CMT #2, will begin to void when the CMT-PBL becomes unable to condense this steam.

The purpose of this study is to provide a description of the cold leg temperature profile at the exit of the cold legs so that their contribution to a potential PTS event can be evaluated. It is therefore important to note that flow is going from the downcomer into the cold leg and not from the cold leg into the downcomer. This means that there is no cold plume falling into the downcomer and no vessel cooldown transient below the CMT-side cold legs that is more severe than the overall vessel cooldown rate . The cold legs on the CMT-side of the facility therefore will not cause PTS.

4.2.1.4 Phase 4 - Vapor Filled Cold Legs

The vapor bubble in the reactor pressure vessel continues to grow. When the ADS valves open the reactor pressure drops rapidly and much of the primary system

liquid volume flashes to steam. This quickly lowers the reactor liquid level and causes the cold legs to fill with steam. The cold legs will refill with water later in the test, but PTS will not be a danger because the reactor pressure is relatively low.

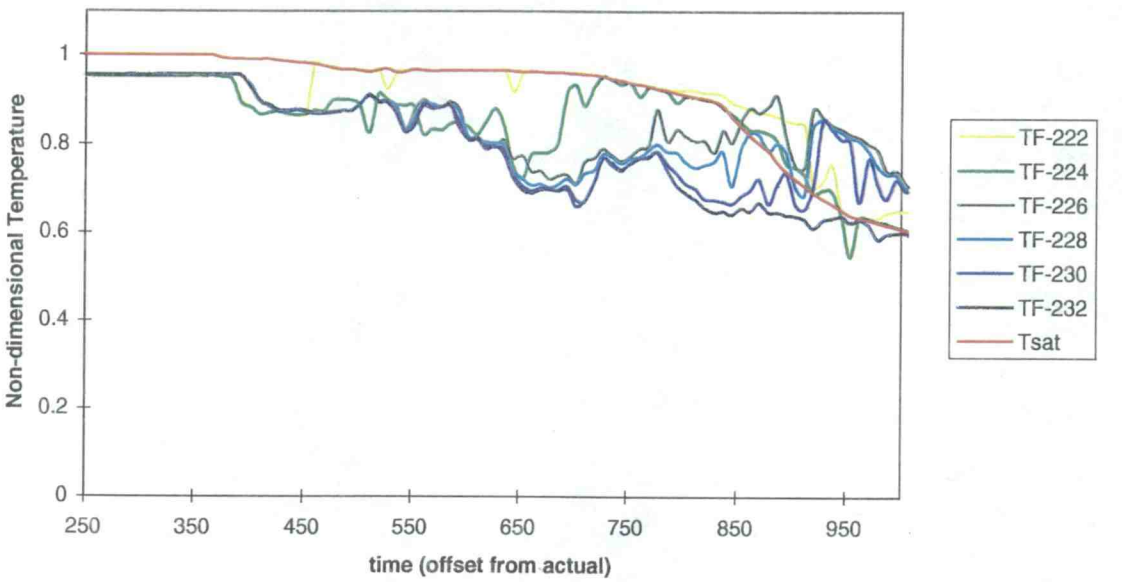

Figure 4-26 - Cold leg #4 temperature profile as measured by the thermocouple rake within the cold leg.

4.2.2 Thermal Stratification on the PRHR-Side

There is an observed difference between the magnitude of thermal stratification on the PRHR- and CMT-sides of the facility. Thermal Stratification of the PRHR-side of the facility can be as much as 100° F larger. This greater stratification is directly related to the injection of cold water from the PRHR into the steam generator, whereas the CMT-side of the facility does not have any sources of

water colder than the downcomer fluid. Figure 4-26 shows a plot of the vertical thermocouple rake in cold leg #4 on the PRHR-side of the facility.

The PRHR-side cold legs go through three phases early in the LOCA. These phases are similar to those experienced by the CMT-side but with different bulk flow direction. The phases are as follows;

1. natural circulation
2. two-phase cold leg "stagnation"
3. vapor filled cold legs

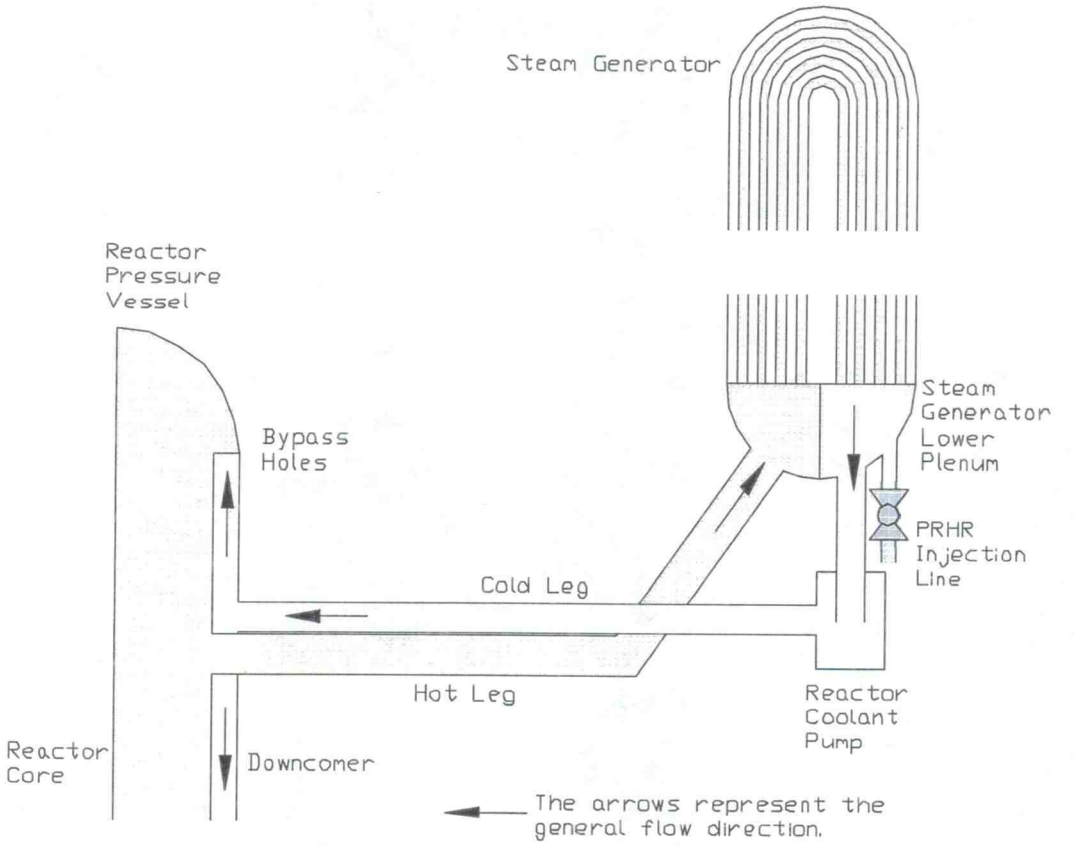

Figure 4-27 - Schematic of natural circulation on the PRHR-side of the facility.

4.2.2.1 Phase 1 - Natural Circulation

The natural circulation stage is very similar to the natural circulation phase of the CMT-side except that it is influenced by the PRHR injection stream. A schematic of this condition is shown in Figure 4-27. Natural circulation flow, which is large compared to the PRHR flow (Figure 4-28), dominates the cold leg. Because the natural circulation flow is so much larger than the PRHR flow the PRHR injection plume is thoroughly broken up and completely mixed; therefore a uniform cold leg temperature is obtained.

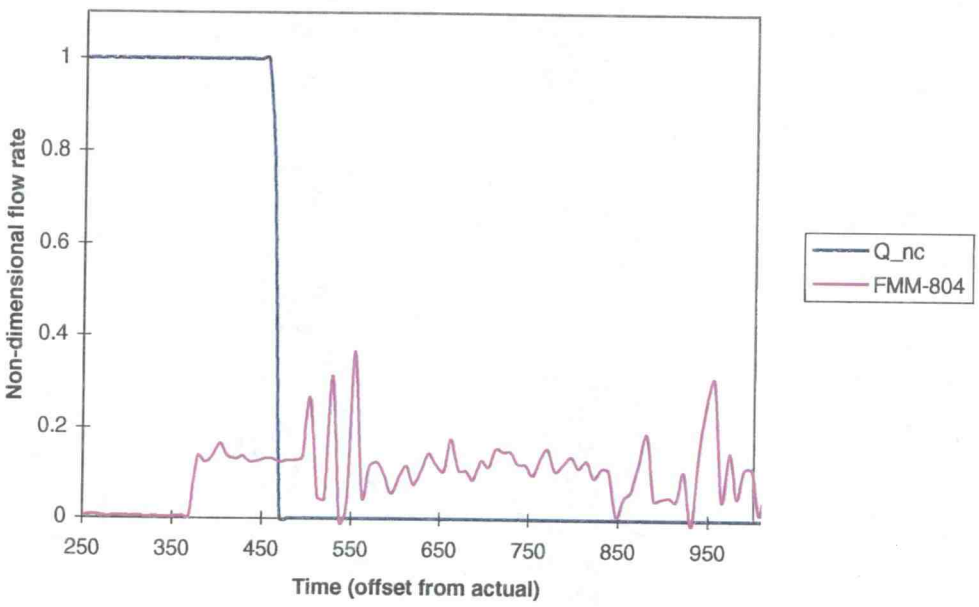

Figure 4-28 - Estimated natural circulation and PRHR flow rate comparison.

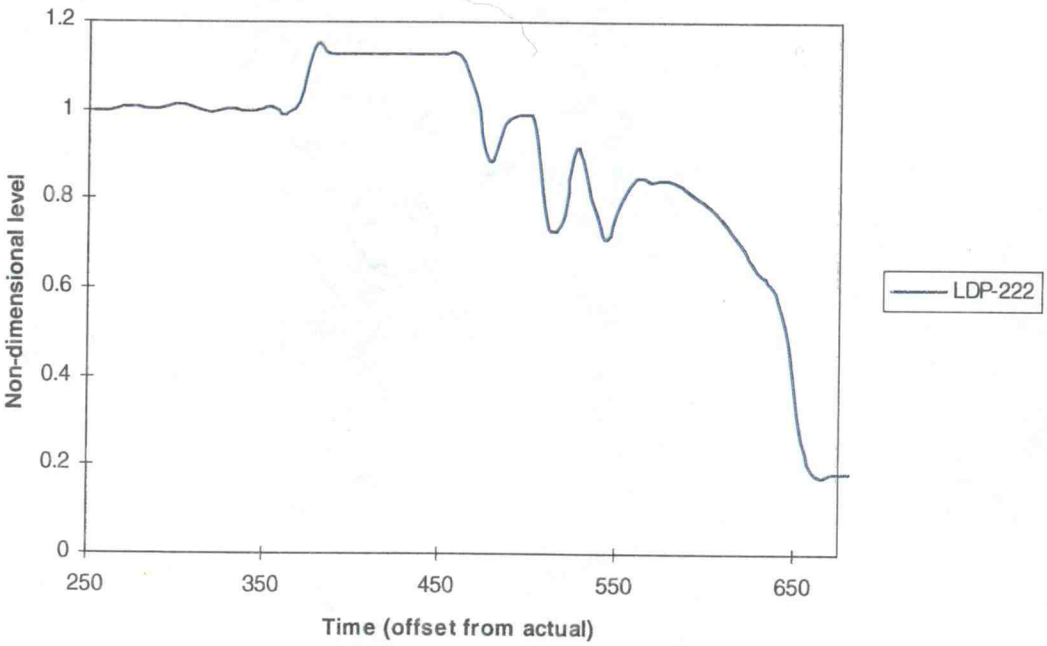

Figure 4-29 - Steam generator #2 collapsed liquid level (cold legs #2 and #4).

The bulk cold leg flow is still cooled noticeably by the PRHR operation, though. Again, this phase continues until the steam generator void becomes large enough to interrupt natural circulation. Figure 4-29 shows the steam generator collapsed liquid level. This plot suggests that the upper steam generator voids and ends natural circulation at approximately 450 seconds.

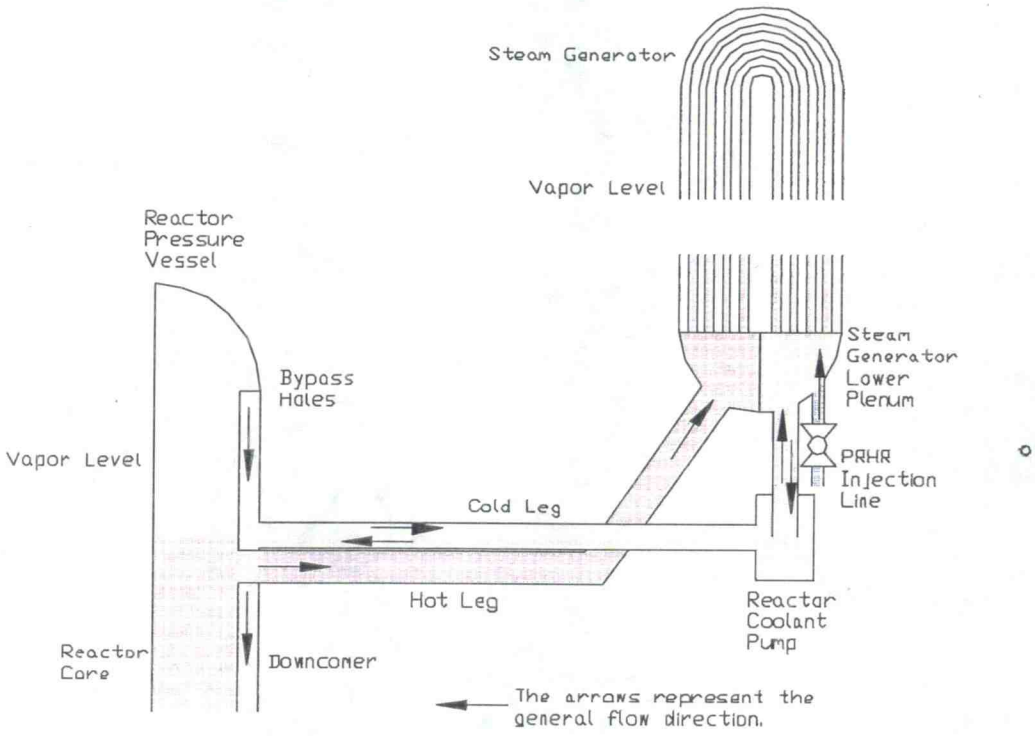

Figure 4-30 - Schematic of two-phase stratification in cold leg #4 (PRHR-side).

4.2.2.2 Phase 2 - Two-Phase Loop Stagnation

When natural circulation stops the primary loop is considered stagnant where stagnation is defined in the same manner as in phase 2 of the CMT-side discussion . The only activity on the PRHR-side of the facility at this point is generated by the PRHR injection. The PRHR flow is much colder than the ambient primary fluid. It is therefore driven by buoyancy forces down into the cold leg and towards the downcomer. Incomplete mixing of the PRHR injection stream may result in the formation of a counter-current flow condition that could result in a colder plume of water exiting the cold leg into the downcomer. The initial temperature of the cold leg plume is the criteria for PTS that must be explored for the reactor under study here.

Figure 4-26 shows a plot of the thermocouple rake in cold leg #4 (PRHR-side). The figure does not conclusively show the existence of a counter-current condition. Other methods must be employed to determine if this condition exists. At this point the PRHR is analogous to the high pressure safety injection (HPSI) systems of common reactors currently in operation and some analysis tools generated for this problem may therefore be used (including the onset criterion of Theofanous). The thermal stratification observed in this plot is significant, but, in every case, it can be credited to the presence of a thin layer of vapor near the top of the cold leg pipe. This suggests that the PRHR injection plume is becoming well-mixed with the ambient fluid in the steam generator lower plenum and the reactor coolant pump prior to entering the cold leg. Therefore, if thermal stratification due to counter-current flow is occurring, the magnitude of the temperature difference is small. A schematic of the natural circulation phase is shown in Figure 4-30.

As previously observed on the CMT-side of the facility, the vapor bubble in the reactor pressure vessel grows and eventually fills the upper downcomer with steam. Because the top of the steam generator is at a much higher elevation than the top of reactor vessel the steam is driven by buoyancy toward the steam generator. To reach the steam generator though requires the formation of a counter-current flow condition in the cold leg. Steam could also form due to boiling in the steam generator U-tubes. The steam generator walls are at a slightly elevated temperature, but because it is so early in the transient the system pressure is high enough that wall temperature is not much greater, if at all greater, than the saturation temperature. The small amount of vapor that is forming in this manner could easily be condensed into the

subcooled liquid within the steam generator. When a counter current flow condition develops to allow the steam generator to begin draining, the cold leg stratifies. Figure 4-31 shows the cold leg #4 temperature profile with its collapsed liquid level. The thermocouple rake shows that the top layer in the cold leg is saturated. The collapsed liquid level plot shows fluctuations, which implies the entrance of vapor. (The large drop in level early in the transient is an artifact created when the reactor coolant pumps are tripped.)

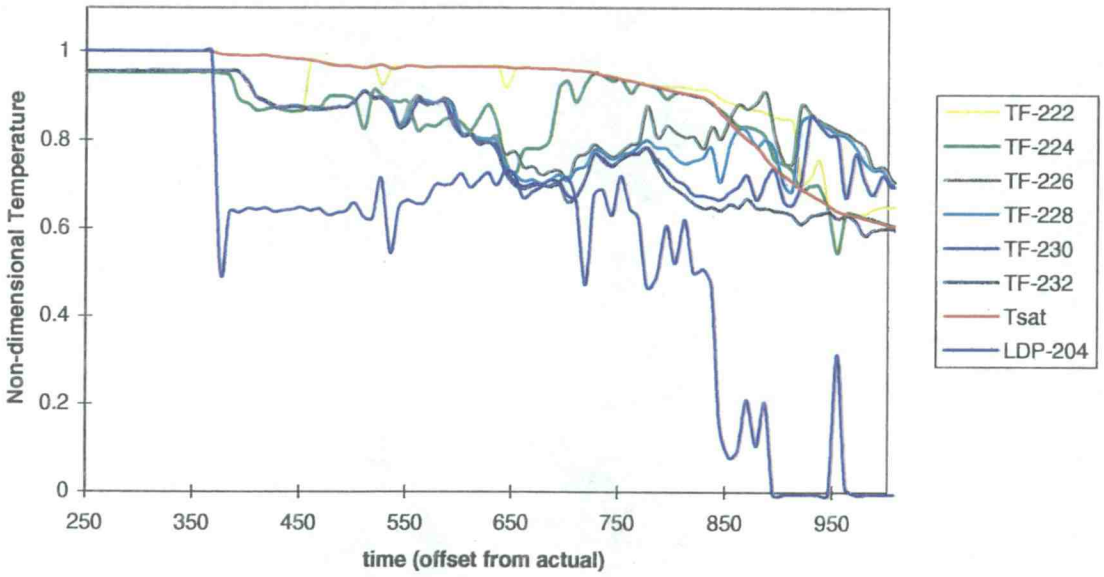

Figure 4-31 - Cold leg #4 temperature profile and collapsed liquid level (LDP-204).

The existence of steam in the cold leg during this period is further supported by Figure 4-32. This figure shows that the upper downcomer has already filled with steam prior to the onset of thermal stratification and the cold leg collapsed liquid level

fluctuations. This suggests that the entrance of vapor into the cold leg was inhibited by the large cumulative flow from natural circulation and PRHR injection.

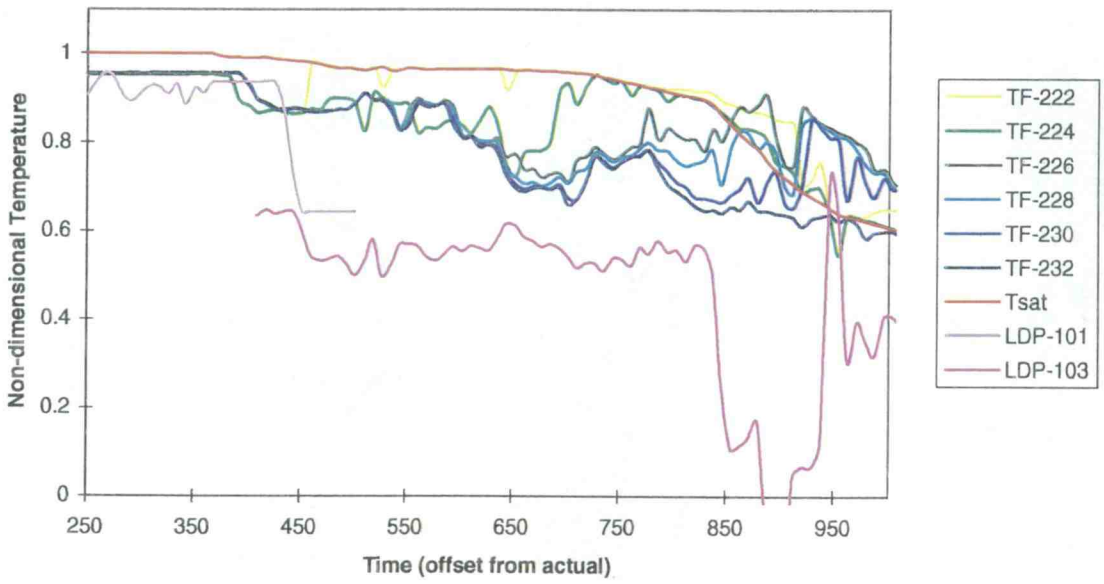

Figure 4-32 - Downcomer collapsed liquid level and cold leg temperature profile.

4.2.2.3 Phase 3 - Empty Cold Legs

As the primary system pressure drops the vapor bubble in the reactor vessel grows and eventually the PRHR natural circulation loop is interrupted by the entrance of steam and the cold legs fill with vapor. By the time the liquid level in the reactor starts to rise enough to fill the cold legs the system pressure is no longer great enough to pose a risk for PTS.

4.3 Degree of Thermal Stratification

It is important to determine the magnitude of the temperature difference between the two fluid streams in the cold leg. To determine this degree of stratification requires a thorough look at the inlet streams and boundaries of each cold leg. During the initial stages of the transient all four cold legs are fed by natural circulation through the steam generator. The cold legs on the PRHR side of the facility are also fed by the PRHR. The PRHR side cold legs should therefore be colder than the CMT-side cold legs during natural circulation. Because the natural circulation flow is much greater than the PRHR flow, the PRHR injection plume is thoroughly broken up and both sets of cold legs are uniform and well-mixed. After the cold legs reach the stagnant stage (i.e. natural circulation stops) the PRHR flow continues to affect the cold legs on the PRHR-side of the facility and the break flow on the CMT-side begins to come from the downcomer. At this point the behavior of the two sets of cold legs becomes very different. The degree of stratification in the CMT-side of the facility is controlled by the temperature of the downcomer and the PRHR-side is controlled by the mixing that occurs between the ambient steam generator fluid and the PRHR injection stream.

Determining the degree of stratification in the CMT-side cold legs requires that the downcomer be described first. Figure 4-20 shows the vertical temperature profile in the downcomer between cold legs #1 and #3. This plot shows that in regions other than directly below the DVI and in the upper downcomer, the liquid is well-mixed and its temperature is uniform. For the purpose of analyzing the cold legs the downcomer can be considered to contain two layers, the saturated vapor region at

the top of the downcomer and the well-mixed subcooled region occupying the rest. The top layer of the stratified downcomer lies at or above the cold leg level and is fed by the downcomer bypass holes. The vapor is held there by its substantially lower than ambient density. The remainder of the downcomer is cooled by the DVI and PRHR injection.

Because the interface between the two layers lies at the cold leg level, they strongly influence the behavior of the cold legs. For the CMT-side of the facility this means that whatever fluid occupies the downcomer will be drawn directly into the cold leg to feed the break and CMT-PBL and that the degree of cold leg stratification will be roughly the same as that of the downcomer. The flow in the non-break cold leg will be substantially smaller because it is not affected much by the break. The non-break cold leg still participates in CMT recirculation; thereby allowing it to draw in fluid from the downcomer annulus.

The cold legs on the PRHR-side of the facility have the potential to stratify into a two or three layer system. In the three layer system the top layer consists of saturated vapor which enters when the upper downcomer fills with steam. The second and third layers can exist if a counter-current flow condition evolves due to incomplete PRHR mixing behavior within the steam generator lower plenum and the cold legs. The PRHR-side cold legs could also settle into a two layer system, saturated steam and a PRHR cooled lower stream. This can occur if the PRHR fluid is mixed well when it is injected into the steam generator lower plenum and falls into and through the reactor coolant pumps. An estimation of the two layer cold stream temperature can be made by considering the fluid temperatures in the lower plenum

and cold legs as slowly varying and affected only by the injection of the PRHR fluid. A more precise description of the fluid within the cold leg and steam generator lower plenum requires a more complex analysis method like the three-dimensional CFD code applied in a later section.

5. COMPARISON WITH ROSA FACILITY DATA

The Large Scale Test Facility (LSTF) of the Japan Atomic Energy Research Institute was modified to simulate the Westinghouse AP600 and to provide data for comparison to the OSU APEX test facility. When in the AP600 configuration the LSTF is more commonly known as the ROSA facility. It is instructive in this case to examine the data generated by the ROSA facility and compare it to that generated by the OSU APEX facility.

The primary objective of the ROSA experiments is to provide data for the assessment of thermal hydraulic safety analysis computer codes. Following assessment, the USNRC will use these codes in the AP600 design certification process. A secondary objective of the experiments is to provide insight into the system response of the AP600 reactor to adverse situations. While LSTF is not an exact scale model of the AP600, it is sufficiently similar to produce the most important thermal hydraulic phenomena associated with AP600.

5.1 Description of Facility

LSTF was designed to simulate thermal hydraulic phenomena peculiar to small break loss of coolant accidents (SBLOCAs) and operational transients in PWRs. It features prototypical component elevation differences, large loop piping diameters, simulated system controls, prototypical primary pressures, and sufficient core power to simulate the core power decay starting within seconds after scram. Although

originally volume-scaled at 1/48 of a typical 3423 MWth Westinghouse-type PWR, the LSTF in the ROSA configuration has a volume ratio of 1/30.5.

The major LSTF modifications made to allow a better representation of the AP600 include the addition of two CMTs, a PRHR, an In-containment Refueling Water Storage Tank (IRWST), CMT pressure balance lines (CMT-PBLs), and an automatic depressurization system (ADS). The plant already had accumulator tanks.

The facility is well instrumented including a large number of thermocouples, flow meters and differential pressure transducers.

5.2 Description of Phenomena

Having thoroughly described the mechanisms that lead to thermal stratification in the cold legs of the OSU APEX facility it is relatively simple to analyze the data from the ROSA facility to determine if the phenomena are comparable. The following is a description of plots that show conditions and behavior that are very similar to that of the PRHR side of the OSU APEX facility.

The first plot of interest, Figure 5-1, is the vertical temperature profile in the PRHR side cold leg. This plot shows the initial cooldown period of the LOCA where the cold leg fluid is well mixed. This well mixed period is immediately followed by a brief single phase thermal stratification and finally a period of two phase stratification that continues until the cold leg empties.

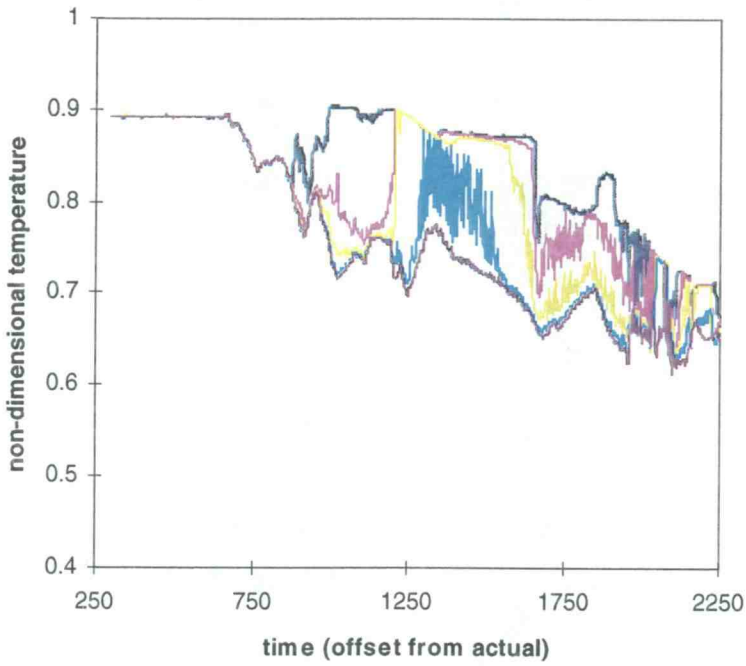

Figure 5-1- Cold leg temperature profile for ROSA facility.

The single phase period occurs when the fluid in the downcomer immediately outside the cold leg entrance increases in temperature enough to provide a buoyancy force large enough to overcome the momentum forces of the fluid flowing out of the cold leg. The increase in temperature is caused by the flow of vapor into the downcomer through the downcomer bypass holes. This vapor forces the hot fluid above the cold leg to move down near the cold leg entrance. Evidence that the initial stratification is single phase is provided by Figure 5-2, which shows the collapsed liquid level in the cold leg. The plot shows a slight level drop that coincides with the initiation of stratification. This dip in level, though, can be credited to the temperature induced density changes in the fluid causing the calibration of the instrument to

change. The cold leg does not actually become two phase until the upper fluid stream reaches the saturation temperature at approximately 1,000 seconds.

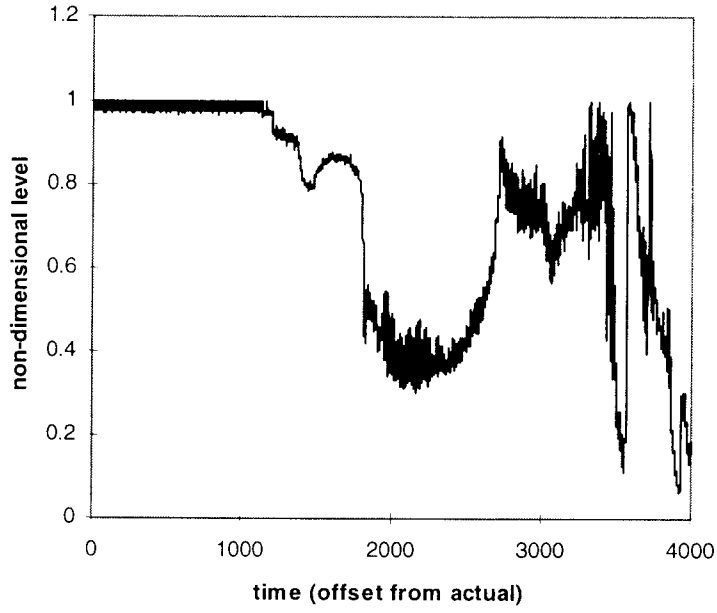

Figure 5-2 - Cold leg collapsed liquid level in the ROSA facility.

The ROSA facility also measures the PRHR flow rate and the total cold leg flow rate. This data is especially useful for comparison with the onset criteria for thermal stratification, which is described later.

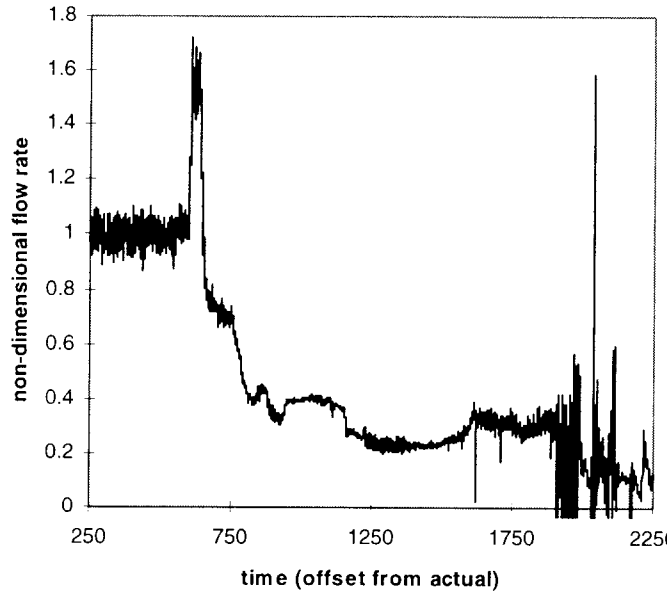

Figure 5-3 - Cold leg liquid flow rate for the ROSA facility.

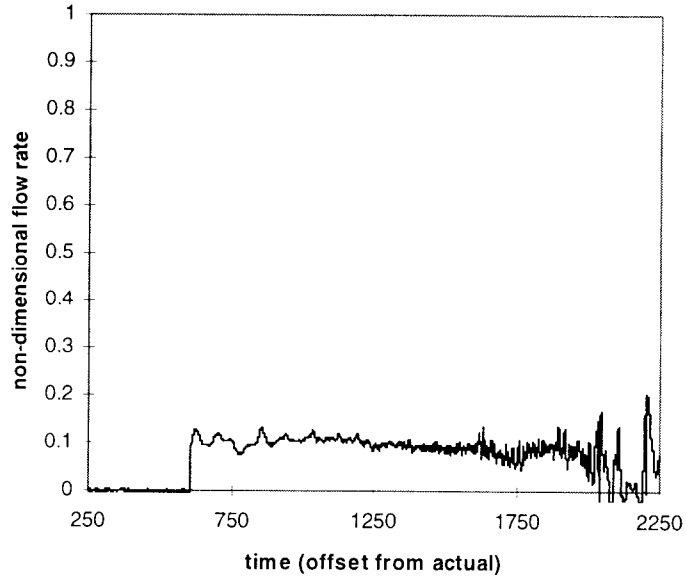

Figure 5-4 - PRHR injection flow rate for the ROSA facility.

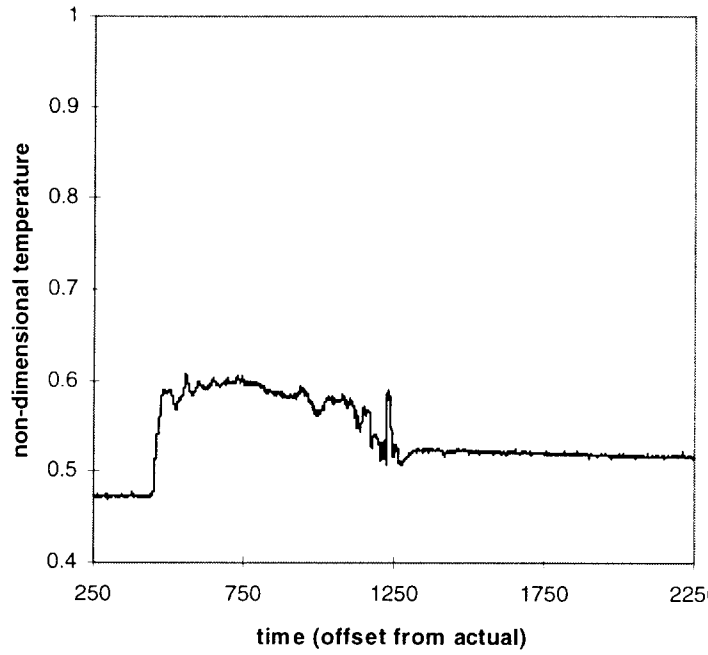

Figure 5-5 - PRHR injection temperature for ROSA facility.

5.1 Comparison with APEX

The ROSA and OSU APEX facility exhibit very comparable behavior. By examining the plots in the Description of Phenomena section regarding thermal stratification in the PRHR side of the facility several key similarities are evident. The most significant similarities are:

- the early well mixed period which precedes the stratification
- the rapid jump to the saturation of the fluid near the top of the cold leg
- the onset of stratification coinciding with the low natural circulation flow rates
- drop in cold leg collapsed liquid level during stratification.

These observations further support the belief that the thermal stratification in the PRHR side cold legs is predominantly a two-phase counter current condition that occurs due to the decline of natural circulation and the formation of a larger vapor bubble in the reactor pressure vessel. The lone difference of importance between the data from the two facilities is the single phase stratification that occurs in the ROSA facility but not the OSU APEX facility. This can be attributed to the height of the downcomer and the time scale in the ROSA facility. The downcomer is much taller and therefore allows a more continuous vertical temperature profile to develop above the cold leg due to conduction, where the OSU APEX facility has a shorter downcomer and therefore the temperature profile is much steeper. The longer time scale of the ROSA facility also affords a longer window for the steady state phenomena to develop, while in the OSU APEX facility the conditions of the system (i.e. downcomer liquid level) may change too rapidly to allow this complicated flow condition to form.

6. DESCRIPTION OF CFX MODEL

The purpose of this research is to provide a tool to predict the onset and degree of thermal stratification that will occur in the cold legs of the OSU APEX facility (and therefore the AP600) during any given flow conditions. A model is necessary because it is both time consuming and expensive to set up and run an experiment for every postulated operating condition. Also, experimental results only offer a glimpse at the actual phenomena occurring within the system. To describe the overall activity of the system, one must extrapolate the information given by a few experimental data points. To observe any particular phenomena occurring within the system, that phenomena must be anticipated and the experiment properly instrumented to report data about the phenomena. A three-dimensional model generated by a computational fluid dynamics (CFD) code on the other hand can predict many phenomena without prior anticipation. Boundary conditions and initial conditions can also be easily changed and their effects evaluated in a short period of time. It is therefore desirable to construct a CFD model of the system and experimentally benchmark it for widespread application.

6.1 Overview of CFX 4.1

CFX 4.1 is a general purpose CFD package which can be used to simulate a wide range of fluid flow and heat transfer processes. The package is comprehensive and includes software to generate the problem geometry, setup the flow solver and analyze the results with flow visualization tools. The heart of the package is the flow solver. The CFX 4.1 flow solver includes the following:

6.1.1 Multi-block meshing

CFX 4.1 has an unstructured multi-block solver, which permits efficient and accurate representation of complex geometries. The mesh is structured within each block, ensuring fast solution of the simulation, while the blocks can be connected in any arrangement to give geometric flexibility.

Using multi-block meshing improves the mesh quality and hence solution accuracy, and allows the user to perform local grid refinement where required. In addition, the multi-block meshes can also expand and contract as prescribed by the user for applications such as piston-in-cylinder flows and detailed free-surface simulations. Furthermore, CFX 4.1 offers a sliding mesh facility, in which grids can be unmatched at inter-block boundaries and can rotate or slide relative to each other. This is especially suited to the simulation of mixing vessel flows, pumps and other rotating machines.

6.1.2 Advanced Turbulence Models

CFX 4.1 provides a selection of advanced turbulence models, including:

- κ-ε turbulence model
- low Reynolds number κ-ε model
- RNG κ-ε turbulence model
- algebraic Reynolds stress model
- differential Reynolds stress model
- differential Reynolds flux model

6.1.3 Multiphase Flows

Individual Particles: The particle-transport model in CFX 4.1 employs a Lagrangian scheme to account for momentum, heat and mass transfer between particles and the continuous phase. Specific modules describe coal and oil combustion and spray particle evaporation.

Continuous and disperse multiphase flow: CFX 4.1 is formulated to handle any number of separate phases: liquids, solids, gases or chemical species, and can therefore model flows in which several types (or sizes) of particles (or bubbles) may be present. In addition, each phase may consist of distinct components: for example water vapor in air, or tracer dye in water.

Free-surface flows: Simulation of sloshing or filling problems is possible with CFX's free-surface model. Surface tension effects can also be included when these are important.

6.1.4 Chemical Kinetics and Combustion Models

CFX's chemical kinetics model allows specification and solution of a chemical system involving several species and reactions. For each species, the program automatically allocates a transport equation and calculates the rate constant, heat release and property changes. Combustion models are available for both controlled and uncontrolled combustion of arbitrary fuels.

6.1.5 Heat Transfer

CFX 4.1 models heat transfer, whether by convection, conduction (including solid regions) or radiation. The radiation module calculates radiative heat transfer,

taking full account of shadowing effects in complex three-dimensional geometries for gray and non-gray systems. The algorithm uses either Monte-Carlo or Discrete-Transfer methods.

6.1.6 High Speed Flows

Proven algorithms handle subsonic, transonic and supersonic flow accurately, and the higher-order differencing schemes available in the software permit efficient calculation of shocks.

6.2 Description of Model

The goal of this work was to create a model of the APEX facility cold legs, which would predict the onset and severity of thermal stratification for a variety of circumstances. It was soon found that the cold leg behavior was extremely dependent on the phenomena occurring in its neighboring equipment, including the steam generator lower plenum and the downcomer. An accurate model of the cold leg phenomena would therefore require the inclusion of these components.

6.2.1 Model Geometry

CFX 4.1 allows the user to construct objects of complex geometry using one of several programs. MESHBUILD was selected for this model. The geometry of the model is generated by creating blocks of cells. Each block consists of six sides that can be deformed into a cube. The user must take care not to overly distort the block. A block that cannot be deformed easily into a cube may make it difficult for the flow solver to accurately model the system. These blocks are then subdivided into cells. The number of cells within the block determines the detail at which the user can

describe phenomena occurring within that block. Many simple systems can be modeled using a single block, but most require the conglomeration of several blocks. This is the case with the cold leg model generated for this analysis. Figure 6-1 and Figure 6-2 show the model and its grid of cells. This model contains 38 blocks and 55,772 cells.

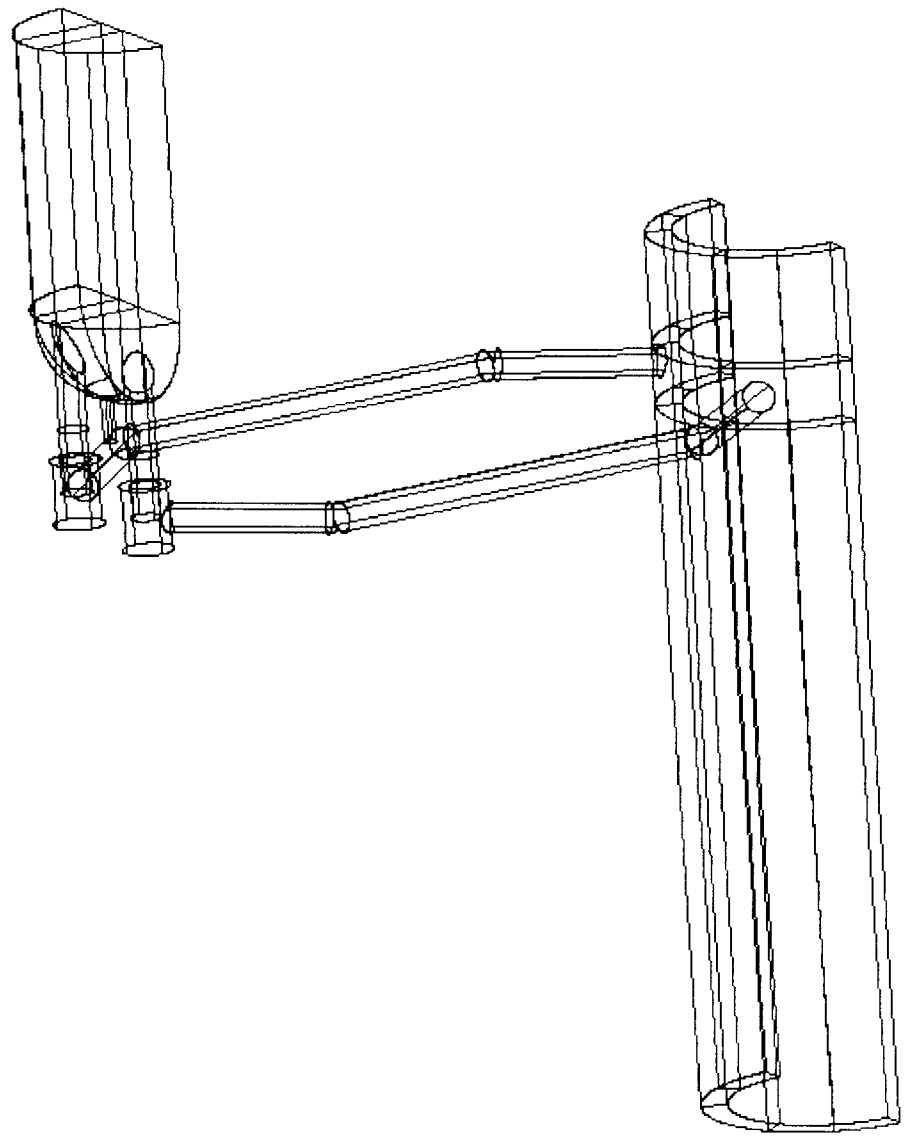

Figure 6-1 - Wire frame drawing of the steam generator lower plenum, cold legs and half downcomer as generated in CFX.

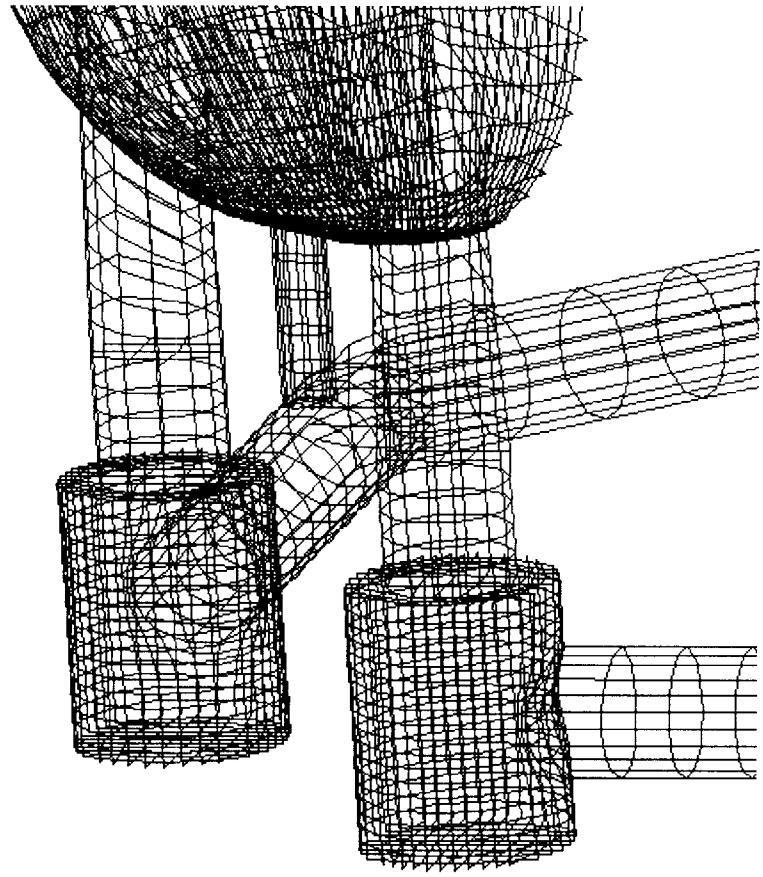

Figure 6-2 - Expanded view of the face grid for the steam generator lower plenum, PRHR, reactor coolant pumps and cold legs.

A model of the entire plant would be difficult to generate and would take a great deal of time to run. The model therefore only consists of the necessary components. The flow conditions at the points where the plant is cut must be easily defined to allow the generation of boundary conditions. The geometry has been cut at the cold side of the steam generator, at the PRHR injection line and at the top and bottom of the downcomer for this purpose. Flow through the steam generator consists entirely of natural circulation flow. This flow is controlled by the decay heat of the

reactor core and can be approximated by experimental correlations generated specifically for the OSU APEX facility. The PRHR flow rate can be approximated using data from a magnetic flow meter (FMM-804). The downcomer bypass flow can be approximated by using the differential pressure across the bypass holes and the Bernoulli equation. (K values for the bypass holes were determined experimentally.) The bottom of the downcomer is considered the only outlet for all the flow into the system.

6.2.2 Solver Options

After creating a mesh that describes the system the flow solver must be set up. To do this the user must enable all the models necessary to appropriately represent all the important physical phenomena occurring within the system. To model the cold leg system required the use of the momentum equations, energy equations (as opposed to using an isothermal model), turbulence models (as opposed to laminar models) and buoyancy models. The momentum and energy equations are obviously required to generate the flow and temperature fields. The turbulence models are necessary because the mixing of the PRHR injection plume with the ambient steam generator lower downcomer is probably turbulent. The driving force for the onset of thermal stratification is buoyancy, which makes it absolutely essential that buoyancy forces be included. The governing equations and models used by CFX to solve this problem are described in detail in the following section.

6.3 CFX Models

This chapter describes the mathematical model equations for fluid flow and heat transfer used by CFX 4.1 in the cold leg model.

6.3.1 Governing Equations

This section describes the governing equations of laminar fluid flow and heat transfer. It should be emphasized that the equations for "laminar flow" are in fact valid for turbulent flows as well. Turbulent flows are just very complex unsteady laminar flows. However, we are limited in our ability to solve these equations accurately for high Reynolds numbers, and we have to resort to turbulence modeling.

6.3.1.1 Transport Equations

The basic set of equations solved by the program for laminar flows is comprised of equations for the conservation of mass and momentum and, in non-isothermal flow, energy. The Navier Stokes equation is reserved for the equations of motion. These equations consist of the continuity equation

$$\frac{\partial \rho}{\partial t} + \nabla \cdot \left(\rho U \right) = 0, \tag{6.1}$$

the momentum equation

$$\frac{\partial \rho U}{\partial t} + \nabla \cdot \left(\rho U \otimes U \right) = B + \nabla \cdot \sigma, \tag{6.2}$$

where σ is the stress tensor:

$$\sigma = -\rho\delta + \left(\zeta - \frac{2}{3}\mu\right)\nabla \cdot U\delta + \mu\left(\nabla U + (\nabla U)^T\right), \tag{6.3}$$

and the energy equation,

$$\frac{\partial \rho H}{\partial t} + \nabla \cdot \left(\rho U H\right) - \nabla \cdot (\lambda \nabla T) = \frac{\partial \rho}{\partial t}, \tag{6.4}$$

where H is the total enthalpy, given in terms of the static (thermodynamic) enthalpy h by:

$$H = h + \frac{1}{2}U^2. \tag{6.5}$$

Here ρ is the fluid density, $\boldsymbol{U}$=(U,V,W) the fluid velocity, $\boldsymbol{p}$ the pressure, T the temperature and t is time. Further B is a body force, μ is the molecular viscosity, ζ is the bulk viscosity and λ is the thermal conductivity.

These equations represent 5 transport equations in the 7 unknowns U, V, W, p, T, ρ and h. They are completed by adding two algebraic equations from thermodynamics, the equation of state, relating density to temperature and pressure,

$$\rho = \rho(T, p) \tag{6.6}$$

and the constitutive equation, relating static enthalpy to temperature and pressure

$$h = h(T, p). \tag{6.7}$$

All of the above transport equations can be expressed as a scalar advection-diffusion equation,

$$\frac{\partial \rho \Phi}{\partial t} + \nabla \cdot \left(\rho U \Phi - \Gamma \nabla \Phi \right) = S \tag{6.8}$$

where Γ is the diffusion coefficient, and S is a source or sink term representing creation and destruction of Φ.

6.3.1.2 Buoyancy

This problem is modeled as an incompressible flow where the Boussinesq approximation is sufficient. The density is therefore considered a constant, $\rho=\rho_o$ except in the buoyancy terms of the momentum equations,

$$B = \left(\rho - \rho_o \right) g \,, \tag{6.9}$$

where,

$$\rho = \rho_o \left(1 - \beta \left(T - T_o \right) \right), \tag{6.10}$$

where β is the coefficient of thermal expansion and T_o is the buoyancy reference temperature. When incorporated into the momentum equations the $\rho_o g$ term is absorbed into the pressure gradient and the right hand side of the momentum equation becomes

$$\rho g - \nabla p' = \left(\rho - \rho_o \right) g - \nabla P \,, \tag{6.11}$$

where P is a further modification to the pressure, now with the hydrostatic part removed,

$$P = p' - \rho_o g \cdot x \,. \tag{6.12}$$

6.3.1.3 Heat Transfer

For compressible and incompressible flows, the energy equation is solved for the enthalpy, H. The transport equation has to be closed by supplying the constitutive equation, that is, the relationship between static enthalpy and temperature and pressure, h=h(T,p). The fluid is assumed to be thermally perfect, that is, the static enthalpy is a function of temperature only. Hence, the constitutive equation is given uniquely by specifying the specific heat at constant pressure, as a function of temperature:

$$C_p(T) = \left(\frac{\partial h}{\partial t}\right)_p , \tag{6.13}$$

and a reference temperature, T_{ref}, where static enthalpy is defined as zero. The static enthalpy is then obtained by integrating the previous equation,

$$h = \int_0^T C_p(T')dT' - \int_0^{T_{ref}} C_p(T')dT' . \tag{6.14}$$

Internally, the constitutive equation is assumed to have the following analytic form:

$$h = \overline{C}_p(T)T - \overline{C}_p\left(T_{ref}\right)T_{ref} , \tag{6.15}$$

where $\overline{C}_p$ is an "average specific heat", obtained by integrating equation (6.13):

$$\overline{C}_p(T) = \frac{1}{T}\int_0^T C_p(T')dT' . \tag{6.16}$$

For this problem the specific heat is assumed to be a constant, independent of temperature, so that $\overline{C}_p = C_p$.

It is important to note that all the fluid properties other than fluid density, for example, molecular viscosity, thermal conductivity, diffusivities etc. are assumed to independent of temperature.

For incompressible flow, the kinetic energy $\frac{1}{2}U^2$ in the total enthalpy is assumed much smaller than the internal energy term h. Thus, in this case, the code solves for the static enthalpy;

$$H = h(T, p) \,, \tag{6.17}$$

It is consistent with this approximation to ignore the pressure work term. So, the energy equation solved by the code for incompressible or weakly compressible flow is:

$$\frac{\partial \rho H}{\partial t} + \nabla \cdot (\rho U H) - \nabla \cdot (\lambda \nabla T) = 0, \tag{6.18}$$

Finally, it should be noted that the energy equation is slightly more complicated than the generic scalar advection-diffusion equation (6.8). The convected variable H is different from the variable T governing diffusive transport, and these are in general related by a non-linear algebraic equation. The energy equation is transformed to an advection-diffusion equation for H by replacing the temperature gradient with an enthalpy gradient:

$$\lambda \nabla T = \frac{\lambda}{C_p} \nabla H \,. \tag{6.19}$$

6.3.2 Turbulence Models

6.3.2.1 The Reynolds-averaged equations

Turbulent flows are extremely complex time-dependent flows. They are governed by the laminar flow equations described in the previous chapter. However, it is not feasible to solve these to the required accuracy using current technology, except for low Reynolds numbers in simple geometries. We therefore resort to turbulence models, which solve transport equations for the Reynolds-averaged quantities:

$$\overline{\Phi}(t) = \frac{1}{2\delta t} \int_{\tau-\delta t}^{\tau+\delta t} \Phi(\tau) d\tau \tag{6.20}$$

where δt is a time scale large relative to the time scale of turbulent fluctuations, and small relative to the time scale to be resolved. Splitting fields into their mean and fluctuating parts:

$$\Phi = \overline{\Phi} + \phi$$

and

$$\Psi = \overline{\Psi} + \psi \,,$$

we easily see that Reynolds averaging has the properties:

1. $\overline{\Phi} = \overline{\Phi}$, $\overline{\phi} = 0$
2. $\overline{a\Phi + b\Phi} = a\overline{\Phi} + b\overline{\Phi}$, a, b constant

3. $\overline{\Phi\Psi} = \overline{\Phi}\,\overline{\Psi} + \overline{\phi\psi}$

4. $\dfrac{\overline{\partial\Phi}}{\partial t} = \dfrac{\partial\overline{\Phi}}{\partial t}, \dfrac{\overline{\partial\Phi}}{\partial x^i} = \dfrac{\partial\overline{\Phi}}{\partial x^i}.$

From now on, we drop the bars from Reynolds averaged mean quantities for primitive variables; we retain the bars however for averages involving products of fluctuating quantities. The derivatives of the following results assume that the flow is incompressible.

Applying Reynolds averaging to the continuity equation, the momentum equation and the scalar transport equation, we obtain:

$$\frac{\partial\rho}{\partial t} + \nabla\cdot\left(\rho U\right) = 0, \tag{6.21}$$

$$\frac{\partial\rho U}{\partial t} + \nabla\cdot\left(\rho U\otimes U\right) = B + \nabla\cdot\left(\sigma - \overline{\rho u\otimes u}\right), \tag{6.22}$$

$$\frac{\partial\rho\Phi}{\partial t} + \nabla\cdot\left(\rho U\Phi\right) = \nabla\cdot\left(\Gamma\nabla\Phi - \rho\overline{u\phi}\right) + S. \tag{6.23}$$

Hence the Reynolds averaged continuity equation is the same as the equation that has not been averaged. However, the momentum and scalar transport equations contain turbulent flux terms additional to the molecular diffusive fluxes. These are the

$$\text{Reynolds stress} = \rho\overline{u\otimes u}$$

and the

$$\text{Reynolds flux} = \rho\overline{u\phi}.$$

It is instructive to note that these terms arise from the non-linear convective terms in the unaveraged equations, not the linear diffusive one. They reflect the fact that convective transport due to turbulent velocity fluctuations will act to enhance mixing over and above that caused by thermal fluctuations at the molecular level. At high Reynolds numbers, turbulent velocity fluctuations occur over a length scale much larger than the mean free path of thermal fluctuations, hence the turbulent fluxes are much larger than the molecular fluxes. For completeness, the Reynolds averaged energy equation is:

$$\frac{\partial \rho H}{\partial t} + \nabla \cdot \left(\rho U H + \rho \overline{uh} - \lambda \nabla T \right) = \frac{\partial p}{\partial t}, \tag{6.24}$$

where the mean total enthalpy is given by:

$$H = h + \frac{1}{2} U^2 + k \,. \tag{6.25}$$

Note that the total enthalpy contains a contribution from the turbulent kinetic energy $k = \frac{1}{2}\overline{u^2}$ as well as the mean flow kinetic energy. In incompressible flows, though, the contributions from the mean and turbulent kinetic energies are ignored, as is the pressure work term on the right hand side of the energy equation.

Turbulence models close equations (6.21) - (6.23) by providing models for the computation of the Reynolds stresses and Reynolds fluxes. An eddy viscosity model is the category of the model used in this problem.

6.3.2.2 Eddy viscosity models

The eddy viscosity models model the Reynolds stresses and fluxes algebraically in terms of known mean quantities. To be precise, we have the eddy viscosity hypothesis that the Reynolds stresses can be linearly related to the mean velocity gradients in a manner analogous to the relationship between stress and strain tensors in laminar Newtonian flow:

$$-\rho\overline{u\otimes u} = -\frac{2}{3}\rho k\delta - \frac{2}{3}\mu_T \nabla\cdot U\delta + \mu_T\left(\nabla U + (\nabla U)^T\right). \tag{6.26}$$

Here, $k = \frac{1}{2}\overline{u^2}$ is the turbulent kinetic energy, and μ_T is an additional viscosity, called the eddy viscosity or the turbulent viscosity. This viscosity has to be prescribed.

Analogous to the eddy viscosity hypothesis, we have the eddy diffusivity hypothesis, that Reynolds fluxes of a scalar are linearly related to the mean scalar gradient:

$$-\rho\overline{u\phi} = \Gamma_T \nabla\Phi\,. \tag{6.27}$$

Here, Γ_T is the eddy diffusivity, and this has to be prescribed. Γ_T is usually written as

$$\Gamma_T = \frac{\mu_T}{\sigma_T} \tag{6.28}$$

where σ_T is the turbulent Prandtl number. Eddy diffusivities are then prescribed by specifying the turbulent Prandtl number.

Subject to these hypotheses, the Reynolds averaged momentum and scalar transport equations become:

$$\frac{\partial \rho U}{\partial t} + \nabla \cdot (\rho U \otimes U) = B - \nabla p' + \nabla \cdot \left(\mu_{eff} \left(\nabla U + (\nabla U)^T \right) \right), \tag{6.29}$$

$$\frac{\partial \rho \Phi}{\partial t} + \nabla \cdot \left(\rho U \Phi - \Gamma_{eff} \nabla \Phi \right) = S \tag{6.30}$$

where μ_{eff} is the effective viscosity, and Γ_{eff} is the effective diffusivity, defined by:

$$\mu_{eff} = \mu + \mu_T$$

and

$$\Gamma_{eff} = \Gamma + \Gamma_T$$

and p' is a modified pressure, defined by:

$$p' = p + \frac{2}{3}\rho k + \left(\frac{2}{3}\mu_{eff} - \zeta \right) \nabla \cdot U \,. \tag{6.31}$$

If the body force contains a gravitational field g, then the modified pressure is given by:

$$p' = p + \frac{2}{3}\rho k + \left(\frac{2}{3}\mu_{eff} - \zeta \right) \nabla \cdot U - \rho g x \,. \tag{6.32}$$

The Reynolds averaged energy equation becomes, after transforming the molecular diffusion term using equation 6.19:

$$\frac{\partial \rho H}{\partial t} + \nabla \cdot \left(\rho UH - \left(\frac{\lambda}{C_p} + \frac{\mu_T}{\sigma_H} \right) \nabla H \right) = \frac{\partial p}{\partial t}. \tag{6.33}$$

Note that, although the transformation of the molecular diffusion term may be inexact if enthalpy depends on variables other than temperature, the turbulent diffusion term is correct, subject to the eddy viscosity hypothesis. Moreover, as turbulent diffusion is usually much larger than molecular diffusion, small errors in the latter are immaterial.

Eddy viscosity models are distinguished by the manner in which they prescribe the eddy viscosity and eddy diffusivity. The most popular, due to its wide degree of applicability, is the κ-ε model.

6.3.2.3 The κ-ε turbulence model

The κ-ε turbulence model uses the eddy viscosity hypothesis. The continuity and momentum equations are then:

$$\frac{\partial \rho}{\partial t} + \nabla \cdot (\rho U) = 0 \tag{6.34}$$

and

$$\frac{\partial \rho U}{\partial t} + \nabla \cdot (\rho U \otimes U) - \nabla \cdot (\mu_{eff} \nabla U) = -\nabla p' + B + \nabla \cdot \left(\mu_{eff} (\nabla U)^T \right). \tag{6.35}$$

ρ and U are now the mean fluid density and velocity, μ_{eff} is the effective viscosity and B is the body force.

In the κ-ε model, it is assumed that

$$\mu_T = C_\mu \rho \frac{\kappa^2}{\varepsilon}. \tag{6.36}$$

The transport equations for the turbulent kinetic energy κ and turbulence dissipation rate ε are

$$\frac{\partial \rho \kappa}{\partial t} + \nabla \cdot (\rho U \kappa) - \nabla \cdot \left(\left(\mu + \frac{\mu_T}{\sigma_\kappa} \right) \nabla \kappa \right) = P + G - \rho \varepsilon \tag{6.37}$$

and

$$\frac{\partial \rho \varepsilon}{\partial t} + \nabla \cdot (\rho U \varepsilon) - \nabla \cdot \left(\left(\mu + \frac{\mu_T}{\sigma_\varepsilon} \right) \nabla \varepsilon \right) = C_1 \frac{\varepsilon}{\kappa} \left(P + C_3 \max(G,0) \right) - C_2 \rho \frac{\varepsilon^2}{\kappa} \tag{6.38}$$

respectively, where P is the shear production defined by:

$$P = \mu_{eff} \nabla U \left(\nabla U + (\nabla U)^T \right) - \frac{2}{3} \nabla \cdot U \left(\mu_{eff} \nabla \cdot U + \rho \kappa \right) \tag{6.39}$$

and G is production due to body force defined by:

$$G = G_{buoy} + G_{rot} + G_{res} \tag{6.40}$$

where G_{buoy}, G_{rot} and G_{res} are terms representing production due to buoyancy, rotation and resistances respectively. However G_{rot}=0, and only G_{buoy} is included in the code. Therefore G=G_{buoy} and is defined by:

$$G = -\frac{\mu_{eff}}{\rho \sigma_\rho} g \cdot \nabla \rho, \tag{6.41}$$

which, with the Boussinesq buoyancy approximation, can be written as:

$$G = -\frac{\mu_{eff}}{\sigma_T} Bg \cdot \nabla T - \frac{\mu_{eff}}{\sigma_Y} \alpha g \cdot \nabla Y . \tag{6.42}$$

Note that the second term in P is only non-zero for compressible flows.

6.4 Summary of Model Output

The CFD model was setup to simulate three system conditions on the PRHR side of the OSU APEX facility including:

1. the full natural circulation phase,
2. a reduced natural circulation phase and
3. the loop stagnation phase,

The first and last phases are described in the description of phenomena section and the third phase is included to illustrate the transition between the other two. Boundary conditions at the steam generator inlet were the only difference between these cases. In all three cases, the PRHR inlet flow is the same and there is a moderate flow of water through the bypass holes. The temperature and flow rate for each of these inlet streams is tabulated in the following table.

		Temp. (K)	Flow Rate (GPM)
Full Natural Circulation	PRHR inlet	295	5
	SG flow	477	50
	Bypass Flow	477	2.5
Reduced Natural Circulation	PRHR inlet	295	5
	SG flow	477	20
	Bypass Flow	477	2.5
Loop Stagnation	PRHR inlet	295	5
	SG flow	-n/a-	0
	Bypass flow	477	2.5

Table 6-1 - Boundary conditions for CFX 4.1 models.

A significant simplification to the system was made by assuming that flow through the bypass holes was water instead of steam. This assumption greatly reduces the difficulty of the problem. The assumption undoubtedly reduces the magnitude of the buoyancy forces but it does not eliminate them. The phenomena observed in the models can therefore still be extrapolated to the actual system. The following are summaries of the CFX 4.1 output for these problems.

6.4.1 Full Natural Circulation

CFX 4.1 calculated the velocity and temperature of the fluid at every node of the problem. Figure 6-3 shows the temperature at the system surfaces. A few phenomena are of particular interest in this plot, including, the pool of cold water at the base of the steam generator and the lack of thermal stratification in the cold legs.

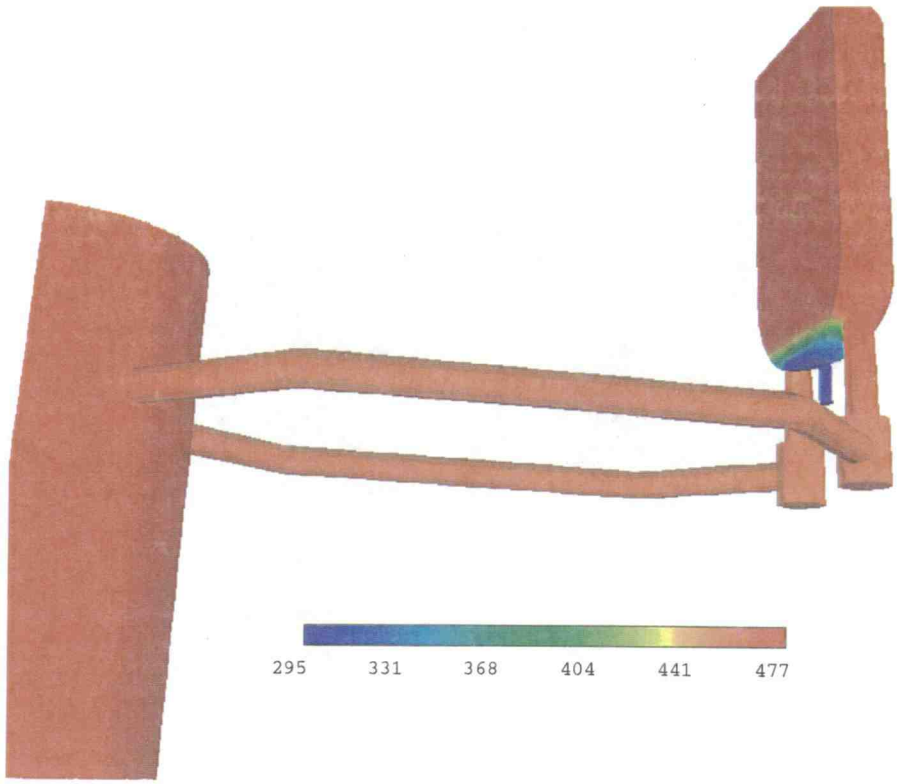

Figure 6-3 - Surface temperatures for the case of full natural circulation as predicted by CFX 4.1.

The following two plots consists of several vertical slices in the cold leg. These slices show cross sectional views of the temperature and velocity of fluid in the cold legs. It is important to note that the flow is one directional and is moving toward the downcomer.

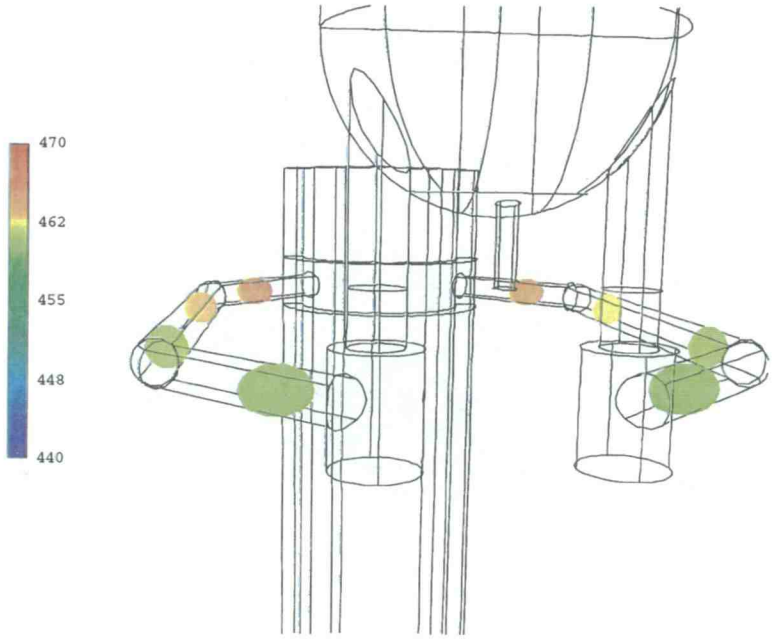

Figure 6-4 - Cold leg temperature profiles for the full natural circulation case as predicted by CFX 4.1.

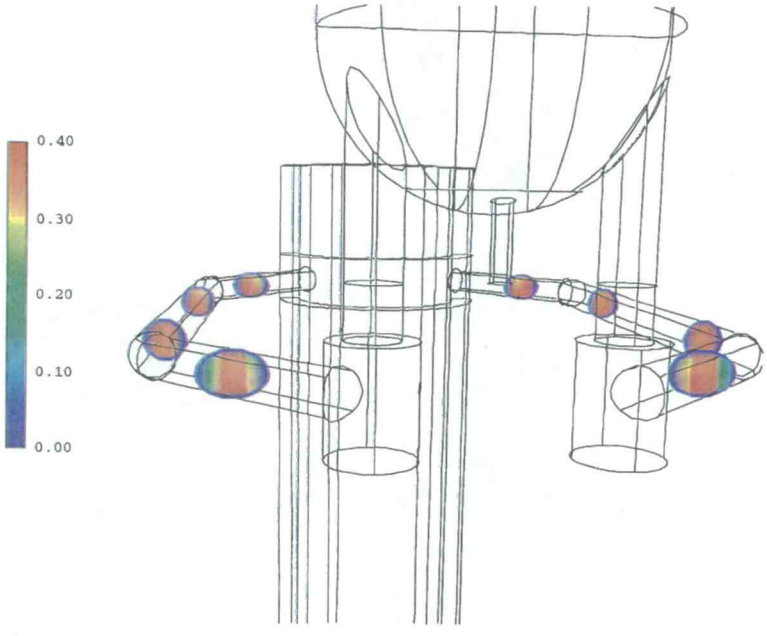

Figure 6-5 - Cold leg velocity profiles for the full natural circulation case as predicted by CFX 4.1.

Another area of interest is the steam generator lower plenum and cold leg penetrations (the connective piping between the steam generator lower plenum and the reactor coolant pumps). Figure 6-6 shows the temperature field in a vertical slice of this region. The cold pool above the PRHR injection nozzle is apparent. Figure 6-7 shows a velocity vector plot of this region. It clearly shows that the all the fluid is moving downward into the reactor coolant pumps.

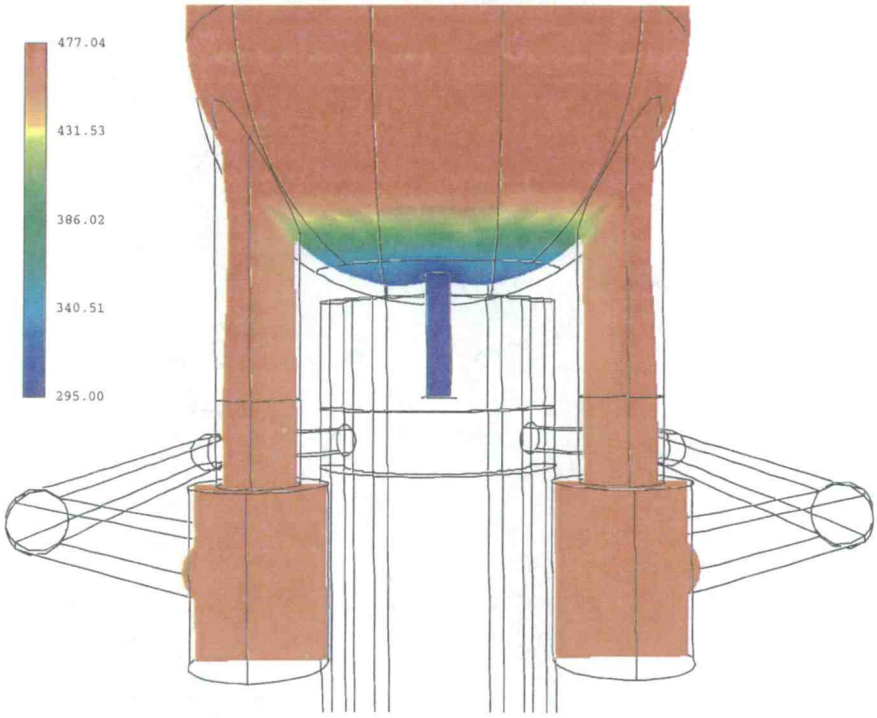

Figure 6-6 - Steam generator lower plenum temperature profile for the full natural circulation case as predicted by CFX 4.1.

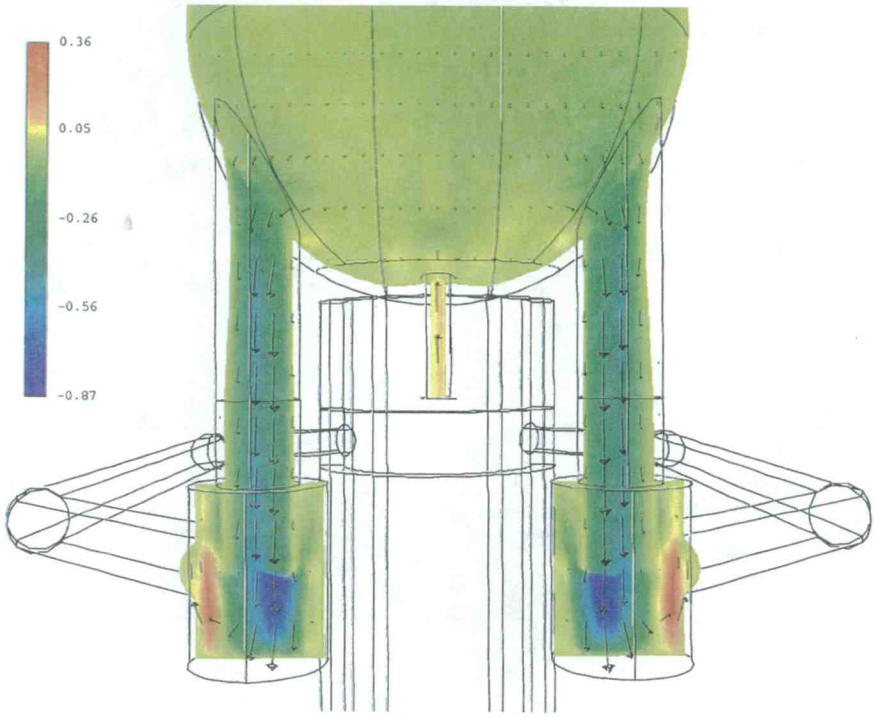

Figure 6-7 - Steam generator lower plenum velocity profile and velocity vectors for the full natural circulation case as predicted by CFX 4.1.

6.4.2 Reduced Natural Circulation

Again, CFX 4.1 calculated the velocity and temperature of the fluid at every node of the problem. Figure 6-8 shows the temperature at the system surfaces. The pool of cold water at the base of the steam generator is present once again and the cold legs are thermally stratified. The magnitude of stratification is approximately 30° Celsius.

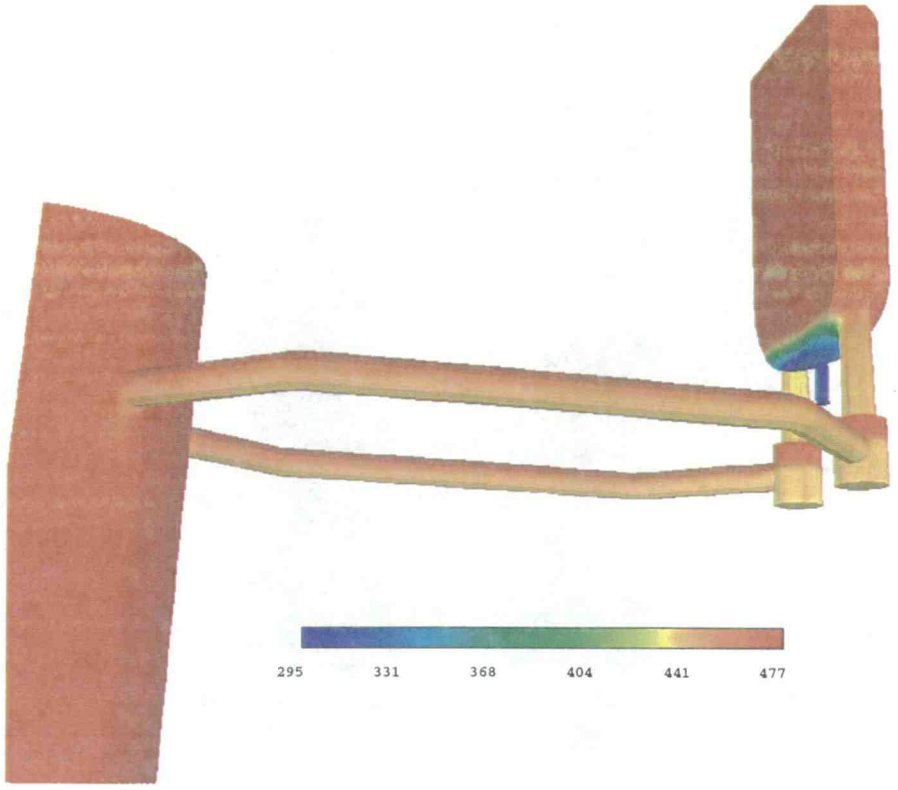

Figure 6-8 - Surface temperatures for the case of reduced natural circulation as predicted by CFX 4.1.

The following two plots consists of several vertical slices in the cold leg. These slices show cross section views of the temperature and velocity of fluid in the cold legs. It is important to note that there is a counter-current flow condition occurring and that the hot fluid on top is moving toward the steam generator and the cold fluid on bottom is moving toward the downcomer.

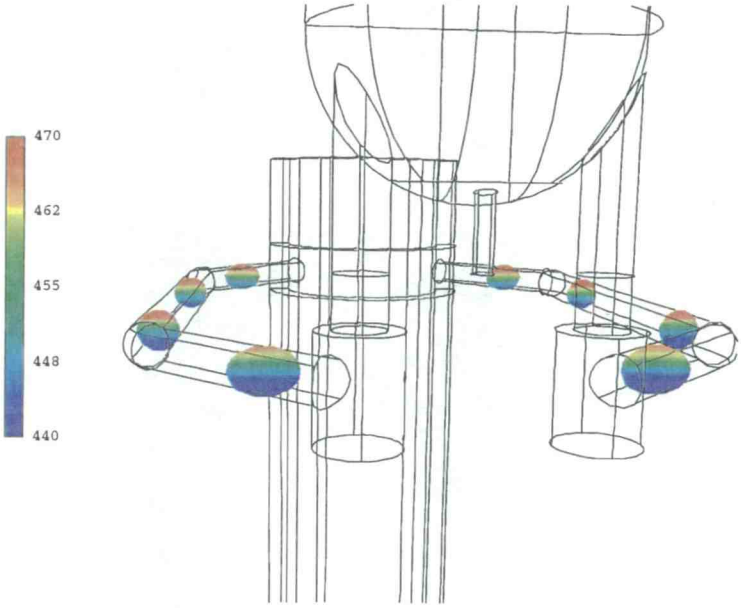

Figure 6-9 - Cold leg temperature profiles for the reduced natural circulation case as predicted by CFX 4.1.

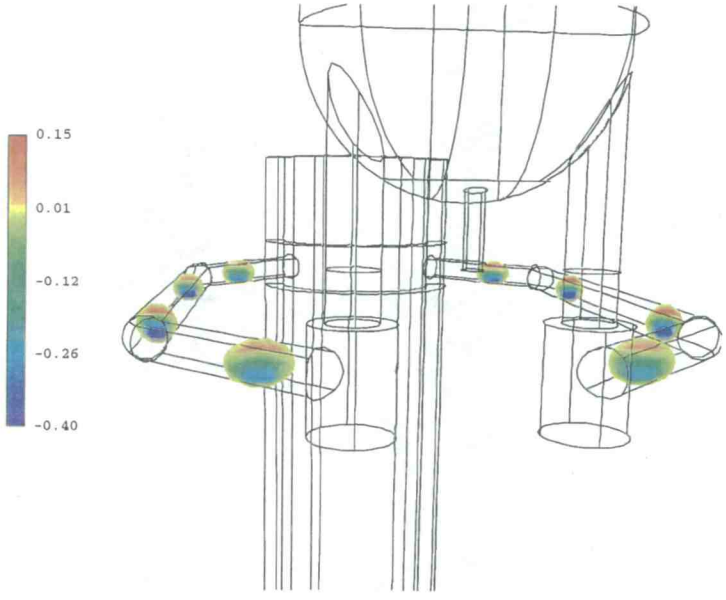

Figure 6-10 - Cold leg velocity profiles for the reduced natural circulation case as predicted by CFX 4.1.

Another area of interest is the steam generator lower plenum and cold leg penetrations. Figure 6-9 shows the temperature field in a vertical slice of this region. The cold pool above the PRHR injection nozzle is apparent. Figure 6-10 shows a velocity vector plot of this region. It clearly shows that the flow is predominantly moving downward into the reactor coolant pumps.

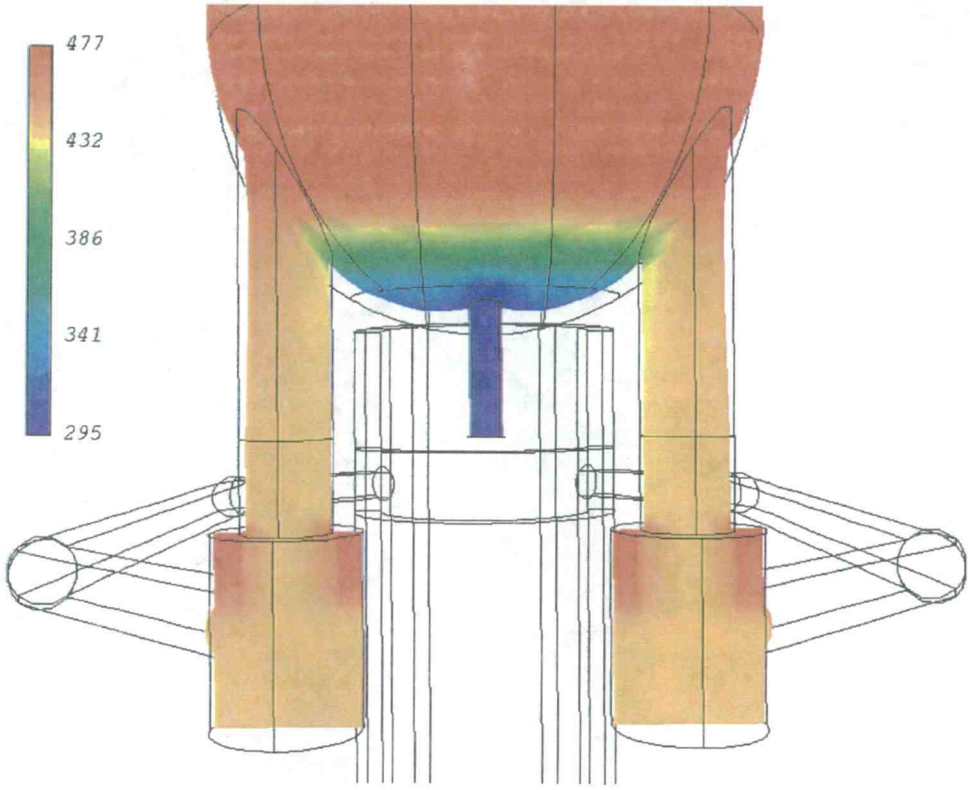

Figure 6-11 - Steam generator lower plenum temperature profile for the natural circulation case as predicted by CFX 4.1.

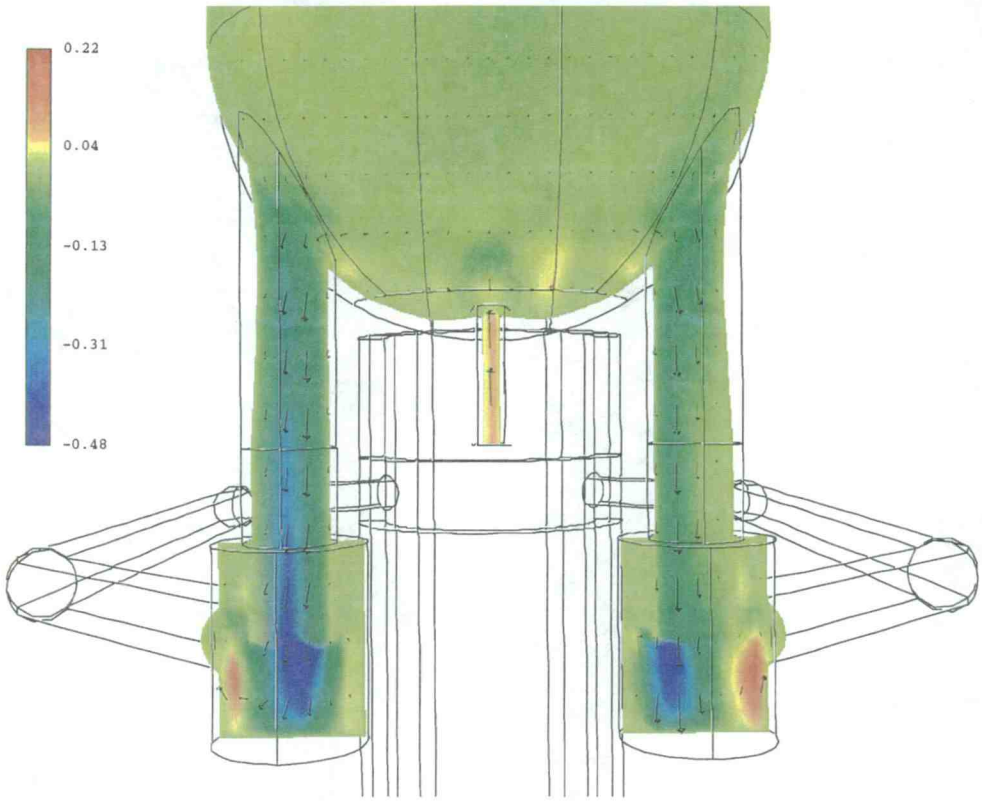

Figure 6-12 - Steam generator lower plenum velocity profile and velocity vectors for the natural circulation case as predicted by CFX 4.1.

6.4.3 Loop Stagnation

The following plots describe the CFX 4.1 output for the case where there is no natural circulation and the primary system is therefore considered stagnant. For this case there is still PRHR injection and downcomer bypass flow. The predicted phenomena are very similar to the reduced natural circulation case except for the non-symmetry between the cold legs and the degree of stratification. Figure 6-13 shows that because the total flow through the cold legs is approximately 1/5 that of the

reduced natural circulation case the back flow from the downcomer is more dominant. This leads to the non-symmetric flow between the cold legs, where one cold leg is dominated by the flow of hot water back toward the steam generator and the other is more thermally stratified and is experiencing a counter-current flow condition.

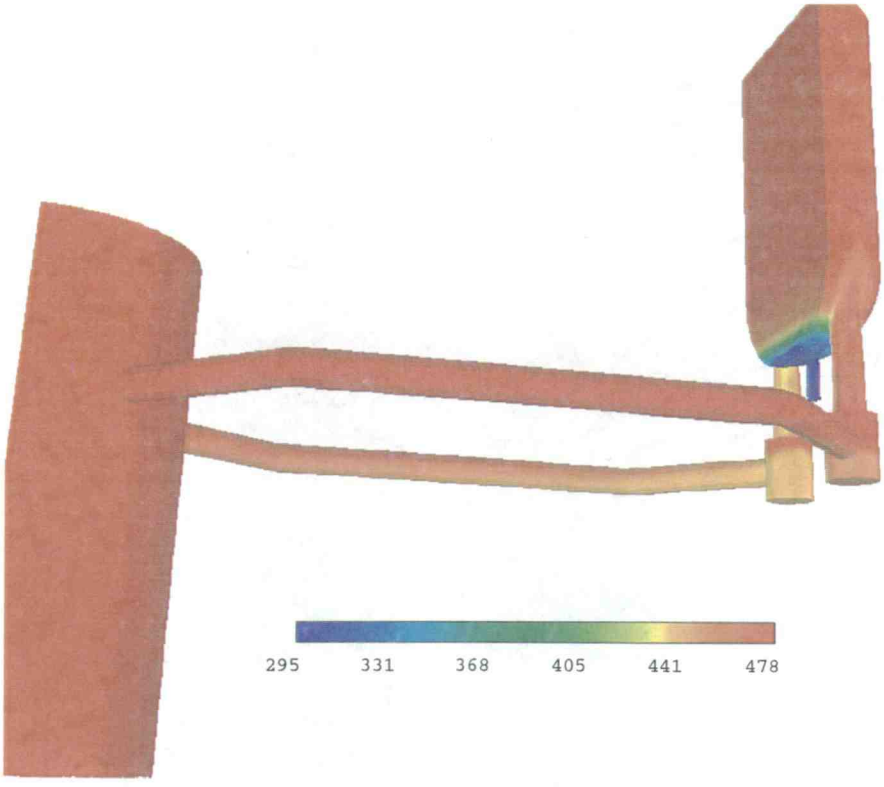

Figure 6-13 - Surface temperatures for the stagnant cold leg case.

Cross sectional plots of the cold temperature and velocity are provided in Figure 6-14 and Figure 6-15. The difference in stratification is clearly shown in these figures.

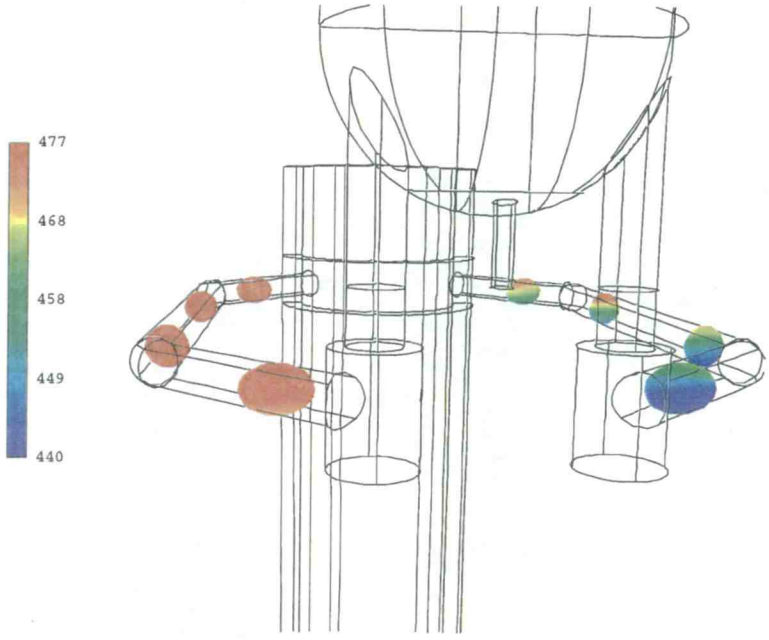

Figure 6-14 - Cold leg temperature profiles for the stagnant loop case as predicted by CFX 4.1.

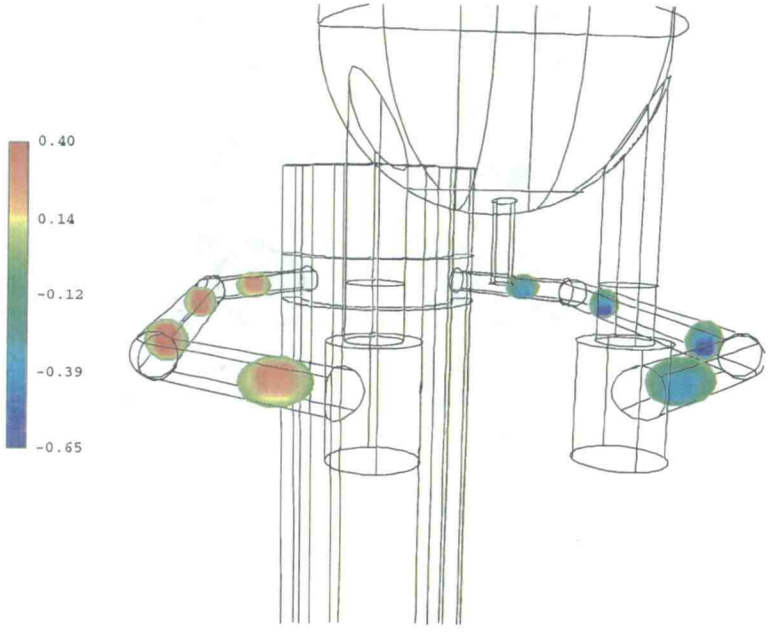

Figure 6-15 - Cold leg velocity profiles for the stagnant loop case as predicted by CFX 4.1.

The following plots show the conditions within the steam generator lower plenum and cold leg penetrations. The strong upward flow of hot water in the left cold leg and the downward flow in the right cold leg are evidence of the non-symmetry of phenomena and illustrate the need for both cold legs in the model.

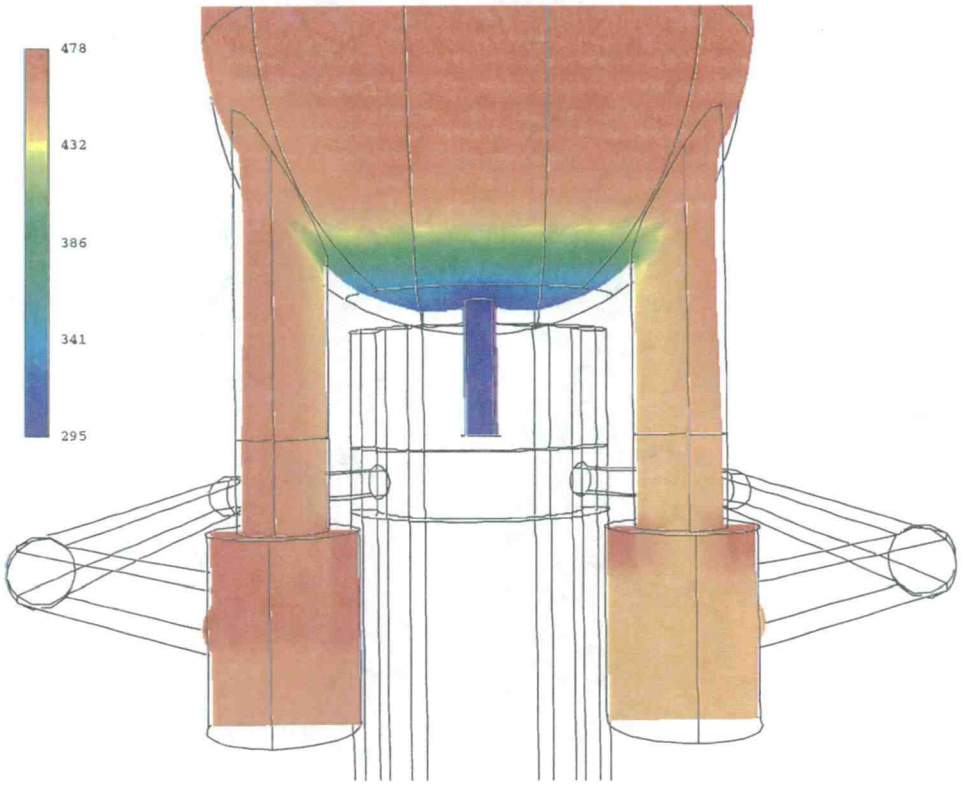

Figure 6-16 - Steam generator lower plenum temperature profile as predicted by CFX 4.1.

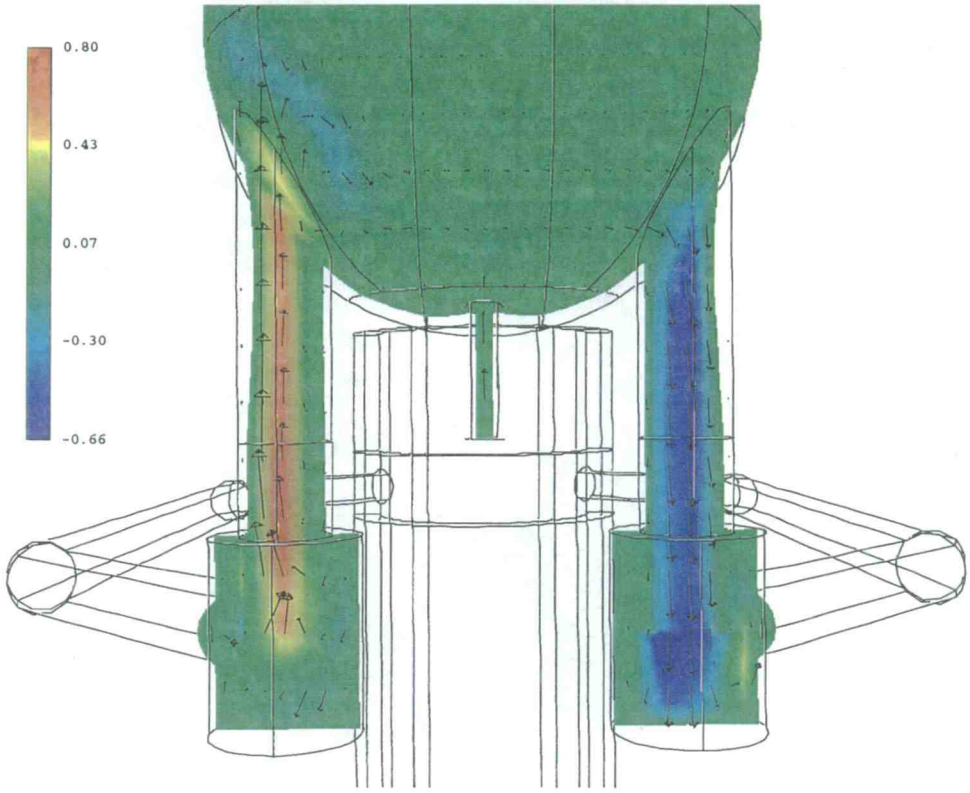

Figure 6-17 - Steam generator lower plenum velocity profile and velocity vectors for the stagnant loop case as predicted by CFX 4.1.

6.5 CFX Application Guidelines

CFX has proven to be a useful tool for the simulation of the behavior of systems like the one described in this report. It accurately predicted many of the large scale phenomena observed in the OSU APEX and ROSA facilities as well as some more local phenomena that occurred within the system (i.e. the plume height of the negatively buoyant PRHR injection stream into the steam generator). Application of the program though did provide some difficulties and required some special

considerations in both the construction of the blocks and the solver parameters. A brief summary of these considerations are discussed here.

The first step to generating a model is to define its geometry and create a nodalized representation of it. CFX allows the user to create groups of connected blocks to model a system. CFX will subdivide each of these blocks into cells to allow them to be connected. If the blocks are defined poorly, the number of cells in the model can become incredibly large. Which is undesirable because the program will solve the governing equations for each cell and the more cells in the model, the longer it will take to run the problem. The problem analyzed here contained roughly 55,000 cells and required approximately 40 hours to solve one problem on a HP workstation. The length of time may be deceiving because the machine was slowed considerable by a shortage of memory which forced the machine to page to disk often and therefore take longer than necessary to solve the problem.

Most of the time it is best to break a system down into a large number of small blocks because this allows CFX to generate a higher quality grid with fewer cells. A high quality grid generally consists of cells that have not been distorted much from a rectangular shape and that change gradually in size. Also, more cells are generally required to subdivide a distorted block than a rectangular block. A higher grid quality therefore generally allows the user to reduce the total number of cells in the problem by making the cells larger.

One of the key decisions in developing a system model is the definition of the system boundaries. It is often not reasonable to model the entire system because it would require a great deal of time and computing power to generate the model, let

alone run the problem. The user must therefore select appropriate place to "cut" the system. In the problem described in this report the cold side of the steam generator was selected because reasonable flow rates could be estimated for natural circulation. Had this not been the case, the extensive modeling necessary to describe the reactor core, hot leg and hot side of the steam generator may have been much too difficult to allow this analysis to be done with CFX or any other CFD code. This also seemed to be a good boundary choice because during stagnation the flow through the steam generator simply stopped and was therefore easy to define. The inclusion of the downcomer was necessary because the boundary condition at the cold leg exit was complicated and difficult to define, especially when compared to the bypass holes and downcomer bottom where the flows were one directional and relatively uniform in temperature. Including a section of the PRHR injection pipe allowed the inlet to have a uniform velocity, which would reach a more realistic fully developed condition prior to entering the steam generator lower plenum. It is advantageous to have the boundaries relatively far from the area of greatest interest because it will allow some of the inaccuracies associated with the roughly approximated boundary conditions to dampen out before reaching these areas (i.e. the opportunity for a uniform velocity profile in a pipe to become fully developed).

The second major step in running a simulation of a system with CFX is to setup the CFX solver. This solver must include commands to enable all the models necessary to predict the phenomena that the user expects to be significant in the problem (i.e. turbulence, heat transfer, buoyancy, etc.). The user must also set the parameters for the numerical solution process. This includes defining the time steps

for a transient problem, selecting the solver types for each governing equation, choosing the under-relaxation factors and the reduction factor for each iteration and a variety of other parameters. For the problem described within this report, it was found that the flow solver tended to be very unstable. The instability was generally associated with the rapid divergence of the turbulence quantities. The instability of the turbulence quantities was overcome by using the "differed correction technique," which gradually increases the effects of turbulence in the governing equations with each iteration until they are fully accounted for only in the final 50% of the iterations on each time step. Further divergence, or simple lack of convergence, was encountered and remedied by reducing the reduction factor and under-relaxation factor for each equation. Reducing the reduction factor for an equation forces the solver to more accurately solve the problem on each iteration before going onto the next iteration. The under-relaxation factor forces the solver to be more conservative about changing the values of thermal hydraulic quantities at a point, which helps prevent overshoot and oscillations about a potential solution. The reduction factor was dropped as low as 10^{-6} for the pressure equation (which affects the continuity equation) for this problem and the under-relaxation factors were dropped to approximately 0.3 for the pressure, momentum and enthalpy equations. Further reduction of these values will cause the solver to approach a converged solution much more slowly and an increase in these values may cause it to converge more rapidly or it may cause it to diverge. Convergence can generally be assumed when the residuals of the problem do not change much from iteration to iteration and they constitute a small percentage (between 5% and 1%) of that quantity flowing into the system and

the average reduction factors for the problem are small (at least 10^{-2}). The residual is a measure of the amount of a quantity which is not conserved by the problem, i.e. mass, energy, etc. It was also necessary to define a very small time step for the first several iterations at the initiation of the transient (0.1 seconds). This allowed the problem to slowly develop the smaller scale flow patterns with the greatest amount of detail, therefore providing a greater degree of stability. The size of the time steps could then be gradually increased, in this case they were as large as 30 seconds at the last time step.

7. Onset of Thermal Stratification

A convenient method for determining if thermal stratification will occur was generated by Theofanous (20) and is described in detail in the literature review section of this report. Because this method is based on analysis done only at the cold leg exit, it can be applied with equal validity in this study by substituting the PRHR for the HPI. Theofanous derived an equation representing a boundary between well-mixed and stratified flow conditions. This boundary is expressed in the following equation,

$$Fr_{PRHR,CL} \approx \left\{1+\frac{Q_{NC}}{Q_{PRHR}}\right\}^{-7/5} \tag{7.1}$$

where $Fr_{PRHR,CL}$ is defined as the following,

$$Fr_{PRHR,CL} = \frac{Q_{PRHR}}{A_{CL}}\left\{gD_{CL}\frac{\rho_{PRHR}-\rho_h}{\rho_{PRHR}}\right\}^{-1/2} \tag{7.2}$$

Where $Fr_{PRHR,CL}$ is the Froude number in the cold legs, Q_{PRHR} is the PRHR injection flow rate, Q_{NC} is the natural circulation flow rate, A_{CL} and D_{CL} are the area and diameter of the cold leg respectively, ρ_{PRHR} is the density of the fluid injected through the PRHR and ρ_h is the density of the fluid at the cold leg exit. Three cold leg conditions can be analyzed to create data points for examination in these equations. The first condition is natural circulation with PRHR injection. The second is the stagnant loop condition described in the description of phenomena chapter. The third and most valuable is the conditions at the transition from well mixed to stratified. A

summary of these values has been included in Table 7-2 and the values have been added to the plot generated by Theofanous in Figure 7-1.

Facility	System Condition	$Fr_{PRHR,CL}$	$1+\frac{Q_l}{Q_{PRHR}}$
APEX	natural circulation	1.2×10^{-1}	11
	stagnation	8.0×10^{-2}	1
ROSA	natural circulation	1.8×10^{-1}	7
	transition (single phase)	1.8×10^{-1}	3.5
	two phase stratified	9.0×10^{-2}	3.5
	stagnation	9.0×10^{-2}	1
CFX	full natural circulation	1.2×10^{-1}	11
	partial natural circulation	1.2×10^{-1}	5
	stagnation	2.1×10^{-1}	1
AP600	natural circulation	1.4×10^{-1}	7
	stagnation	9.5×10^{-2}	1

Table 7-2- Onset Criteria Data.

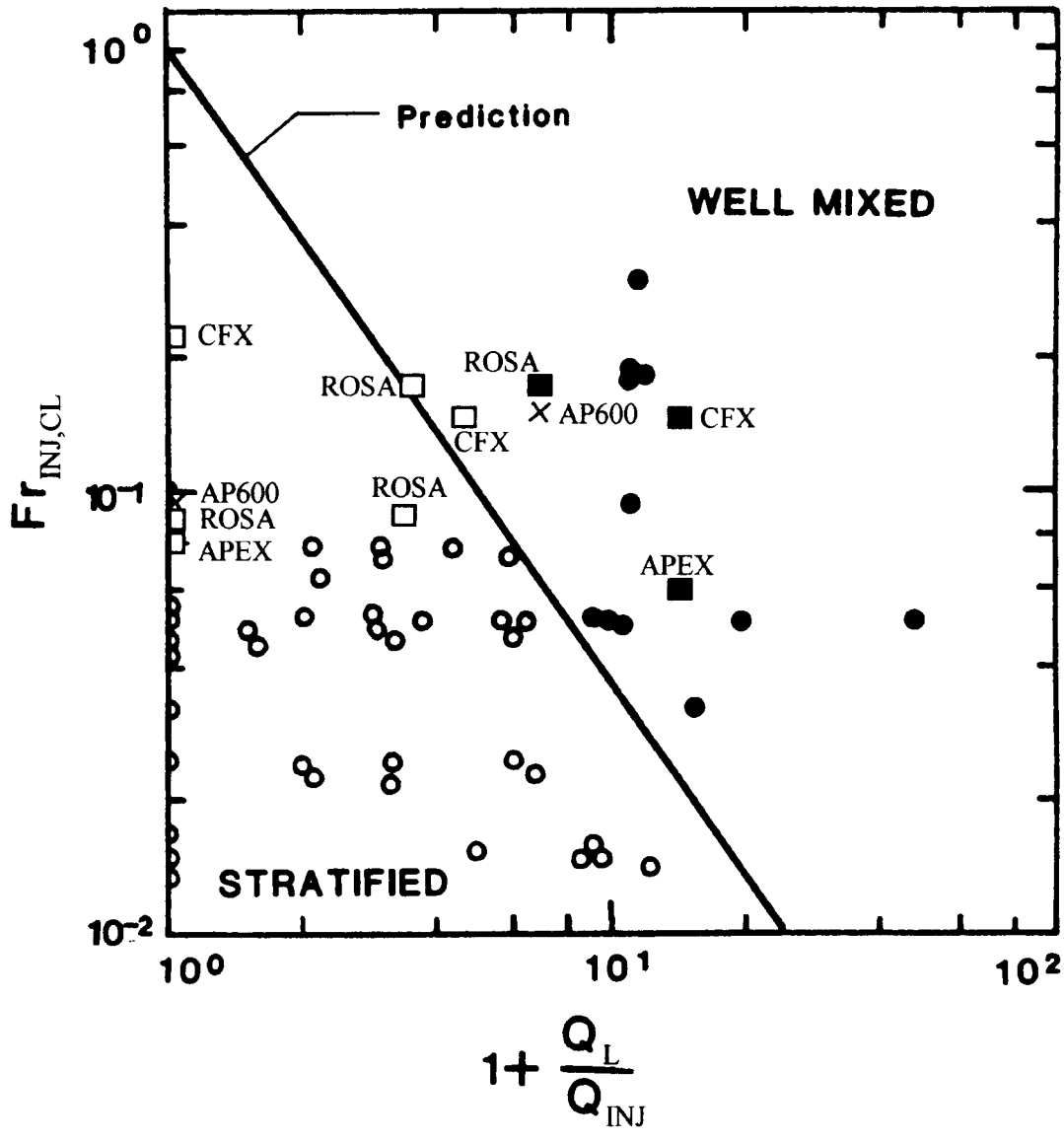

Figure 7-1 - The onset chart developed by Theofanous containing the onset line and data from the CREARE, APEX and ROSA facilities as well as points generated using CFX.

The values calculated for the natural circulation condition clearly lie on the well mixed side of the figure. This is in agreement with the cold leg #4 thermocouple rake in the OSU APEX and ROSA facilities which show that thermal stratification

does not occur when the natural circulation flows are high during the transient. The values calculated for the stagnant cold leg fall on the stratified side of the plot. This is also in agreement with the measured data which shows that two phase stratification accompanies the stagnation of the cold leg. Most instructive though is the transition point calculated for the ROSA facility which falls very near the onset criteria line, further supporting its credibility as a threshold for stratification. The conditions within the AP600 were estimated and plotted on the chart also. The points show that the AP600 will cross the onset threshold during a LOCA in a manner similar to the experimental facilities, meaning that the AP600 will experience a stratification period during a LOCA. The CFX data points were included as well. They show that CFX is reasonably good at predicting the flow conditions in the actual system.

The onset equations were generated by Theofanous with single phase systems in mind, but extension of the model to two phase systems is not unreasonable. The same theory applies and the extension is supported by the agreement of the plotted data.

The onset criteria is useful for determining if thermal stratification could possibly occur within a system without performing a detailed experimental or analytical analysis. It does not provide any insight to the degree of stratification though.

8. CONCLUSIONS/FURTHER WORK

- Thermal stratification in the subcooled blowdown phase of a LOCA was described, as were the factors that cause it on both the PRHR and CMT side of the OSU APEX facility.
- A model was constructed to simulate the thermal hydraulic conditions within the steam generator lower plenum, cold legs and downcomer on the PRHR side of the facility using CFX 4.1, a computational fluid dynamics code.
- A criterion for predicting the onset of thermal stratification, based on the cold leg Froude number and the ratio of the natural circulation and the PRHR injection flow, was established.

Oregon State University has constructed a test facility for the purpose of investigating the performance of the Westinghouse AP600 nuclear reactor safety systems. Analysis of the data resulting from this investigation revealed that the fluid within all four cold legs of the plant would become thermally stratified during the subcooled blowdown phase of a LOCA. The cause of these phenomena was unclear and thermal stratification had been identified by the NRC as a significant factor in assessing the risk of pressurized thermal shock (PTS) in a reactor following safety water injection. In current generation nuclear reactor systems, thermal stratification is caused by incomplete mixing of the cold high pressure safety injection (HPSI) water within the cold leg. This system is not included in the OSU APEX facility. Upon further review of the experimental data it was discovered that the stratification was two phase and consisted of saturated vapor at the top of the cold leg and subcooled

liquid on the bottom. The magnitude of stratification was greater on the PRHR side of the facility than on the CMT side due to the PRHR injection stream in the steam generator lower plenum. It was also established that the PRHR side cold legs developed a counter current flow condition where steam from the reactor pressure vessel was flowing into the downcomer, through the cold legs and into the steam generator while subcooled liquid was flowing out the steam generator, through the cold legs and into the downcomer. The potential for single phase thermal stratification that might increase the risk of PTS still existed in this side of the facility if the PRHR injection stream remained unmixed in the cold leg. The CMT side of the facility, however, developed a co-current flow condition. Steam was flowing from the reactor pressure vessel and into the steam generator and CMT-PBLs while subcooled liquid was being drawn into the cold leg and out the cold leg break. This flow condition establishes that the CMT side cold legs will not contribute to the risk of PTS.

The second stage of this work was to develop a model for predicting thermal stratification in the cold legs for the purpose of evaluating the risk of PTS. CFX 4.1, a computational fluid dynamics code, was selected for this task. By judiciously choosing the boundaries to cut the system, a model of the PRHR side cold legs and the attached components was created. This model contained the steam generator lower plenum, the PRHR injection line, approximations of the reactor coolant pumps and their connective piping, two cold legs and one half the downcomer. Inlet flows consisted of the natural circulation flow, PRHR injection flow and reactor downcomer bypass hole flow. All inlet flows were assumed to be single phase liquid. The flow

solver required a great deal of under-relaxation to avoid instability. A summary of the model predictions follows:

- predicted a well mixed cold leg for the case of full natural circulation
- predicted mild stratification for the case of reduced (1/2 of full) natural circulation
- for the stagnant loop case the model predicted thermal stratification and a global circulation pattern between the cold legs in which flow from the downcomer into the steam generator dominated in one cold leg and flow from the steam generator into the downcomer dominated in the other.

The third objective of this study was to provide an onset criteria for thermal stratification. In his work, Theofanous developed a criterion for current generation nuclear reactors which was intended for use with single phase systems. This criterion was benchmarked against data from experiments at the CREARE facility. The derivation of the criteria though does not make any assumptions which invalidate it for two phase systems. Data from the OSU APEX facility, ROSA facility and CFX models have been added to this plot. Despite the departure from single phase systems, the criteria shows good agreement with the data. Also shown on the plot are data points estimating where the Westinghouse AP600 would fall during natural circulation and loop stagnation. The stagnation point lies in the stratified region of the plot and the natural circulation point lies in the well mixed region, which suggests that the full scale AP600 will exhibit a transition between the two conditions similar to the test facilities.

Further work is recommended in several areas, including the following:

- include two phase phenomena in the CFX model
- further exploration of the possible formation of single phase stratification in the subcooled liquid layer of the cold leg
- improvement of the natural circulation flow estimates for the OSU APEX facility and AP600
- explore the possible formation of a global recirculation pattern
- verify the existence and determine the significance of the cold puddle in the base of the steam generator lower plenum

To more accurately match the CFX model to the facility will require that the two phase phenomena be included. A first step in this direction can be accomplished by changing the fluid flowing into the downcomer bypass holes from saturated liquid to air, which is a default gas for the code. This change would also require the inclusion of some of the two phase flow models and additional fluid properties. Most significantly though, the problem will become less stable and the parameters controlling it will need to be manipulated.

The work previously performed in this area has emphasized the formation of a counter current single phase flow condition in the cold leg. This attention was given because this flow condition resulted from incomplete mixing of cold injection flow and could lead to rather severe local vessel cooldown rates. Large cooldown rates could increase the risk of pressurized thermal shock (PTS). This flow condition is important because the system analysis codes currently used by the NRC only model one-dimensional, well mixed conditions and are therefore incapable of predicting it. Although it is clear that the stratification is primarily two phase for this reactor there is

is a possiblity that the subcooled liquid region of the cold leg could develop a single phase stratified counter current flow condition as well. To observe this flow condition would require the addition of instrumentation to the OSU APEX facility and to model it would require modification of the CFX model to include two phase phenomena.

To improve the experimental evaluation of the onset criteria will require knowledge of the natural circulation flow rate in the cold leg. Data describing this flow rate for a given test would permit the definition of the actual transition from well mixed to stratified, where the current data for the OSU APEX facility only offers a point at full natural circulation and loop stagnation. Knowledge of the cold leg flow rates will also assist in the exploration of the global recirculation pattern predicted by CFX for the loop stagnation case.

Another phenomena of interest predicted by CFX was the pool of cold water in the base of the steam generator lower plenum. Verification of this pool, followed by further evaluation of its significance is recommended.

BIBLIOGRAPHY

1. APEX Testing Facility, NRC-11 Quick Look Report, Reyes Jr., J., Franz, S., and Groome, J., Corvallis OR, Oregon State University, 1995.

2. Chao, J., et. Al., Analysis of Mixing With Direct Safety Injection Into the Downcomer Region of a Westinghouse Two-Loop PWR (NSAC-63), Nuclear Safety Analysis Center, EPRI, Palo Alto, California, May 1984.

3. Chen, M. J., et. Al., Simulation of a Thermal Hydraulic Transient in a Pipe Using the COMMIX-1A Computer Code, Argonne National Laboratory, Argonne, Illinois, February 1980.

4. Chen, M. J., et. Al., Turbulence Modeling in COMMIX Computer Code, Argonne National Laboratory, Argonne, Illinois, April 1984.

5. Chexal, B., et. Al., EPRI Research and Application Efforts on Reactor Vessel Pressurized Thermal Shock, EPRI, Palo Alto, California, October 1983.

6. Daly, B. J., Three Dimensional Calculations of Transient Fluid Thermal Mixing in the Downcomer of the Calvert Cliffs-1 Plant Using SOLA-PTS, NUREG/CR-3704, Los Alamos, New Mexico, April 1984.

7. Domanus, H. M., et. Al., COMMIX-1A: A Single-Phase Computer Program for Thermal Hydraulic Analysis of Single and Multicomponent Systems, Volume II: Assesment and Verification, Argonne National Laboratory, Argonne, Illinois, December 1983.

8. Domanus, H. M., et. Al., Three-Dimensional Analysis of Thermal and Fluid Mixing in Cold Leg and Downcomer of PWR Geometries, Argonne National Laboratory, Argonne, Illinois, December 1983.

9. Gardener, G.C., Motion of Miscible and Immiscible Fluids in Closed Horizontal and Vertical Ducts, International Journal of Multiphase Flow, Vol. 3, pp. 305-318, 1977.

10. Hashemi, A, el. Al., Thermal Mixing in a Rectangular Geometry Model of a Cold Leg with High Pressure Injection and a Downcomer, EPRI, Palo Alto, California, March 1983.

11. Levy, S., An Approximate Prediction of Heat Transfer During Pressurized Thermal Shock, S. Levy Incorporated, Campbell, California, June 1982.

12. Levy, S., Downcomer Annulus Thermal Shock for Beaver Valley Power Station, S. Levy Incorporated, Campbell, California, June 1983.

13. Levy, S., el. Al., Simplified Predictions of Pressurized Thermal Shock, S. Levy Incorporated, Campbell, California, October, 1983.

14. McGriff, R., et. Al., Analysis in the Cold Leg and Downcomer of a Westinghouse Three-Loop Plant During a SBLOCA (NSAC-62), Nuclear Safety Analysis Center, EPRI, Palo Alto, California, May 1984.

15. Reyes Jr., Dr. Jose N., Low-Pressure Integral Systems Test Facility Scaling Report, Jan 1995, Westinghouse Electric Corporation, Pittsburgh Pennsylvania., 1994.

16. Rothe, P. H., et. Al., Fluid and Thermal Mixing in a Model Cold Leg and Downcomer with Vent Valve Flow, EPRI, Palo Alto, California, 1982.

17. Rothe, P. H., et. Al., Thermal Mixing in a Model Cold Leg and Downcomer at Low Flow Rates, EPRI, Palo Alto, California, March 1983.

18. Schetz, J. A., Injection and Mixing in Turbulent Flow, American Institute of Aeronautics and Astronautics, New York, NY, 1980.

19. Selby, D. L., NRC FIN No. B0829, Oak Ridge National Laboratory, Oak Ridge, Tennessee, October 1985.

20. Theofanous, T. G., el. Al., Decay of Buoyancy Driven Stratified Layers with Applications to Pressurized Thermal Shock (PTS), Purdue University, West Lafayette, Indiana, May 1984.

21. Theofanous, T. G., et. Al., REMIX: A Computer Program for Temperature Transients Due to High Pressure Injection After Interruption of Natural Circulation, Purdue University, West Lafayette, Indiana, May 1986.

22. Theofanous, T. G., et. Al., Buoyancy Effects in Overcooling Transients Calculated for the NRC Pressurized Thermal Shock Study, Purdue University, West Lafayette, Indiana, May 1986.

23. Theofanous, T. G., et. Al., A Unified Interpretation of One-Fifth to Full-Scale Thermal Mixing Experiments Related to Pressurized Thermal Shock, Center for Risk Studies and Safety, University of California at Santa Barbara, April 1991.

24. Tuomisto, H., et. Al., Thermal Mixing in a Semiannular Downcomer With Interacting Flows from Cold Legs, Imatran Voima Oy, Helsinki 10, Finland, October 1986.

25. Tuomisto, H., et. Al., Application of the REMIX Thermal Mixing Calculation Program for the LOVIISA Reactor, Imatran Voima Oy, Helsinki 10, Finland, October 1987.

26. Turner, J. S., Buoyancy Effects in Fluids, Cambridge University Press, New York, NY, 1973.

NOMENCLATURE

Symbols

A	Area	μ	Viscosity
β	Thermal Expansion Coefficient	P	Pressure
C_p	Specific heat for a constant pressure process	Q	Heat
		ρ	Density
D	Pipe inside diameter	T	Temperature
g	Gravity	t	Time
Fr	Froude number	U	Velocity
H	Enthalpy	V	Volume
h	Convective heat transfer coefficient		
$\dot{m}$	Mass flow rate		

Subscripts

c	Pertaining to parameters involved with the cold leg cold stream.
CL	Pertaining to parameters involved with the cold leg.
e	Pertaining to parameters involved with entrainment.
h	Pertaining to parameters involved with the cold leg hot stream.
HPI	Pertaining to parameters involved with the HPI system.
l	Pertaining to parameters involved with the primary loop.
m	Pertaining to parameters involved with mean quantities.
mm	Pertaining to parameters involved with the mixed mean fluid.
PRHR	Pertaining to parameters involved with the PRHR.
T	Pertaining to parameters involved with the turbulent quantities.
W	Pertaining to parameters involved with the pipe walls.

Acronyms

ACC	Accumulator	LOCA	Loss of coolant accident
ADS	Automatic Depressurization System	NRC	Nuclear regulatory commission
AP600	Advance Plant 600 megawatt	OSU	Oregon State University
APEX	Advanced Plant EXperiment	PRHR	Primary Residual Heat Removal heat exchanger
BAMS	Break and ADS measurement system		
CFD	Computational Fluid Dynamics	PT	Pressure transducer
CMT	Core Makeup Tank	PTS	Pressurized thermal shock
DP	Differential pressure transducer	RCP	Reactor coolant pump
DVI	Direct Vessel Injection	RMM	Regional Mixing Model
IRWST	Incontainment Refueling Water Storage Tank	RPV	Reactor Pressure Vessel
		SG	Steam generator
FMM	Magnetic Flowmeter	TF	Thermocouple